UiA University of Agder

Design and Analysis of a Novel Semi-submersible Floater Supporting a 5MW Wind Turbine

Sara Abd Ali Najim

Internal supervisor
Zhiyu Jiang, Associate professor at University of Agder
External supervisor
Xiangjun Kong, Senior Engineer at NOV APL

This master's thesis is carried out as a part of the education at the University of Agder and is therefore approved as a part of this education. However, this does not imply that the University answers for the methods that are used or the conclusions that are drawn.

Universiy of Agder,Spring 2021
Faculty of Engineering and Science
Department of Engineering Sciences

Master

Mandatory Self Declaration

Den enkelte student er selv ansvarlig for å sette seg inn i hva som er lovlige hjelpemidler, retningslinjer for bruk av disse og regler om kildebruk. Erklæringen skal bevisstgjøre studentene på deres ansvar og hvilke konsekvenser fusk kan medføre. Manglende erklæring fritar ikke studentene fra sitt ansvar.

1.	Jeg/vi erklærer herved at min/vår besvarelse er mitt/vårt eget arbeid, og at jeg/vi ikke har brukt andre kilder eller har mottatt annen hjelp enn det som er nevnt i besvarelsen.	☒
2.	Jeg/vi erklærer videre at denne besvarelsen: - ikke har vært brukt til annen eksamen ved annen avdeling/universitet/høgskole innenlands eller utenlands. - ikke refererer til andres arbeid uten at det er oppgitt. - ikke refererer til eget tidligere arbeid uten at det er oppgitt. - har alle referansene oppgitt i litteraturlisten. - ikke er en kopi, duplikat eller avskrift av andres arbeid eller besvarelse.	☒
3.	Jeg/vi er kjent med at brudd på ovennevnte er å betrakte som fusk og kan medføre annullering av eksamen og utestengelse fra universiteter og høgskoler i Norge, jf. Universitets- og høgskoleloven §§4-7 og 4-8 og Forskrift om eksamen §§ 31.	☒
4.	Jeg/vi er kjent med at alle innleverte oppgaver kan bli plagiatkontrollert.	☒
5.	Jeg/vi er kjent med at Universitetet i Agder vil behandle alle saker hvor det forligger mistanke om fusk etter høgskolens retningslinjer for behandling av saker om fusk.	☒
6.	Jeg/vi har satt oss inn i regler og retningslinjer i bruk av kilder og referanser på biblioteket sine nettsider.	☒

Publishing Agreement

Fullmakt til elektronisk publisering av oppgaven

Forfatter(ne) har opphavsrett til oppgaven. Det betyr blant annet enerett til å gjøre verket tilgjengelig for allmennheten (Åndsverkloven. §2).

Alle oppgaver som fyller kriteriene vil bli registrert og publisert i Brage Aura og på UiA sine nettsider med forfatter(ne)s godkjennelse.

Oppgaver som er unntatt offentlighet eller tausehetsbelagt/konfidensiell vil ikke bli publisert.

Jeg/vi gir herved Universitetet i Agder en vederlagsfri rett til å gjøre oppgaven tilgjengelig for elektronisk publisering:	☒ JA	☐ NEI
Er oppgaven båndlagt (konfidensiell)?	☐ JA	☒ NEI
(Båndleggingsavtale må fylles ut) - Hvis ja:		
Kan oppgaven publiseres når båndleggingsperioden er over?	☐ JA	☐ NEI
Er oppgaven unntatt offentlighet? (inneholder taushetsbelagt informasjon. Jfr. Offl. §13/Fvl. §13)	☐ JA	☒ NEI

Preface

This master thesis is written as the concluding part of a Master in Civil Engineering at the University of Agder, Faculty of Engineering Sciences. The research was conducted in the Spring of 2021, and constitutes for 30 ECTs.

The goal with this master thesis is conducting a preliminary design of a novel semi-submersible concept, named the twin fish floater system. The thesis investigates possibilities and challenges with the given design, and demonstrates the potential for an innovative design.

It is a wish that the content of the report is interesting to the reader, and that the research will be of great use in the further development of the offshore wind industry.

I would like to extend my sincerest gratitude to my supervisors, Dr. Zhiyu Jiang, Associate professor at University of Agder and Dr. Xiangjun Kong, Senior Engineer at NOV APL. For your immense knowledge, round the clock availability, support and attention for detail: Thank you both. It has been a privilege and an honour to have you as my supervisors and work with you. I have learned a lot.

I would also like to thank my family and friends for their immense support. Last, but not least I would like to thank my classmates and teachers at University of Agder for making these 5 years a unforgettable period.

Best regards
Sara Abd Ali Najim
11 of June 2021 - Grimstad.

Summary

The wind industry has been rapidly evolving in recent years, moving from onshore to offshore locations. For deep waters, floating wind turbines are more cost-effective than bottom-fixed ones, and semi-submersible floating wind turbines are especially advantageous compared to other concepts because of their relatively small draft and good towability for installation. This master thesis focuses on preliminary design and analysis of a novel semi-submersible floating wind turbine supported by a twin fish floater and positioned by a single-point mooring system. Hydrostatic and hydrodynamic analysis are first carried out to select a floater with decent dynamic properties. Then, a two-component mooring system is designed with a turret connected to the twin fish floater. Dynamic analysis of the coupled wind turbine-floater-mooring system is performed under a few extreme environmental conditions. Results identify the motion characteristics of the twin fish floater with single point mooring and show that the extreme mooring line tensions satisfied the design criteria. This study contributes to a better understanding of the proposed novel system under wave conditions. In future, detailed structural analysis will be included in a more comprehensive study to evaluate the feasibility of the concept.

Figure 2: Illustration proposed by thesis of novel twin fish floater concept.

List of Abbreviations

Abbreviation	Description
BEM	Blade Element Momentum
CM	Centre of Mass
DNV	Det Norske Veritas
DoF	Degrees of freedom
CoB	Center of Bouyancy
CoG	Center of gravity
GL	Germanischer Lloyd
GM	Gravity metacentric Height
JONSWAP	Joint North Sea Wave Project
RAO	Response amplitude operator
MSL	Mean Sea Level
MWL	Mean water level
NREL	National renewable energy laboratory
RAO	Response amplitude operator
QTF	Quadratic Transfer Functions
ULS	Ultimate Limit State
MSL	Mean Sea Level
MWL	Mean water level
NREL	National renewable energy laboratory
TLP	Tension Leg Platform
ZOB	Vertical Center of Buoyancy
ZOG	Vertical Center of Gravity

Contents

List of Figures

List of Tables

1 | Introduction

In recent years, the effect of global warming has become more visible and led to larger impacts on society, both economic and social [14].To reduce carbon emissions while fulfilling the increasing energy demand, renewable energy is a good option[15]. Amongst all options, wind energy shows good potential due to its low cost, reliability and zero-emissions during operation. Also, there has been an increase in energy demand. It is expected that the energy demand will increase in the next decades[16]. From 2011 to 2020, the capacity from offshore wind power worldwide increased from approximately 3776 MW to 34 367 MW and it has potential for significant expansion [17]. Several companies are seeing the potential for wind energy and are investing into this renewable energy technology[18].

Although onshore wind currently has greater turnover than offshore wind [19], there is an increase in resistance towards use of onshore wind . There are several reasons for that, such as visual and sound pollution for the populations in which wind turbines are erected [20]. Compared to onshore wind, offshore wind has advantages such as: Stronger, and less turbulent wind at sea than at land , unlimited construction area compared to placing wind turbines on land and easier transportation of large wind turbines using ships instead of using roads [21].

There are many different offshore wind turbines in use.In general we can divide between fixed and floating structures [21]. The fixed structures in use today are used for sea depths of about 50 metres. Some examples in commercial use are the monopile, jacket or tripod structure. For sea depths of more than 50 metres, floating structures prove to be more cost efficient. For floating wind turbines, we can distinguish between spar, semi-submersible and the TLP[22].

Figure 1.1: Different offshore structure foundations for wind turbines [1]

Spar floaters is a gravity based structure requiring a large draft to stay stable. The necessary draft requires that the structure is built on water depths of 100 metres or more. Also, transportation and assembly of the spar floater requires good weather conditions. **Tension leg platform (TLP)** use tendons to achieve stability, and limit the motions of the structure. However, there is a risk for a coupling effect between the wind turbine and the tendons. Installation of TLP may also be difficult. **Semi-submersible** is a waterplane area structure with great flexibility. The semisubmersible may be used on both small and great water depths, and relies on ballasting to achieve stability. The manufacturing and assembly is done at the dock before the structure is towed to site, ensuring great quality and eliminating the need for barges and marine cranes. Semi-submersibles have been built using different materials, such as steel, concrete or hybrid structures. From the reasoning above, the semi-submersible structure proves to be a good option for further investigations[22].

Figure 1.2: Spar floater [2]

Figure 1.3: Pelastar TLP [3]

Figure 1.4: WindFloat [4]

A mooring system is a traditional way of keeping the structure at place. A mooring system can be constructed from a number of lines (chain,rope or a combination of both) with their upper ends (fairlead) attached to the structure, while the lower end (anchor) is fastened to the sea bed [9] [11]. The typical type of mooring systems in use is catenary mooring lines in a spread mooring system [23].It obtains the restoring force mainly by lifting and lowering the weight of the mooring line. In a spread mooring system, several pre-tensioned anchor lines are arrayed around the structure to keep it in position. The system requires significant length of anchor lines lying on the sea bed [9].

Many semi-submersible concepts have been proposed, the 5MW CSC [23], WindFloat [4], Trifloater [24] , ideol concept with a damping pool [25]. Most of these semi-submersible concepts are copied from the oil industry and use a catenary system to take up large forces. For the existing mooring systems used for semi-submersible structures, only spread mooring systems have been used. The twin fish floater is a structure with biomimetic characteristics,taking up little forces since it will rotate depending on loads inflicted on it. It will therefore reduce the number of mooring lines from several to only one.

According to Karimirad et. al , the price of the generated electricity is dependent on several factors such as design of support structure, installation, grid connection, operation and maintenance.The costs for floating offshore wind turbines exceed their bottom-fixed counterparts, and researchers are searching for opportunities for cost reduction[26].The feasibility of different floating concepts need to be studied and innovate structure which may aid in maturing the offshore industry.

However, significant analyses needs to be conducted for a novel structure. A coupled analysis is a good methodology to determine the overall influences of environmental loads on the structure. In a coupled analysis it is possible to study the influence of the mooring/riser system on the floater. Several tools can be used, such as SIMO-RIFLEX, where SIMO computes the vessel motion, and RIFLEX is used for modelling of the mooring system, and calculates forces and motions in the mooring system. Together, the vessel motion from SIMO is included in the equations for the mooring system [12].

As the wind energy industry is being foretold to become a "1 Trillion $ industry" [27], further investigations within cost effective wind turbine systems will encourage further use and growth of the technology. Therefore in this thesis, a novel semisubmersible wind turbine system, is studied. A single point mooring system is designed and a coupled analysis is conducted to properly asses the structure's responses.

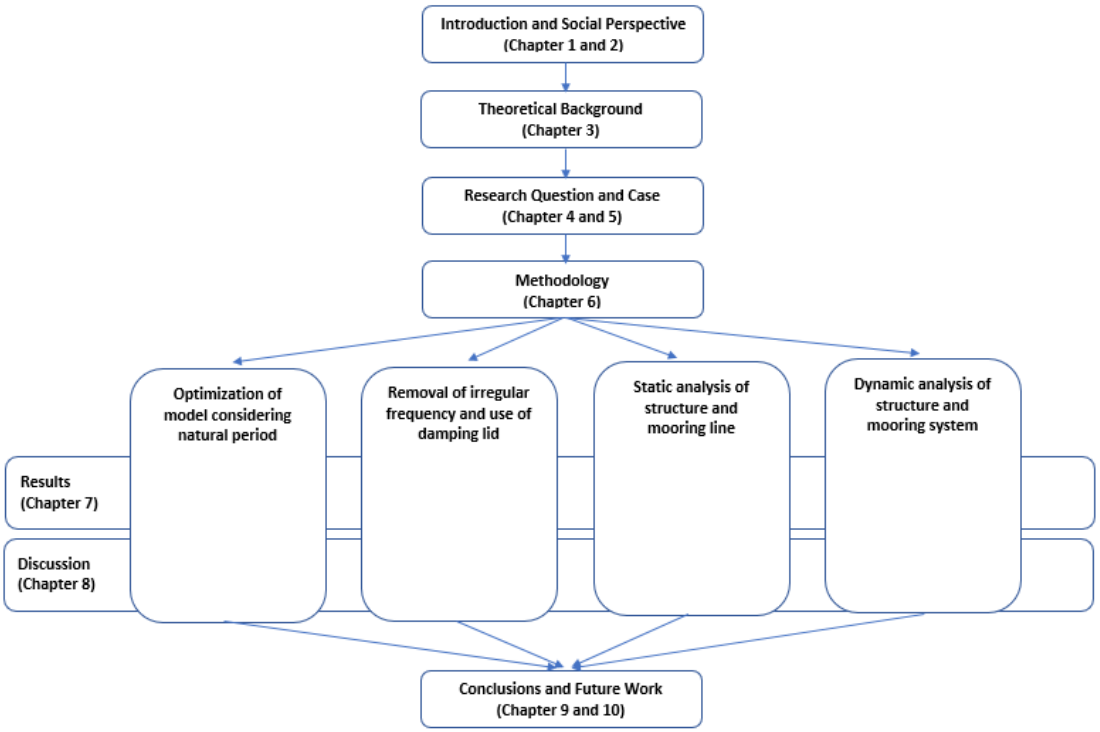

Figure 1.5: Overview of the report structure

This thesis contains the following chapter sections:

Chapter 1: Introduction
Gives a background for the thesis, brief scope introduction and the structure of the thesis.
Chapter 2: Social perspective
Shows the social perspective and importance of investigating novel designs of offshore floating structures.
Chapter 3: Theory
Presents the theoretical background of the thesis. Different classical literature and fundamental hydrostatic and hydrodynamic theory is presented.
Chapter 4: Scope
Main research question with sub-questions and necessary limitations for the thesis.
Chapter 5: Case
Presents case, and data of the twin fish floater with used software and location with belonging loads.
Chapter 6: Methodology
Methodology for modelling and analysis conducted in the thesis.
Chapter 7: Results
The results of the thesis is presented.
Chapter 8: Discussion
Discusses the results presented in the previous chapter. Shares the same structure as the result chapter.
Chapter 9: Conclusion
Presentation of conclusions from the master thesis
Chapter 10: Recommendations
Presents fields which should be investigated further.
Chapter 11: References and **Chapter 12: Appendix**

2 | Significance of the work

In recent years, the effect of global warming has become more visible and led to larger impacts on society, both economic and social. Some consequences of global warming are more frequent and intense droughts, storms, rising sea levels, melting glaciers and warming oceans have had effect on people and the wildlife population of the world. The carbon emissions caused by humans and industry are only amplifying the effects of global warming [14].

According to statistics, non-renewable energy sources such as fossile fuel make up more than 70 percent of the electricity generation in the OECD countries in 2018. The rest is adressed to renewable energy sources [28]. From research, it is clear that the non-renewable energy sources have had significant impact on the emission of CO_2 [14] , and thereby impacting global warming. To reduce carbon emissions while fulfilling the increasing energy demand, renewable energy is a good option. Amongst all options, wind energy shows good potential due to its low cost, reliability and zero-emissions during operation. Also, there has been an increase in energy demand. It is expected that the energy demand will increase in the next decades [16]. From 2011 to 2020, the capacity from offshore wind power worldwide increased from approximately 3776 MW to 34 367 MW and it has potential for significant expansion [17].The potential for wind power is immense, and large parts of the world have good prospects for increased use of wind power, as shown below [5]. Increased use of wind power will generate more workplaces worldwide [16].

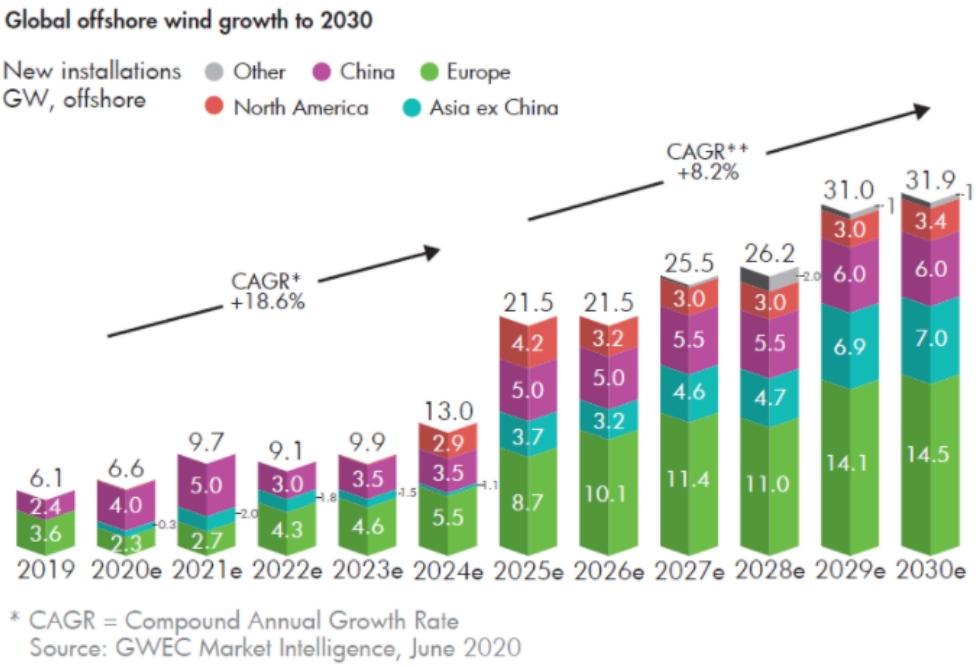

Figure 2.1: Predicted offshore wind growth to 2030 [5]

Although onshore wind currently has greater turnover than offshore wind [19], there is an increase in resistance towards use of onshore wind. There are several reasons for that, such as visual and sound pollution for the populations in which wind turbines are erected [20]. Compared to onshore wind, offshore wind has advantages such as: Stronger, and less turbulent wind at sea than at land and unlimited construction area compared to placing wind turbines on land [22].

Norway is a country which relies on the sea. Regarding energy, Norway has mostly been related to oil and gas, and water power [29]. Recently, Norway is focusing on new renewable energy sources such as wind to reduce the reliability on oil and gas [30]. A report by Multiconsult mapped the turnover of the renewable energy sources in Norway year 2019. Compared to 2018 the turnover increased by about 30 percent in 2019. The turnover from sale to clients in Norway was 25.9 billion NOK. Half of the amount was in onshore wind power. Offshore wind was the only sector which experienced growth in export in 2019 of the renewable energy sources. Hydropower is the sector which employs the most people, while offshore wind employs the second most people within the renewable energy sector (17 percent) [19]. The government and companies are investing in offshore wind power. The Hywind Tampen project by Snorre and Gullfaks platforms is the worlds first renewable power for offshore oil and gas, while it is the largest wind farm in the world [31].

Locally, the companies in Agder is investigating the advantages with floating offshore wind in the collaborative project, "Flytende Havvind". The unique gathering of companies in Agder offers great opportunity, and may generate many new workplaces[30].

As stated by Karimirad et al: for every possible site for installation of offshore wind turbines and depending to wave and wind characteristics, seabed properties and social conditions, the usage of floating wind turbines at some water depth is indicated as the most appropriate mainly due to cost related issues. The development of offshore wind turbines in deep waters requires further investigation. The issues related to design configuration of the support structure,installation, grid connection, operation and maintenance have significant effects on cost of produced electricity [26].

The costs for floating offshore wind turbines exceed their bottom-fixed counterparts, and researchers are searching for opportunities for cost reduction. Good, and feasible floating wind turbines with a cost effective design will potentially increase the use of the technology, and open for more workplaces.

3 | Theory

This chapter introduces the theories used in the software and programs used in completing the master thesis. Potential flow theory is used by both SIMA and HydroD to calculate dynamic responses of the structure. For a parked wind turbine, airfoil aerodynamics can be applied to calculate the overall wind forces on the turbine blades. When the turbine is operating, wind turbine theory, and various corrections are used in RiFlex. Also, the sea environment, forces and fundamental concepts within hydrostatics and hydrodynamics are presented.

The following assumptions are set for the theory presented in this chapter [32]:

1. The water is incompressible
2. Viscosity plays no role
3. Surface tension plays no role
4. The water surface is plane
5. The floating bodies are rigid
6. The sea bed is impermeable, therefore the velocity vertical component is zero.

3.1 Aerodynamics of wind turbine

3.1.1 Airfoil aerodynamics

In severe wind conditions , the wind turbine will stop working and the blades will be in a feathered position. In such a case, aerodynamics for an operating wind turbine is no longer appropriate. It is unreasonable to use blade element/ momentum theory. Instead, strip theory can provide a good estimation for aerodynamic loads acting on a parked wind turbine.

An airfoil element (see below) will be exposed to a flow with a certain degree of attack. The forces which will act on the blade is a lift force normal to the incoming wind direction, a drag force inclined with inflow and a pitching moment pointing from positive lift force direction to inflow direction.

Several terms are necessary to know. The dashed line is the mean camber line, the position is between the upper and lower surface of the airfoil. The black line is the chord line , and connects the leading edge in the front and trailing end. Camber is the length between the mean camber line and the chord while the thickness is the distance from the upper to the lower surface. Angle of attack is the angle between inflow direction and chord line. The span of the blade is the total length of the blade.

The lift force (La) is the force perpendicular to the wind direction , and a non dimensional lift

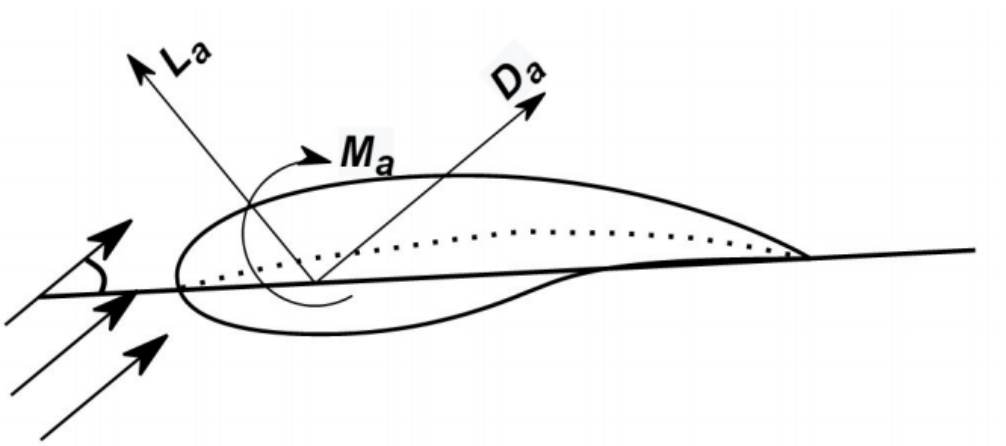

Figure 3.1: Airfoil element with loads [6]

coefficient defined as:

$$C_L = \frac{L_a}{0.5\rho_a u_i^2 A_c} \tag{3.1}$$

Drag force (Da) is a parallell to the inflow direction, and similarly, the drag coefficient can be expressed as:

$$C_D = \frac{D_a}{0.5\rho_a u_i^2 A_c} \tag{3.2}$$

Pitch moment (Ma) is positively defined pointing from lift forces to drag force and pitch moment coefficient is expressed as.

$$C_M = \frac{M_a}{0.5\rho_a u_i^2 A_c} \tag{3.3}$$

For the above equations, ρ_a is the air density , u_i represents inflow speed , A_c is the blade area and c is chord length.

Lift coefficient, drag coefficient and pitch coefficient are expressed with respect to angle of attack. When the inflow angle equals to zero, the aerodynamic forces are relatively small on the airfoil. With an increasing angle of attack, all forces will increase. Lift forces will drop after the stall angle.Drag coefficient will keep increasing with the angle of attack , as well as the speed. In general, we will arrive at a peak value around 90 degrees [33].

3.1.2 Operating wind turbine aerodynamics

The main purpose of an onshore or offshore wind turbine, is extracting kinetic energy from the wind to generate electricity.Even though the described principles and mechanisms are in general the same, a floater has larger motions compared to an onshore fixed tower due to the flexibility of the wind turbine and the combined effect of wind, wave and current. These motions can have a large impact on the aerodynamics of the rotor and the blades.

There are two general aerodynamic models for wind turbines; The Blade Element/Moment (BEM) method used together with corrections for tip loss, hub loss, dynamic stall and dynamic wake. Another way is the GDW – Generalized Dynamic Wake model which is an acceleration potential method and originally developed for helicopters.

SIMA uses the BEM for aerodynamic calculations. However, since no analysis has been conducted considering an operational wind turbine in this thesis, no further theory regarding an operational wind turbine will be presented [33].

3.2 Sea environment and relevant terms

All offshore structures are exposed to waves in one way or another. Waves can be generated in different ways, such as by wind, by a moving structure, astronomical forces or earthquakes [34].

The gravity and surface tensions works to level out the sea surface, but it also allows the waves to propagate. Waves induced by winds are very irregular, but the superposition principle is used to study the effect of a irregular wave by looking at it as a composition of many harmonic waves with different amplitudes [34].

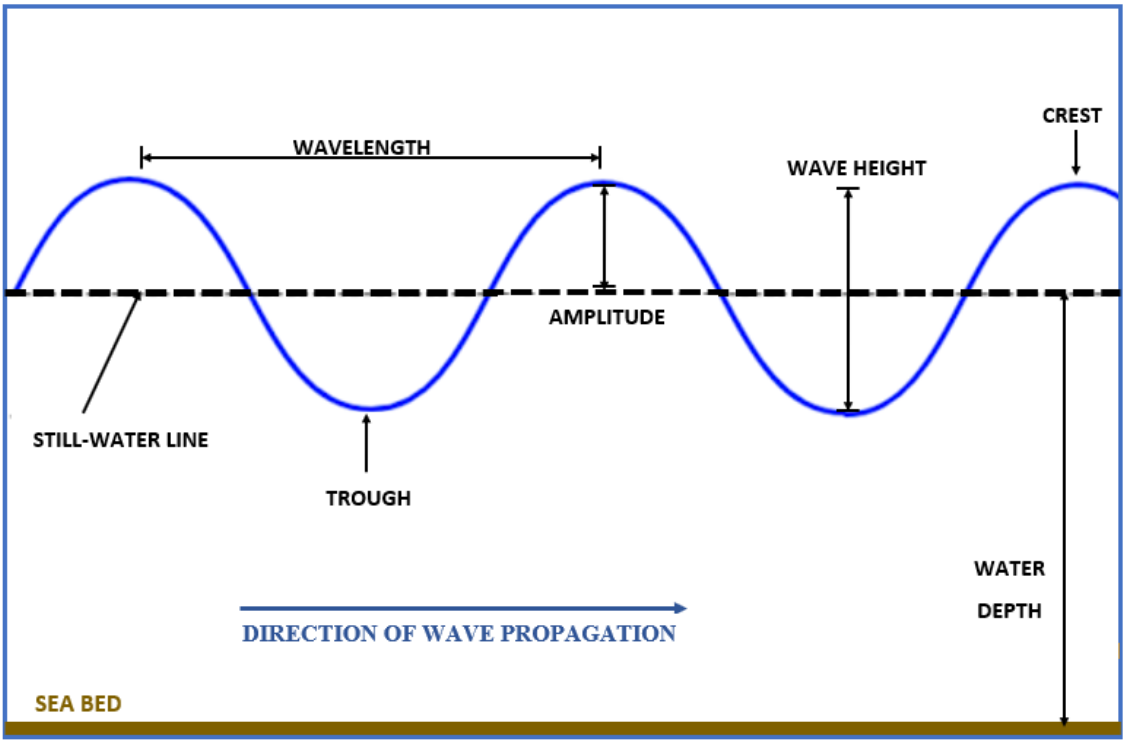

Figure 3.2: Overview of technical terms for waves [7]

3.2.1 Wave height

The wave height is the vertical distance from the wave crest to the wave through on any wave. On a sinusodial wave the wave height will be two times multiplied with the wave amplitude. The significant wave height is the average of $\frac{1}{3}$ of the waves.

3.2.2 Wave period

The wave period T is the time, usually defined in seconds, a wave uses to complete one cycle, i.e from one wave crest to another. The term is important to understand natural periods and resonance later in the theory chapter. Wave period is inversely proportional to wave frequency f.

$$T = \frac{1}{f} \tag{3.4}$$

The wave frequency f is defined as the number of waves that pass a fixed point in a given time [34].

3.2.3 Wave spectrum

Local waves, generated by wind is modelled by spectral density functions. There are several different spectral density functions, such as the Pierson-Moskowitz spectrum, the JONSWAP spectrum or the Ochi - Hubble spectrum.

The single peak spectras used to simulate North Sea environment, is the JONSWAP spectrum. In 1968 and in 1969 an extensive measurement program, called the Joint North Sea Wave Project was carried out for 100 miles into the North Sea.The spectral formulation applies for fetch-limited or coastal wind generated seas.

The Jonswap spectrum is a modified Pierson-Moskowitz spectrum. The PM spectrum is most frequenctly used for developed seas. It has been derived for wave spectral formulations.

It is given by:

$$S_{PM}(\omega) = \frac{5}{16} H_s^2 \omega_p^4 \omega \exp\left(-\frac{5}{4}(\frac{\omega}{\omega_p})^{-4} \right) \tag{3.5}$$

While the JONSWAP spectrum is given by:

$$S_j(\omega) = A_\gamma S_{PM}(\omega) \gamma e^{-0,5\left(\frac{\omega-\omega_p}{\sigma\omega_p}\right)^2} \tag{3.6}$$

Where $S_{PM}(\omega)$ is the Pierson-Moskovitz spectrum , ω is the angular frequency , H_s is the significant wave height, T_p is the spectral peak period , γ is the non dimensional peak shape parameter, σ is the spectral width parameter with $\sigma_a = 0.07$ for $\omega \leq \omega_p$ and $\omega_b = 0.09$ for $\omega > \omega_p$. Finally, A_γ is the normalizing factor [11].

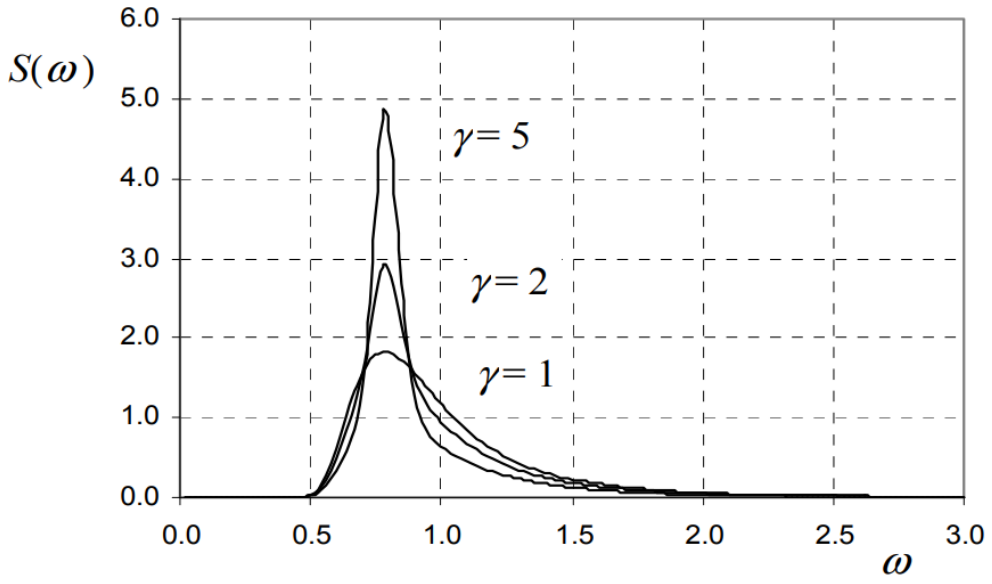

Figure 3.3: JONSWAP spectrum with variable peak shape parameter [8].

3.3 Hydrostatics of Offshore Structures

In this section the hydrostatic theory for offshore floating structures is presented.

3.3.1 Hydrostatic Stability

The notion of stability is related to the position of equilibrium. If we consider any random structure, a force or a moment exerted on it will lead to one of three possible scenarios [32]:

1. The structure will return to its initial equilibrium position, meaning that the structure is stable.
2. The structure's position will continuously change, meaning that the structure is unstable.
3. The structure remains in its changed position until a force or moment will act on it, forcing it to return to the original position or change to a different position, meaning that the structure is in neutral equilibrium.

The figure below shows several important characteristics which are necessary in describing the hydrostatic characteristics for a floating body.

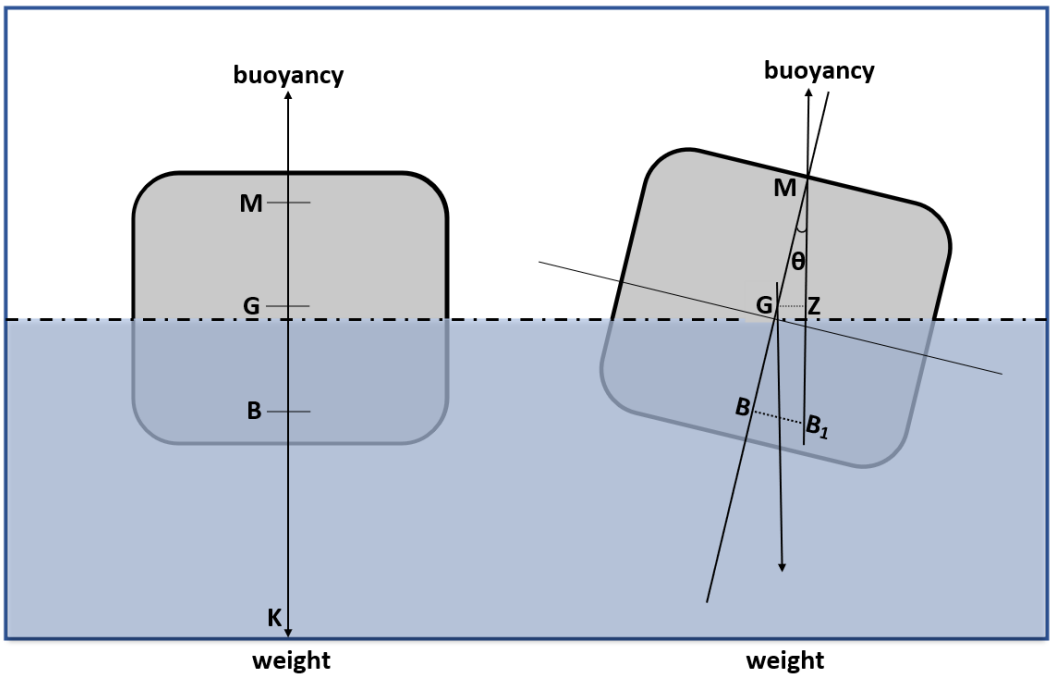

Figure 3.4: Parameters influencing the static stability of a structure [7]

The center of gravity,G, is defined as the point within the structure in which all mass may be concentrated to a force vector in the negative z-direction. The center of bouyancy, denoted by B, is the centre of volume for the submerged part of the structure, where bouyancy may be simplified to a force vector in positive z direction. The metacentre,M, is defined as the point in which a vertical line through a heeled centre of bouyancy crosses the vertical line for the original centre of buoyancy. The metacentric height, GM, is the distance between the centre of gravity and the metacentre. A larger metacentric height will give a higher righting moment in a heeled state. Rightning moment refers to the rightning arm between G and B1. If this is poorly designed, the structure will capsize [32].

3.3.2 Archimedes principle

Archimedes principle states that a body lowered in fluid will be subjected to an upward force equal to the weight of the fluid displaced. Archimedes principle can be derived from Pascal's principle.

For a floating structure the following two rules are of importance:

1. Archimedes principle: Sum of all forces needs to be zero.
2. Stewin's law: Sum of all moments need to be zero

For a floating body, two forces will always act: The buoyancy force acting upwards and the gravity force acting downwards.If these forces are aligned in x and y direction the moments will be zero.

We therefore have the following formula:

$$\rho g \nabla - gm = 0 \tag{3.7}$$

Where ρ is the density of water , g is the gravity acceleration and ∇ is the displaced volume of the structure. The right side is the bouyancy force, while the left side represents gravity force.

$$\rho g \nabla = gm \tag{3.8}$$

If a structure is floating freely, then the horizontal, vertical and rotational equilibrium has been achieved. Horizontal equilibrium is not relevant until the mooring system is designed. Rotational equilibrium is achieved when the center of buoyancy and center of gravity are located on the same vertical line.

The centre of bouyancy is dependent of the submerged part of the structure . The center of bouyancy only changes when draft,trim or heel occurs. Under the influence of a light heeling, the vertical line will intersect with the center line of a structure in a point. The distance between the center of gravity and the metacentre indicated by a point M, the metacentre. The higher GM value is , the better is the initial stability of the structure.

The center of gravity and the center of buoyancy will not always remain on the same vertical line. The new center of buoyancy which we get when the structure heels, will result in a new vertical line. The distance, GZ, is the horizontal distance between these two lines. The greater the rightning arm is , the better is the structure's ability for stabilization [32].

3.3.3 GZ-curve

For a floating body which experiences a heel with an angle ϕ the stability moment can be calculated in the following way as presented below:

$$M_s = \rho g \nabla \overline{GZ} \tag{3.9}$$

$$M_s = \rho g \nabla \overline{GN_\phi} sin\phi \tag{3.10}$$

$$\rho g \nabla (\overline{GM} + \overline{MN_\phi}) sin\phi \tag{3.11}$$

Which leads to the $\overline{GZ}$ being equal to:

$$\overline{GZ} = \overline{GN_\phi} sin\phi = (\overline{GM} + \overline{MN_\phi}) sin\phi \tag{3.12}$$

$\overline{GZ}$ is a good indication of the stability of the structure.

The GZ curve has several important characteristics useful in evaluation of the stability of a structure;

1. The slope at the origin
2. Range of stability
3. The maximum GZ value
4. Angle of deck immersion
5. Area under the stability curve

The **slope at the origin** or **tangent to the GZ curve** represents the metacentric height GM.The **range of stability** is the range which the GZ curve has positive values. The negative values for the GZ curve represents areas where the structure loses stability. If the angle has positive GZ value, than the structure will return to its original state when moment is removed. For **maximum GZ value** is the largest heeling moment the structure can resist. **Angle of deck immersion** is represented on the GZ curve as an inflection point. **Area under the stability curve** up to a certain angle represents the amount of energy in which the structure can absorb from wind, or other external effects [32].

3.4 Linear Wave theory

Linear wave theory, also known as airy wave theory, describes propagation of waves on the surface of a fluid. Velocity potentials are used in the description of the theory, which are a result of a derivation of a potential function.

The velocity potential is given by the following formula:

$$\Phi_\omega(x, z, t) = P(z) * sin(kt - \omega t) \tag{3.13}$$

Several requirements need to be fulfilled, such as:

1. Laplace equation
2. Boundary condition for sea bed
3. Free surface dynamic condition
4. Free surface kinematic boundary condition

The velocity potential for each direction in the x,y,z axis are given by the following formulas:

$$v_x = \frac{\delta \Phi_\omega}{\delta x} \tag{3.14}$$

$$v_y = \frac{\delta \Phi_\omega}{\delta y} \tag{3.15}$$

$$v_y = \frac{\delta \Phi_\omega}{\delta z} \tag{3.16}$$

The continuity formula is given by the equation:

$$\frac{\delta^2 \phi_\omega}{\delta x^2} + \frac{\delta^2 \phi_\omega}{\delta z^2} = 0 \tag{3.17}$$

The continuity equation in combination with Laplace equation results in:

$$\nabla^2 \Phi_\omega = \frac{\delta^2 \Phi_\omega}{\delta x^2} + \frac{\delta^2 \Phi_\omega}{\delta y^2} + \frac{\delta^2 \Phi_\omega}{\delta^2 z} = 0 \tag{3.18}$$

Since we assume that the particles on a fluid surface only moves in the **x-z** plane then v_y will equal zero and therefore $\frac{\delta^2 \Phi_\omega}{\delta y^2} = 0$.

Boundary condition for the seabead states that the seadbed is assumed impermeable and that the vertical flow velocities of the particles at the seabead are zero.

$$\delta \frac{\Phi_\omega}{\delta z} = 0 \text{ for } z = -h \tag{3.19}$$

The free surface dynamic boundary condition states that a pressure p at the surface equals the atmospheric pressure. Bernoulli equation can be simplified to the formula below if free surface dynamic boundary condition is considered. For $z = \zeta$ the equation will be zero.

$$\frac{\delta \Phi_\omega}{\delta t} + \frac{p}{\rho} + gz = C \tag{3.20}$$

The final condition, which is the free surface kinematic boundary condition states that the particles vertical velocity will equal the vertical velocity of that fluid surface is considered.

$$\frac{\delta \Phi_\omega}{\delta z} = \frac{\delta \zeta}{\delta t} \tag{3.21}$$

This results in the Cauchy-Poisson condition given by the following formula for z=0.

$$\frac{\delta z}{\delta t} + \frac{1}{g}\frac{\delta^2 \Phi_\omega}{\delta t^2} = 0 \tag{3.22}$$

The boundary conditions explained above are used in the boundary element method for calculating hydrostatic and hydrodynamic issues [32].

3.5 Hydrodynamic Loads

In general, the forces in which a floating body is exposed to can be divided into two sections:

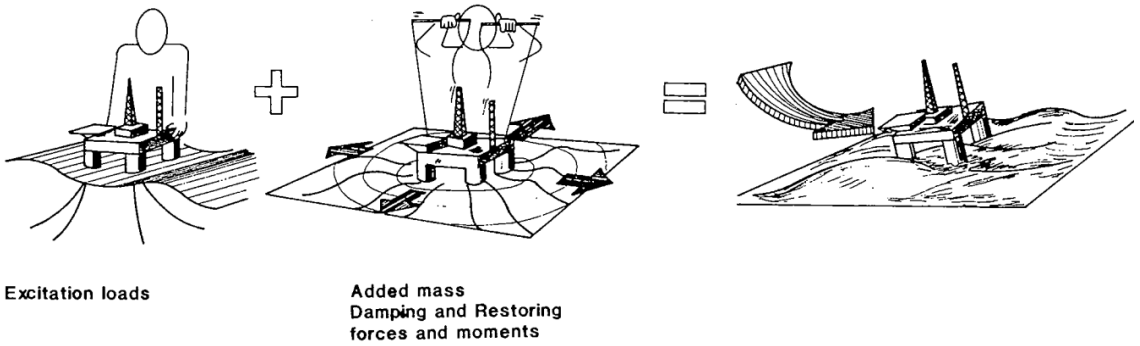

Figure 3.5: Superposition of forces on a floating offshore structure [9].

1. Forces on a structure exposed to regular waves while being restrained. These forces are named Froude-Krylov forces and diffraction forces and moments.
2. Forces on a structure in still water which is forced to oscillate. These forces are added mass, damping and restoring forces.

For cases where *Linear Wave Theory* applies, the superposition principle is valid for obtaining the total hydrodynamic forces on a structure.

3.5.1 Radiation and Diffraction

When multiply forces is acting on a body, the resulting force can be obtained using the superposition principle. A structure is affected by passing waves and waves generated by the structure itself when it oscillates. Radiation is related to the concepts added mass, damping and restoring loads. If we imagine that the structure is forced to oscillate in still water, the radiating waves represents the energy taken out of the system. The diffraction loads are from the passing waves affecting the structure given that the structure is fixed.

3.5.2 Added mass and radiation damping

Added mass and damping is a result of a forced harmonic rigid body motion. The motion will cause outgoing waves from the structure which results in pressure on the surface from the fluid where the particles oscillate with different amplitudes. These forces and moments are calculated by integrating over the defined surface. The pressure can be obtained from the velocity potential and from the boundary method, a numerical calculation method often used for offshore structures.

Linear theory can describe wave induced motions and loads on semi-submersibles. The non-linear effects are vital when studying severe sea states and for investigating the horizontal motions of a moored structures. If we consider regular waves with an amplitude far from breaking, linear theory will result in that the wave induced motions and load amplitudes are linearly proportional to the wave amplitude. Therefore, to obtain the results for irregular waves, we use the superposition principle as represented by the figure above [9].

3.6 Motions and responses of floating structures

Below the relevant theory regarding the motions and responses of a floating offshore structure is presented. The DOF's for a floating structure,equation of motions and the natural periods are presented.

3.6.1 6 DOF of a floating structure

For a offshore structure, there are six different motions. Semi-submersible structures have the least vertical motions of the different structures, and therefore has large workability. The degrees of freedom for a floating structure are the three rotational; pitch, yaw and roll and the three translatory; heave, surge and sway [35].

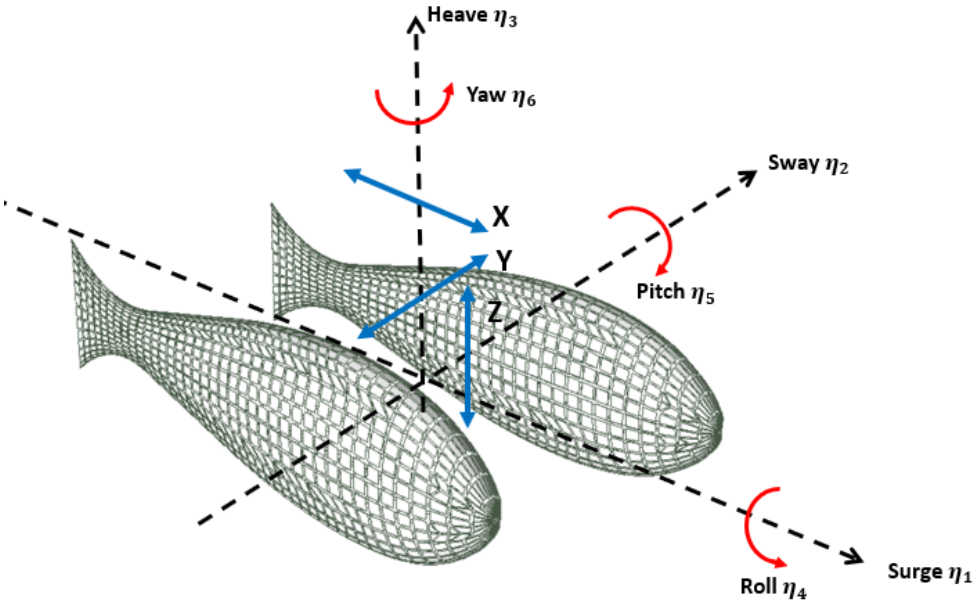

Figure 3.6: The six DOF's shown on the twin fish floater [7]

Table 3.1: Degrees of freedom with definition

Degree of freedom	Definition
Surge	Translation along longitudinal axis, x-axis.
Sway	Translation along lateral axis, y-axis.
Heave	Translation along the vertical axis, z-axis.
Roll	Rotation along longitudinal axis, x-axis.
Pitch	Rotation along lateral axis, y-axis.
Yaw	Rotation along vertical acis, z-axis.

3.6.2 Equation of motion

An equation of motion describes the motion of an object in relation to time. The foundation for the equation of motion is Newton's second law.

The simplified form of the equation is the following for frequency domain analysis:

$$(M + A)\ddot{x} + B\dot{x} + Cx = F_{exc} \tag{3.23}$$

M represents the mass of the structure, A equalts the added mass of the structure, B is the damping, while C represents the hydrostatic restoring force.

If a structure has 6 DOFs the equation can be reformulated to the following:

$$\sum_{k=1}^{6}[M_{jk} + A_{jk})\ddot{\eta}_k + B_{jk}\dot{\eta} + C_{jk}\eta_k] = F_j e^{-i\omega_e t} \tag{3.24}$$

For values of j = 1,2..5,6 [9].

3.6.3 Natural periods

Natural periods of a system with more than one DOF can be found by first estimating an answer for the second order differential equation, which is a variant of Newtons' second law for a spring term.

$$M\ddot{x} + Kx = 0 \tag{3.25}$$

Here, we can guess:

$$x = \Phi cos(\omega t + \phi) \tag{3.26}$$

Where Φ is the eigenvectors, ω is the angular frequency, t is the time and ϕ is the phase of the oscillation.

Through double differentiation of equation above and insertion of the guessed solution x from Eq.3.26 an equation for natural periods emerge:

$$(K - \omega^2 M)\phi = 0 \tag{3.27}$$

K represents the stiffness matrix.

To solve this equation for the system when it is in motion the solution is when $K - \omega^2 M) = 0$. That means that the matrix is singular and the solution can be written as [9]:

$$det|K - \omega^2 M| = 0 \tag{3.28}$$

3.6.4 Response amplitude operators

Response amplitude operators are functions showing the effect of the sea on the floating structure. Displacement RAOs define the response of the structure, for one particular degree of freedom, to a period and wave direction.

For regular wave conditions the response amplitude operator, RAO, can be calculated by dividing the response amplitude by the excitation amplitude of the structure.

$$(M + A)\ddot{x} + B\dot{x} + Cx = F_{exc} \tag{3.29}$$

With $x = ae^{iwt}$ and $F_{exc} = F_0\zeta_a e^{iwt}$

Where a is the distance the floater has moved and ζ_a is the wave amplitude. The figure shows an example for surge.

Inserting for F_{exc}, x and its derivatives give:

$$(M + A)(-\omega^2 ae^{iwt}) + B(i\omega ae^{i\omega t}) + C(ae^{i\omega t}) = F_0\zeta_a e^{iwt} \tag{3.30}$$

Since the RAO is the motion divided by amplitude this will give [9]:

$$RAO = \frac{a}{\zeta_a} = \frac{F_0}{-\omega^2(M + A) + iwB + C} \tag{3.31}$$

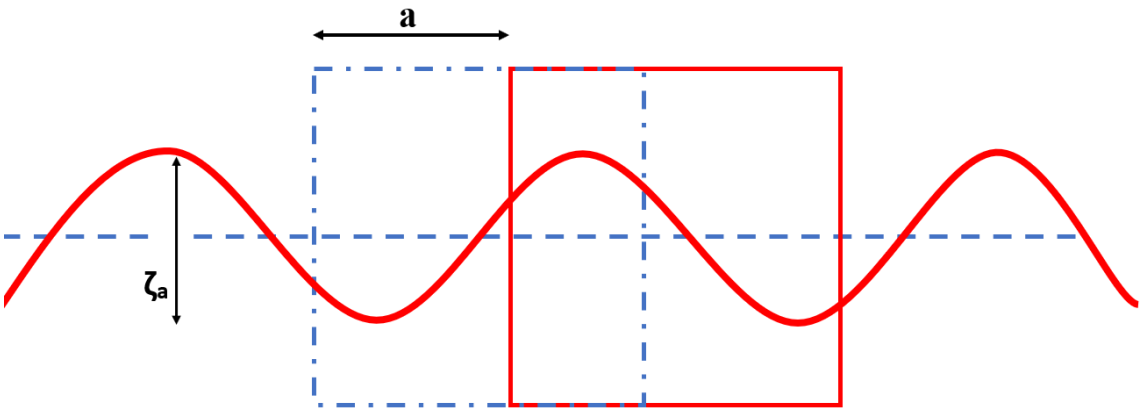

Figure 3.7: RAO shown for a arbitrary figure [modified after [10]

3.7 Coupled analysis of floating wind turbine system

In this section the theory behind a coupled analysis is presented as well as relevant formulas. The relevant standards and documents are explained briefly.

3.7.1 Coupled analysis

DNV GL had a joint industry project on coupled analysis of floating wind turbines. The aim was to develop a recommended practise for floating offshore wind turbines to aid the industry to meet the FOWT design requirements . Serve as a reference document between project stakeholders, to agree and align the methods for the design and analysis of FOWTs, and serve as a guideline for designers, suppliers, purchases and regulators [36].

The document covers general design requirements, environmental conditions, numerical modeling, scale-model testing and validation, FOWT controllers, and load case set-up and data analysis. It is stated that the practice has several gaps, but that it should be read in combination with other standards.

In general, a site-specific load analysis based on the design basis shall be performed, where aero-elastic and hydrodynamic effects. The analysis can be performed for one or a few locations. Wind loading is also essential for prediction of global motion response of floaters. Accurate modelling of wind effects is of importance. For some floating systems, and load cases, the wind loads can be the dominating excitation.

It is evident that the coupling effect between the force on the wind turbine and the motion of a floater is important to consider, and this applies to all concepts. For a FOWT, there is a strong coupling effect between the floater motions and the turbine forces. The occuring coupling can be explained as by that the motion of the floater will influence the aerodynamic inflow conditions to the turbine and will introduce inertial loads on the wind turbine.

The forces on the turbine will influence the motions of the floater mainly through hydrodynamic excitation and damping forces. The natural periods of the floater motion may be altered by the wind turbine.Aerodynamics of the wind turbine can contribute to the floater stability with either a positive or negative damping, but the influence depends on external conditions and the control system.

For some installation types a coupling may occur between the station keeping system and the floater: Wind and wave frequency motions of the floater will influence the forces in the mooring system. Also, the motions of the station keeping system will excert forces on the floater, generally as restoring forces, damping and excitation forces. Careful considerations need to be taken to variations and environmental input parameters, suitable adjustment of calculation parameters for the specified FOWTs [36] [37].

3.7.2 Equation of motion in time domain

From potential flow theory, the equation of motion for the time domain can be written in the following way

$$(M + A)\ddot{x} + B\dot{x} + Cx = F_{exc} \tag{3.32}$$

The frequently used method for solving the equation is the convolution integral. If considering the

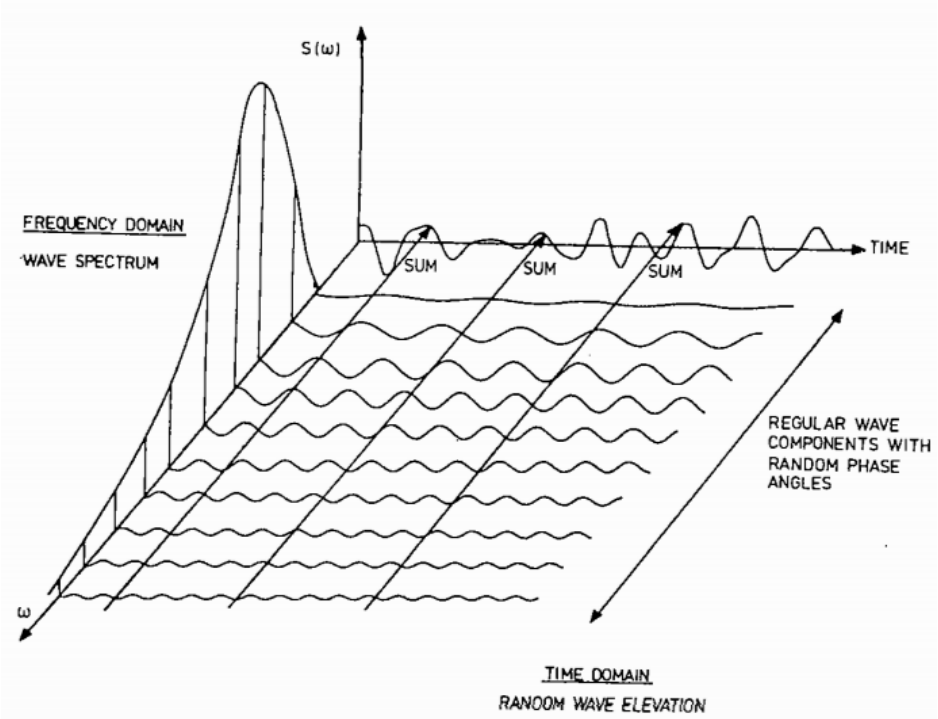

Figure 3.8: Principle of wave loads in frequency domain and time domain analysis [9].

radiation part of the problem (only the frequency dependent coefficients):

$$\mathbf{RF}(t) = A(\omega)\ddot{x} + B(\omega)\dot{x} \tag{3.33}$$

Assuming that the right term varies sinusodially at one frequency only, equation can be written to the frequency domain in the following way:

$$\mathbf{RF}(\omega) = (-\omega^2 A(\omega) + i\omega B(\omega))\eta_a(\omega) \tag{3.34}$$

We can use the following relations to rewrite the equation:

$$A(\omega) = A_\infty + a(\omega), A_\infty = A(\omega = \infty) \tag{3.35}$$

$$B(\omega) = B_\infty + b(\omega), B_\infty = B(\omega = \infty) = 0 \tag{3.36}$$

The equation can therefore be rewritten into:

$$RF(\omega) = -\omega^2 A_\infty \eta_a(\omega) + (i\omega a(\omega) + b(\omega))i\omega\eta_a(\omega) \tag{3.37}$$

Applying inverste Fourier transformation results in the following equation:

$$RF(t) = A_\infty \ddot{x}(t) + \int_{-\infty}^{\infty} h(t-\tau)\dot{x}(\tau)d\tau \tag{3.38}$$

Physically, $(h-\tau)=0$ for $t<0$. And causality imply that $h(t-\tau=0$ for $\tau>t$. The equation 3.38 can therefore be rewritten to the following:

$$RF(t) = A_\infty \ddot{x}(t) + \int_0^t h(t-\tau)\dot{x}\tau d\tau \tag{3.39}$$

Substituting equation into equation ,the equation of motion for time domain will be the following:

$$(M + A_\infty)\ddot{x} + Cx + \int_0^t h(t-\tau)\dot{x}(\tau)d\tau = F \tag{3.40}$$

where the retardation function $h(\tau)$ is calculated through a transformation of the frequency dependent added mass and potential damping

$$h(\tau) = \frac{1}{2\pi}\int_{-\infty}^{\infty}(b(\omega) + i\omega a(\omega))e^{i\omega t}d\omega \tag{3.41}$$

Using that the $b(\omega) = b(-\omega)$ and $a(\omega) = a(-\omega)$

$$h(\tau) = \frac{1}{\pi}\int_0^{\infty}(b(\omega)cos(\omega\tau) - \omega a(\omega)sin(\omega\tau))d\omega \tag{3.42}$$

From the causality $h(\tau) = 0$ for $\tau < 0$; The process can not have any memory effect of the future. This suggests that the two parts of the integral must be opposite for $\tau < 0$ and identical for $\tau > 0$, or mathematically:

$$h(\tau) = \frac{2}{\pi}\int_0^{\infty} b(\omega)cos(\omega\tau)d\omega = -\frac{2}{\pi}\int_0^{\infty}\omega a(\omega)sin(\omega\tau)d\omega \tag{3.43}$$

Basen on the function given above , the retardation function can be found either using frequency dependent potential damping coefficients or added mass coefficients [38].

3.7.3 Solution Technique

The force vector F, from the equation .... can be found in the following way:

$$F = F^1 + F^2 + F_{drag} + F_{mooring} + F_{wind} \tag{3.44}$$

Using the panel method in HydroD, the first order wave excitation loads can be found. HydroD solves the potential flow problem using WADAM solver. To find the second order wave loads F^2 can also be obtained in HydroD by solving the quadratic transfer functions with a free surface model. These wave loads are transformed into first order and second order transfer functions in SIMO by importing the results. The forces from the mooring line are calculated by Riflex, and added to the right side of the equation of motion at each time step.

The solution of equation of motion in time domain is based on an incremental process using the dynamic time integration scheme according to Newmark β family methods. The Newton-Raphson iteration is used to assure equilibrium between the internal and external forces [38].

3.8 Mooring system and stationkeeping

In the section below the theory behind keeping an offshore structure at place and calculations for catenary mooring system will be presented.

3.8.1 Mooring system

A floating offshore structure is kept at place, against wind, waves and current forces by using mooring systems and thrusters [9]. We divide the different systems which keep a structure at place, we mainly divide them into three: Active system, Passive system or a combined system. The passive system refers to implementation of a mooring system. Active system uses thrusters to keep the structure at place, while a combined system uses both thrusters and mooring system for keeping the structure at place. For a floating offshore wind turbine, only mooring systems are used to keep the structure at place [11].

A mooring system consists of a number of lines or cables which are attached to the structure at different points. The low ends are anchored to the sea bed. For mooring lines, either chain, rope or a combination of both can be implemented.

Inspired by offshore oil structures, a spread mooring system is often used for semi-submersible wind turbine systems. The mooring system consists of pre-tensioned anchor lines that are arranged around the structure to hold it in the desired place. A spread mooring system will give a offshore structure a fixed heading, forcing the structure to take up great forces. Spread mooring systems are used in applications requiring long service life, in any water depth and for any size of a vessel.

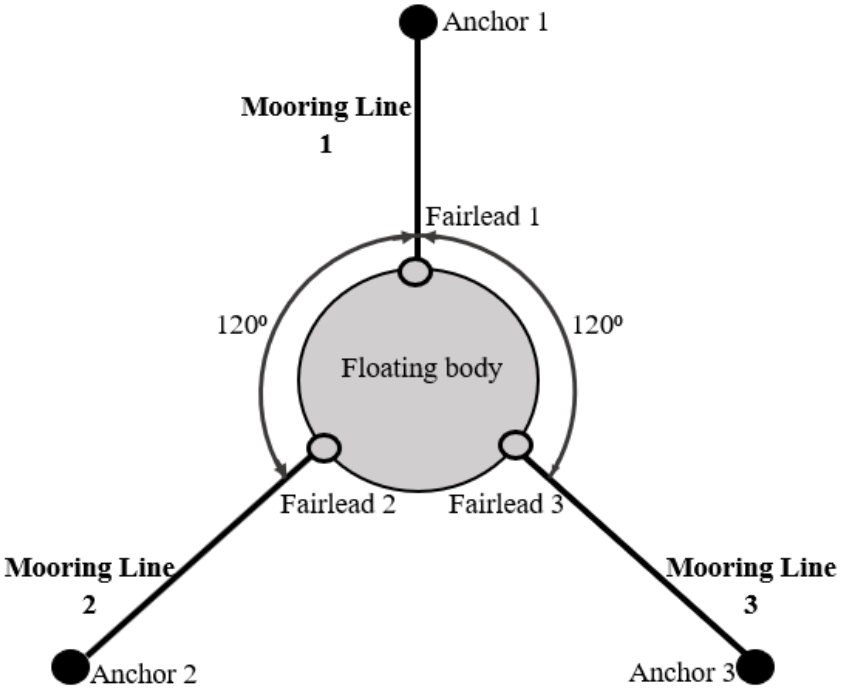

Figure 3.9: Illustration for a spread mooring system on a spar floater [7]

A vessel which is single point moored can rotate freely with the environment, obtaining minimum mooring loads. The lines can be made up of chain or rope. Usually a combination of different elements are used to achieve heavy lines at the bottom and light line at water level. This is done to achieve great stiffness as well as light lines.

Initial tension or pre-tension of the mooring lines are achieved by winches installed on the offshore vessel. The mooring cables have an effective stiffness composed of both the elastic and geometric stiffness.

In the design of a mooring system, the joint probability of extreme environmental conditions is used as a basis for designing mooring system. Determining the long term statistics, the data of the extreme condition on waves, wind and current the joint probabilities have to be considered.Both the values of the extreme weather components and directions need to be determined. In the DNV document it is stated that the most unfavourable load combination will be used as design criteria of the mooring system.

A mooring element can have one of the following shapes presented [11]:

1. Taut mooring line
2. Catenary mooring line
3. Mooring line with a clump weight
4. Mooring line with a spring buoy

As stated before, for semi-submersible structures catenary mooring lines are used to keep the structure at place. The figure below shows the most common different mooring lines today.

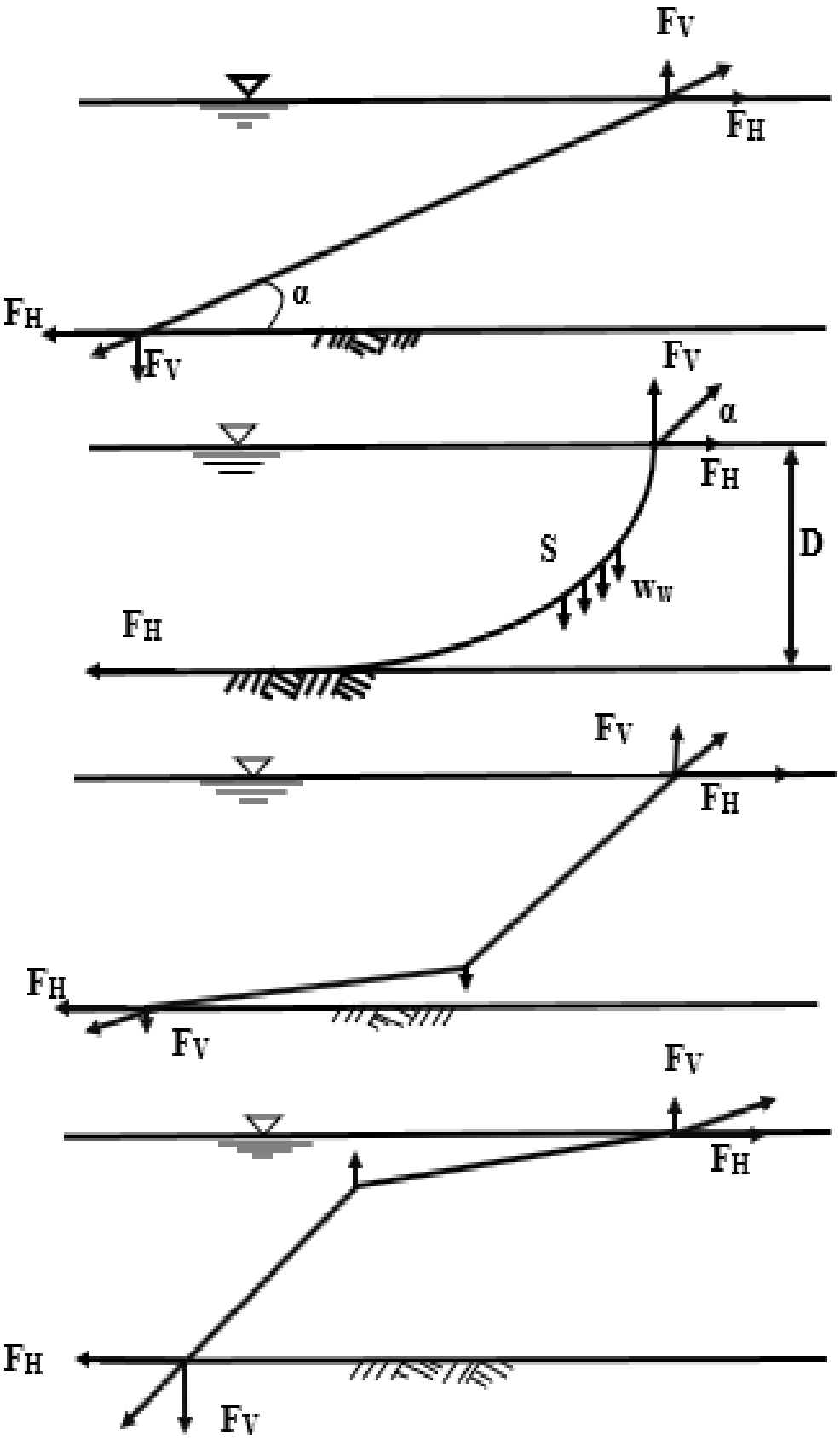

Figure 3.10: Different principles of catenary mooring lines [7] based on [11]

3.8.2 Catenary mooring line

In this section the explanation provided by OM. Faltinsen in Sea Loads on Ships and Offshore structures. The general formulas and derivation for the catenary mooring lines:

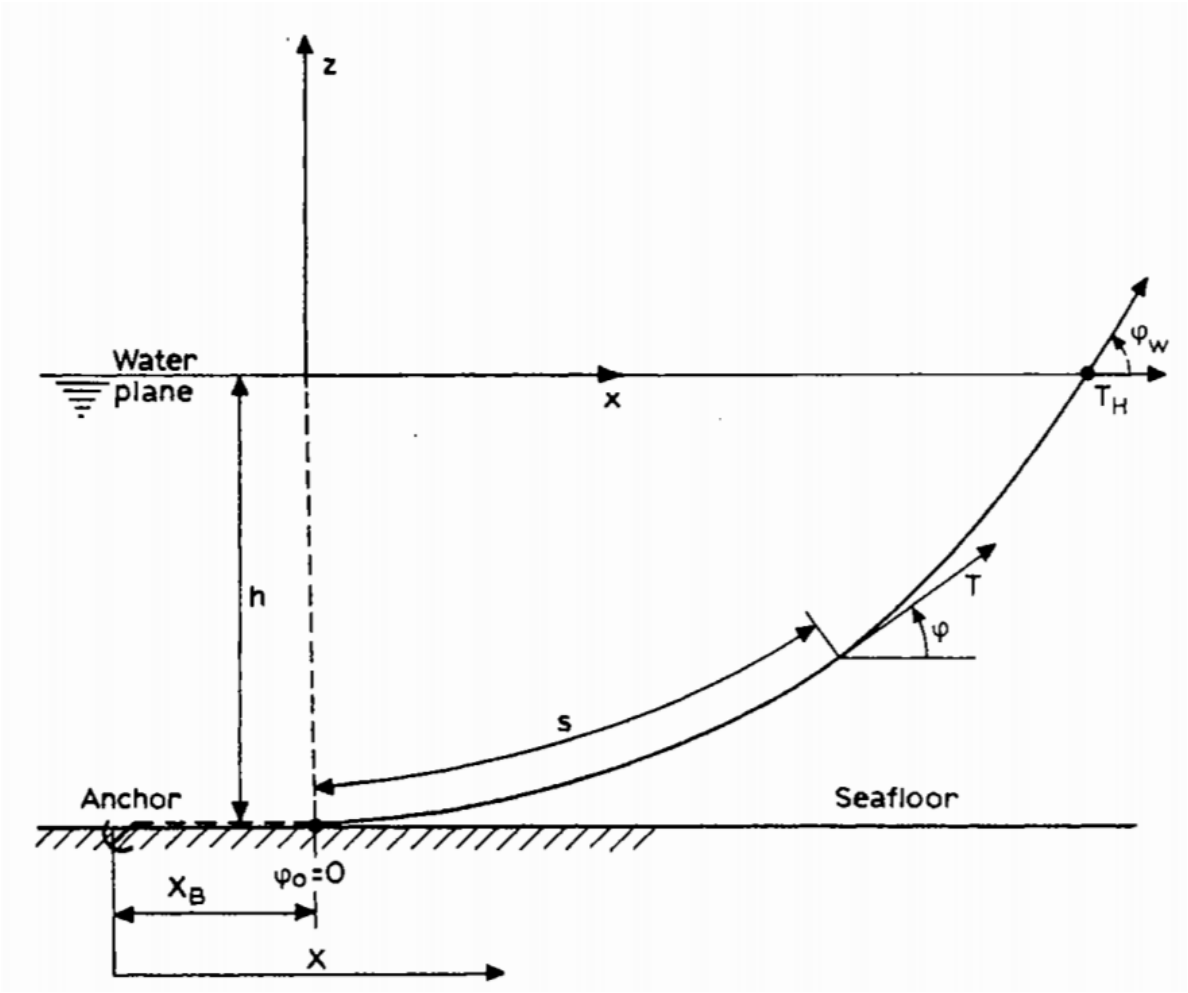

Figure 3.11: General illustration of cable line with symbols [9]

We assume that the structure is moored at calm sea, and that the coordinate system is set as defined in the figure: The vertical axis, z-axis is positive upwards while the horizontal axis is the x - axis.

The mooring line is curved, with the anchor attached to the sea bed.

For chains, the bending stiffness is neglected. The elasticity of the mooring line is usually neglected, but is accounted for in extreme conditions. Figure 3.12 presents an example of a mooring line element and forces which are excerted on it.

F and D are the mean hydrodynamic forces per unit length, in normal and tangential direction. ω is the weight per unit length of line in water. A is the cross sectional area of the cable line. E is the elastic modulus, while T is the line tension.

Correction forces are implemented for ω; $-\rho g A_z$ and $-\rho g A_z - \rho A dz$ at the ends of the element;

$$dT - \rho g A dz = [\omega sin\phi - F\frac{1+T}{AE}]ds \tag{3.45}$$

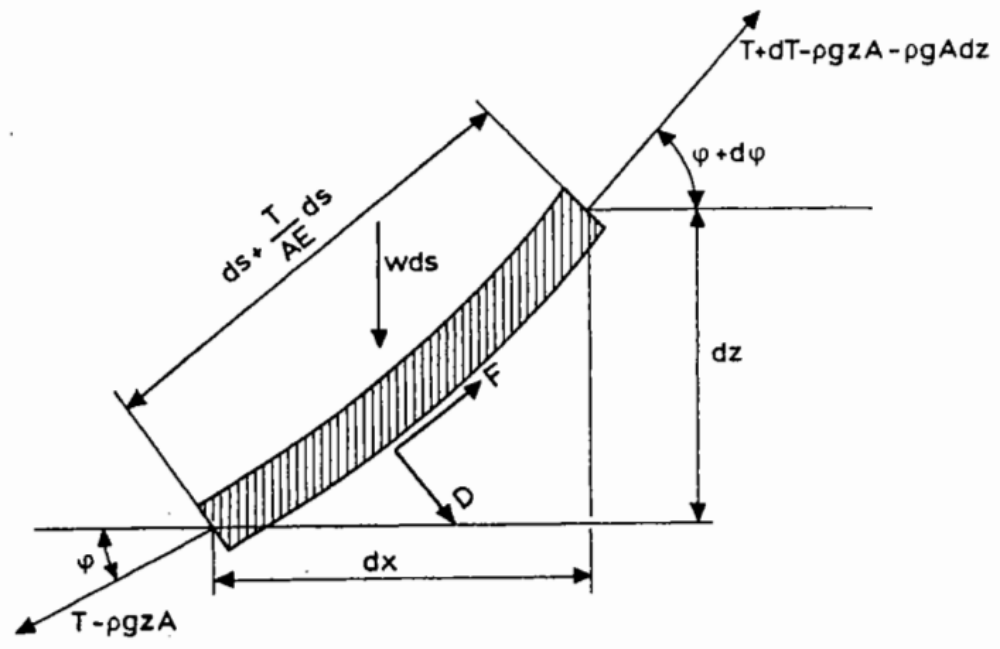

Figure 3.12: Illustration for an element of a mooring line [9]

$$Td\phi - \rho g A_z d\phi = [\omega cos\phi + D\frac{1+T}{AE}]ds \tag{3.46}$$

For non-linear equations we neglect F and D and assume that the line is inelastic and has a constant weight distribution.

$$T' = T - \rho g z A \tag{3.47}$$

$$dT' = \omega sin\phi ds \tag{3.48}$$

$$T'd\phi = \omega cos\phi ds \tag{3.49}$$

$$dT' = \omega sin\phi ds \tag{3.50}$$

$$T'd\phi = \omega cos\phi ds \tag{3.51}$$

When dividing the two equations:

$$\frac{dT'}{T'} = \frac{sin\phi}{cos\phi}d\phi \text{ in other words } T' = T'_0\frac{cos\phi_0}{cos\phi} \tag{3.52}$$

By integrating the following is achieved:

$$T'd\phi = \omega cos\phi ds \tag{3.53}$$

$$s - s_0 = \frac{1}{\omega}\int_{\phi_0}^{\phi} \frac{T_0'}{cos\theta}\frac{cos\phi_0}{cos\theta}d\theta = \frac{T_0' cos\phi_0}{\omega}[tan\phi - tan\phi_0] \tag{3.54}$$

since $dx = cos\phi ds$

$$x - x_0 = \frac{1}{\omega}\int_{\phi_0}^{\phi} \frac{cos\phi_0}{cos\theta}d\theta = \frac{T_0' cos\phi_0}{\omega}(log\frac{1}{cos\phi} + tan\phi) - log(\frac{1}{cos\phi_0} + tan\phi_0)) \tag{3.55}$$

$dz = sin\phi ds$ we find that:

$$z - z_0 = \frac{1}{\omega}\int_{\phi_0}^{\phi} T_0' \frac{cos\phi_0 sin\theta}{cos^2\theta}d\theta \tag{3.56}$$

$$z - z_0 = \frac{T_0' cos\phi}{\omega}[\frac{1}{cos\phi}] - \frac{1}{cos\phi_0} \tag{3.57}$$

ϕ_0 is the point of contact between cable line and sea bed.

$\phi_0 = 0$ so we get that:

$$T_0' = T' cos\phi \tag{3.58}$$

$$T_H = T cos\phi_w \tag{3.59}$$

We find that $T_0' = T_H$

The coordinate system selected $x_0 = 0$ and $z_0 = -h$ for $s_0 = 0$.

$$\frac{x\omega}{T_H} = log\frac{1 + sin\phi}{cos\phi} \tag{3.60}$$

$$sinh\frac{\omega x}{T_H} = \frac{1}{2}(\frac{1 + sin\phi}{cos\phi} - \frac{cos\phi}{1 + sin\phi}) = tan\phi \tag{3.61}$$

$$cosh(\frac{\omega x}{T_H}) = \frac{1}{2}(\frac{1 + sin\phi}{cos\phi} + \frac{cos\phi}{1 + sin\phi} = \frac{1}{cos\phi} \tag{3.62}$$

$$\frac{T_H}{\omega} sinh(\frac{\omega}{T_H}x) \tag{3.63}$$

$$z + h = \frac{T_H}{\omega}[cosh(\frac{\omega}{T_H}x) - 1] \tag{3.64}$$

Line tension is found by combining several equations.

$$T - \rho g z A0\frac{T_H}{cos\phi} = T_H + \omega(z + h) \tag{3.65}$$

$$T = T_H + \omega h + (\omega + \rho g A)z \tag{3.66}$$

The vertical component T_z is found through the formula below:

$$dT'_z = d(T'sin\phi) = dT'sin\phi + T'cos\phi d\phi \tag{3.67}$$

$$\omega sin^2\phi ds + \omega cos^2\phi ds \tag{3.68}$$

That gives $T'_z = \omega s$ or $T_z = \omega s$

For finding the minimum length L_{min} of the chain if gravity anchors are used; A gravity anchor cannot be exposed to vertical forces from the anchor lines. If we consider intact mooring system and a broken line situation:

Forces for a movable anchor, and how the forces can be moved to a platform. Movable anchors can only take up a little of the vertical forces before the holding forces are reduced drastically. Vi therefore have to limit the calculations to the cases where the chain is horizontal with the anchor.

Current and waves will give hydrodynamic forces on the anchor chain (anchor line). If the hydrodynamic forces are neglected, then it is assumed that the anchor line is in a vertical plane going through the tangation point at the bottom and the fastening of the platform. Moments caused by the stiffness of the anchor line , for a chain this is a valid assumption, and for a wire the bending is large and therefore this can be accepted.

To find the minimum length of the cable lines we will have to use the following equations:

$$l_s = asinh(\frac{x}{a}) \tag{3.69}$$

$$h = a[cosh(\frac{x}{a}) - 1] \tag{3.70}$$

$$a = \frac{T_H}{\omega} \tag{3.71}$$

by combining the equations given above, we see that:

$$l_s^2 = h^2 + 2ha \tag{3.72}$$

Hence, the maximum tension in the cable can be written as:

$$T_max = T_H + wh \tag{3.73}$$

The necessary minimum cable length is therefore determined by the following formula:

$$l_min = h(2\frac{T_max}{wh} - 1)^{\frac{1}{2}} \tag{3.74}$$

The horizontal distance between the anchor and the fairlead position X is:

$$X = l - l_s + x \tag{3.75}$$

The relation between X and T_H is:

$$X = l - h\sqrt{1 + 2\frac{\omega}{hT_H}} + \frac{T_H}{\omega} cosh^{-1}(1 + \frac{h\omega}{T_H}) \tag{3.76}$$

When the chain is elastic, extensional stiffness EA needs to be taken into consideration. In this case, the horizontal stiffness could be expressed using the following formula:

$$T_H = \frac{T_z^2 - (\frac{\omega^2 l_s^2}{2AE})^2}{2(\omega h - \frac{\omega^2 l_s^2}{2AE})}) \tag{3.77}$$

Horizontal distance of the floating part of the elastic cable is given by the following:

$$x = \frac{T_H}{\omega} log(\frac{\sqrt{T_H^2 + T_z^2} + T_z}{T_H \omega}) + \frac{T_H}{AE} l_s \tag{3.78}$$

3.9 Contour Line Method

Design of offshore structures requires reliable calculations for loads and responses corresponding to an exceedance probability. All sources of inherent randomness needs to be accounted for. For linear problems this can be easily solved, but for non-linear issues this may be a complex and time consuming issue. Environmental contour lines are used for obtaining proper estimates of long term extremes utilizing a short term analysis. The long term joint distribution of mean wind speed at 10 meter height (U_w), the significant wave height H_s and the spectral peak period(T_p) and the sites shown in the article are acquired by fitting 10 years environmental hindcast data by using the procedure described by Johanessen et al in a separate paper. The 50-year contour surfaces at five different sites are presented for extreme response analysis

The article by Luan presents load effects corresponding to 50 year wind and wave conditions, with the necessary theoretical background [39].

When wind and wave power are estimated separately, the marginal distributions for both are given. Extreme conditions with combinations of U_w , H_s and T_p can be selected along the contour surface. Long term distributions of wind and wave directions are not considered in the article. It is assumed that the wind and wave are collinear and always have the same direction.

Marginal distribution of mean wind speed U_w The results indicate that 1-hour mean wind speed at 10m height (U_w) follows a two-parameter Weibull distributions. The probability density function is given by the following:

$$f_{U_w}(u) = \frac{\alpha_u}{\beta_u}\Big(\frac{u}{\beta_u}\Big)^{\alpha_u - 1} exp\Big[-\Big(\frac{u}{\beta_u}\Big)^{\alpha_u}\Big] \tag{3.79}$$

α_u and β_u denote the shape and scale parameters. f() refers to the probability density.

For the joint distribution of H_s and T_p - If only wave data is to be considered a joint PDF of H_s and T_p can be established:

$$f_{H_s,T_p}(h,t) = f_{H_s}(h) f_{T_p|H_s}(t|h) \tag{3.80}$$

The Lonowe model is used, which is a cross between Weibull and Log model.

For values where $h \leq h_0$

$$f_{Hs}(h) = \frac{1}{\sqrt{2\pi}\sigma_{LHM} h} exp(-\frac{1}{2}(\frac{ln(h) - \mu_{LHM}}{\sigma_{LHM}})^2) \tag{3.81}$$

But if $h > h_0$ the following formula applies:

$$f_{Hs}(h) = \frac{\alpha_{HM}}{\beta_{HM}}(\frac{h}{\beta_{HM}})^{\alpha_{HM}-1} exp[-(\frac{h}{\beta_{HM}})^{\alpha_{HM}}] \tag{3.82}$$

The formulas below are used to calculate the necessary distributions for generating an environmental contour line:

$$\mu_{LTC} = c_1 + c_2 h \tag{3.83}$$

$$\sigma^2_{LTC} = d_1 + d_2 exp(d_3 h) \tag{3.84}$$

$$\alpha_{HC} = a_1 + a_2 u^{a_3} \tag{3.85}$$

$$\beta_{HC} = b_1 + b_2 u^{b_3} \tag{3.86}$$

$$\mu_{T_p} = \bar{T}_p(u,h) = \bar{T}_p(h)[1 + \theta(\frac{u - \bar{u}(h)}{\bar{u}(h)})^{\gamma}] \tag{3.87}$$

$$\bar{T}_p(h) = e_1 + e_2 h^{e_3} \tag{3.88}$$

$$\bar{u}(h) = f_1 + f_2 h^{f_3} \tag{3.89}$$

$$v_{T_p}(h) = k_1 + k_2 exp(hk_3) \tag{3.90}$$

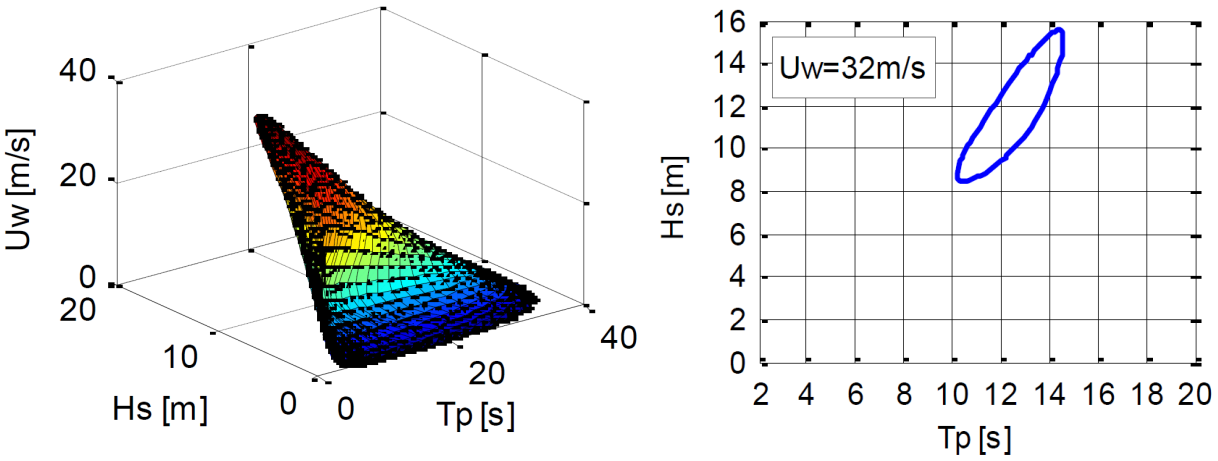

(a) 3D contour line

(b) 2D contour line

Figure 3.13: Environmental Contour lines

4 | Scope

The wind industry has had a tremendous growth in the last few decades, and the demand is increasing. Installation of new wind turbines has currently been moving away from onshore to offshore wind as well as moving from shallow to deep sea.

The costs for floating offshore wind turbines exceed their bottom-fixed counterparts, and researchers are searching for opportunities for cost reduction. These floating offshore wind turbines are assembled before they are towed to location, removing the need for complicated installations done at sea, and heavy machinery. The semi-submersible designs are preferred due to the flexibility regarding sea depth at installation site. However, several questions arise in how the system will behave, and investigations of feasibility of a novel design is extensive. For the existing semi-submersible designs investigated, spread mooring systems are used in keeping the structure at place. By rather designing structures with a single point mooring system , then the cost related to the mooring system will be significantly reduced.

Hence, a novel semi-submersible floater supporting the 5MW wind turbine has been proposed in this thesis. The structure is moored with a single point mooring system. The aim is to design a system with good static and dynamic responses. The entire structure with floater, wind turbine, and mooring system needs to be included in the analysis conducted to study the coupling effect between the different parts of the system.

4.1 Research Question(s)

The main research question for this thesis is therefore:

How can the twin fish wind turbine system be designed?

With the following subquestions to aid in answering the main question:

1. *What are the dynamic characteristics of the system under influence of environmental loads?*
2. *How can the mooring system of the twin fish wind turbine system be designed to keep the structure at place?*

The first research question is related to investigate the dynamic characteristics of the entire system together. The global movement of the structure is investigated for different conditions.

The second research question is related to designing a mooring system for the twin fish. The main goal is designing a single point mooring system, which is different from the usual spread mooring system used for the semi-submersible structures.

4.2 Limitations

Since this is a study of a novel concept, it was difficult selecting limitations in the project, since there was no clear idea of possible difficulties which can arise with the design. The preliminary design of the model was conducted in a pre-project in the fall of 2020, and the work presented here is a continuation and further optimization of the final model presented in that work. When I use the term *optimization* it is not a properly correct optimization since the process does not involve theories within design of experiments to select the variables; the design procedure was based on iterations. However, the selections were conducted considering reasonable, practical values, and were thoroughly studied.

Several limitations have been set to answer the research question properly in the given time. The environmental loads investigated are for the ULS case, for a return period of 50 years. The external loads applied were found using a environmental contour line for a given location presented in a separate research article. Some values for parked condition were presented in a table, and a case with minimal loads also has been included for comparison. Current loads are not included in the analysis. Since the analysis conducted in this thesis is for a ULS state, then I am considering a parked wind turbine condition, and therefore the wind forces can be neglected. Operational loads are not investigated in the thesis.

For the mooring system, a few design variables were set before any analysis were conducted. These were that it is generally more popular to use a chain system in shallow water, while a combination of chain and wire system is used in deep waters. Also, the mooring system needs to fulfill several design requirements, given in a design standard.

The design of the wind turbine is not conducted, further references is given to the design requirements for the wind turbine presented in a separate standard [8]. Economic considerations have not been made in the thesis, except for reasonable material choice.

The structural calculations of the hull and support structure has not been done. Detailed design of the support system has also not been conducted. Fatigue considerations have not been done.

Finally, no economic considerations have been made in this thesis.

5 | Case and Materials

In this chapter the twin fish floater concept will be presented with size, parameters, and the complete models for each program. The wind turbine, loading conditions and model in SIMO-RIFLEX is also presented as well as limitations and assumptions set for each analysis and procedure.

5.1 Preliminary twin fish model data

In the preproject the main goal for the preliminary design was to fulfil the following two basic requirements:

1. The floater must have sufficient buoyancy to supporting wind turbine tower.
2. The floater must ensure sufficient restoring force to keep the hydrostatic stability of the floating wind turbine.

The twin fish floater is a novel concept proposed with biomimetic characteristics, with two fish shaped structures connected by a support structure for a wind turbine. The preliminary model design was established in a preproject conducted the Fall of 2020 [40], based on a original twin fish with given measurements. The size of the twin fish was scaled, and shifted to achieve good hydrostatic and hydrodynamic results. In the preproject - thesis, the novel design was compared to two other semi-submersible concepts, the V-semi [26] and the 5MW CSC [23], showing good results. The final characteristics of the twin fish floater is presented below.

Table 5.1: Characteristics of the twin fish floater.

Characteristics	**Symbol**	**Value**
Depth [m]	F_H	19.997
Length [m]	L_F	76
Width [m]	W_F	7.197
Plate width[m]	P_W	15
Support length[m]	S_L	9
Support width[m]	S_W	6.5
Fin length[m]	F_L	17.1
Plate height [m]	S_H	1.75
Support height [m]	T_H	3
Freeboard [m]	W_H	3.3
Displaced volume [m^3]	∇	8001.50
Shift of fish [m]	L_s	15
Distance between fish [m]	2* L_S	30
COG of the floater [m]	-	(9.69 , 0 , -10.58)
COB of the floater [m]	-	(10.19 , 0 , -7.33)
COG of the system [m]	-	(10.17 , 0 , -5.25)

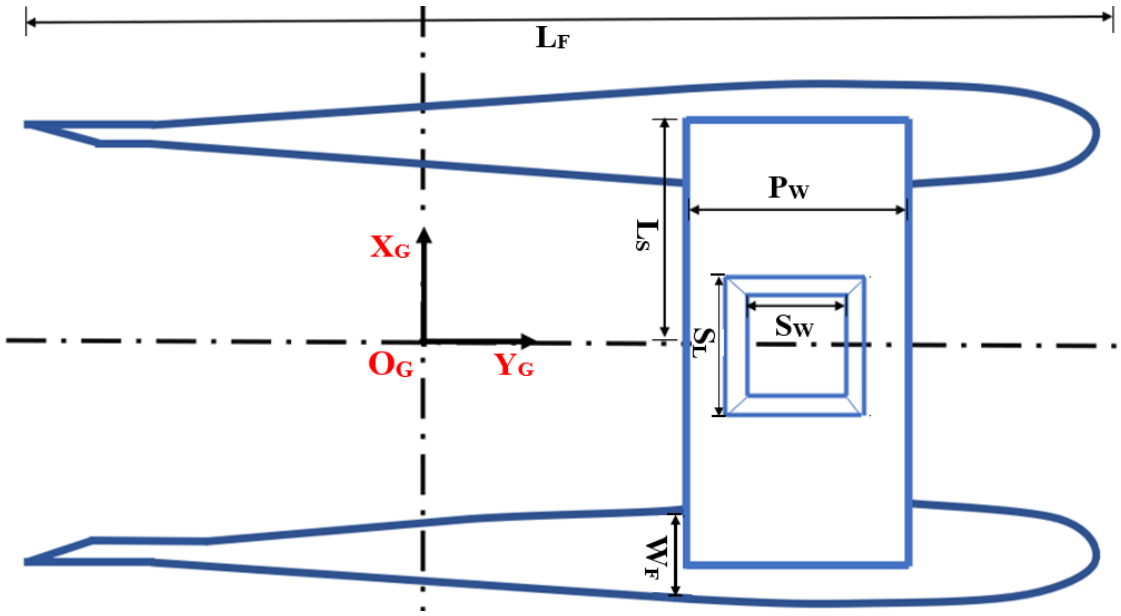

Figure 5.1: Overview of the twin fish floater with parameters

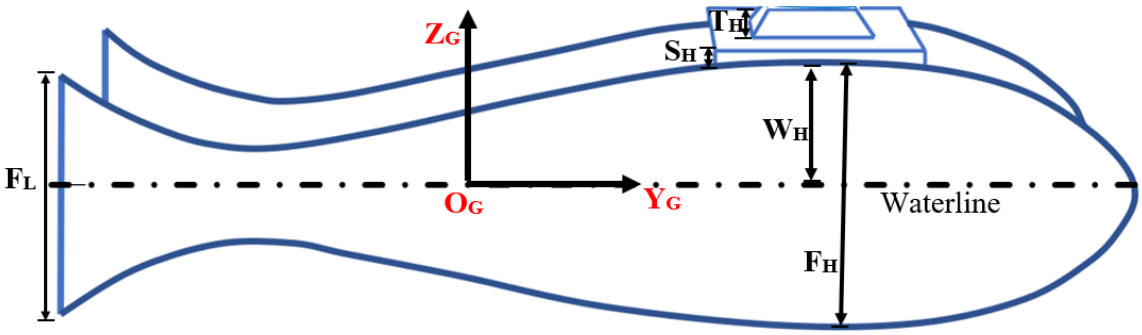

Figure 5.2: Side view of the twin fish floater with parameters

5.2 NREL offshore 5-MW baseline wind turbine

To support concept studies to assess new offshore wind technology, specifications for a representative wind turbine was presented in two reports by Jonkmann et al [41] [42]. The wind turbine is a conventional, three-bladed upwind variable-speed variable blade-pitch-to-feather-controlled turbine. The design was created by obtaining broad design specifications from turbine producers, emphasizing REpower 5MW machine. The detailed information which was missing was filled in by a composite of publicly available data from projects such as the DOWEC, RECOFF, and WindPACT.

The tower properties are dependent on the support structure to carry the rotor-nacelle assembly.The type of support structure will also depend on installation site, where the properties of the installation site will depend on water depth, soil type and wind and wave severity. In the report by Jonkman the properties of the tower is given according to a land based version of the NREL 5MW baseline wind turbine [41]. But in the second report, the data for a tower mounted on a spar floater is given [42]. This has been used for the tower in the thesis.

The table on the next page is an overview of the qualities for the 5MW wind turbine presented by Jonkmann et. al.

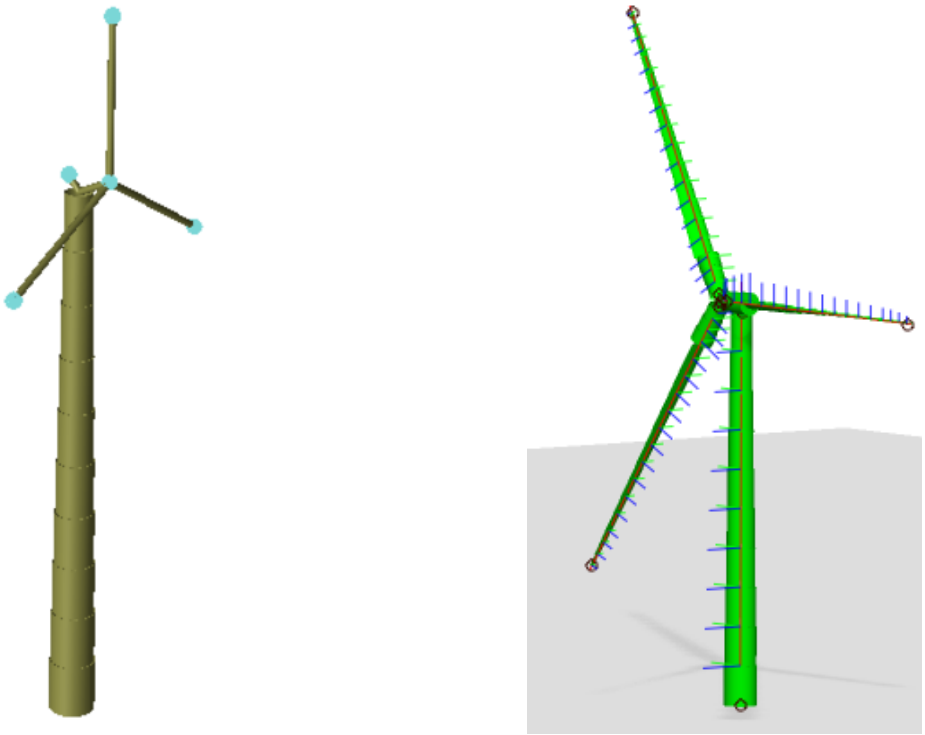

(a) Wind turbine in GeniE (b) Wind turbine in SIMA

Figure 5.3: Models of the wind turbine

Table 5.2: Main characteristics of the 5MW wind turbine.

Description	**NREL 5MW**
General information	
Rating	5MW
Configuration	Upwind, 3 blades
Control	Collective pitch
Drivetrain	Multiple stage gearbox
Rated wind speed	11.4 m/s
Cut-in,Cut-out wind speed	3 m/s , 25 m/s
Cut-in, Rated rotor speed	6.9 rpm , 12.1 rpm
Rated tip speed	80 m/s
Maximum thrust	750 kN
Geometry information	
Rotor, Hub diameter	126 m , 3 m
Hub height	90 m
Tower height	87.6 m
Overhang,Shaft tilt	5 m , 5°
Pre-cone	-2.5°
Mass	
Rotor mass	110t
Nacelle mass	240t
Tower mass	347.5t
Total mass	697.5t
Overall COG	(-0.2m,0m,64.0m)

Thw wind turbine were modelled with the same specifications in GeniE and SIMO-Riflex.

5.3 Parameters natural period study

For optimization of the natural period, the structure needs to be lowered, without compromizing the stability of the structure or the hydrodynamic qualities. The following values were first selected, but based on these results more iterations needed to be done. The next variables were selected after the below were run in HydroD.

Table 5.3: Characteristics of the studied cases.

	Case number				
Characteristics	**1**	**2**	**3**	**4**	**5**
Lowered [m]	0.5	1.0	1.5	2.0	2.5
Freeboard [m]	2.8	2.3	1.8	1.3	0.8
Displaced mass [tonne]	8284.27	8381.20	8451.19	8493.44	8506.45
ZOB of the floater [m]	-7.5	-8	-8.5	-9.0	-9.5
ZOG of the system [m]	-5.85	-6.42	-6.97	-7.50	-8.0
Displaced volume [m^3]	8082.21	8176.78	8245.06	8286.28	8298.97

The freeboard is defined as the distance from the water level to the top of the structure above water.

The requirements set in cooperation with the supervisors which need to be fulfilled so that the results can be considered reasonable is defined in the following table:

Table 5.4: Restrictions for characteristics of the floater.

Characteristics	**Value**
Natural period	
Heave [s]	20-30
Roll [s]	20-40
Pitch [s]	20-40
Metacentric height	
GMT [m]	≥ 0.5
GML [m]	≥ 0.5

The regular natural periods for semi-submersible structures are between 20-30 seconds. Too large values will result in bad responses. The GMT and GML requirements are given in a standard as a requirement for stability.

5.4 Damping of the structure

The irregular frequencies which might appear in the responses of the structure, is removed by introducing a internal lid within the two fish hulls in the structure. Two different internal lids have been tested, one created in HydroMesh and one in Multisurf.

For the moonpool between the two fish hulls a plate was created and meshed. Most of the damping was introduced through this lid to counteract the effect of the moonpool, but damping was also added to the structure through the crtical damping matrix for roll and yaw. Several sensitivity analysis were conducted in HydroD to find the best suitable damping values, and combination of these values, for the twin fish floater.

Table 5.5: Values for moonpool damping and critical damping studied.

Characteristics	Value [%]
Damping moonpool	
	0 to 200; 25 value step
	200 to 400;50 value step
Damping roll	
	2 to 10; 2 value step
Damping yaw	
	1 to 9; 2 value step

The internal lids from both the programs and the damping lid for the moonpool is shown in the figures below.

The function with the internal lid is creating a cover for the internal surface in the fish hulls. Two were created in different programs, Multisurf and HydroMesh, to assess reliability of the modelling

The edges of the damping lid for the moonpool follows the shape of the twin fish floater.

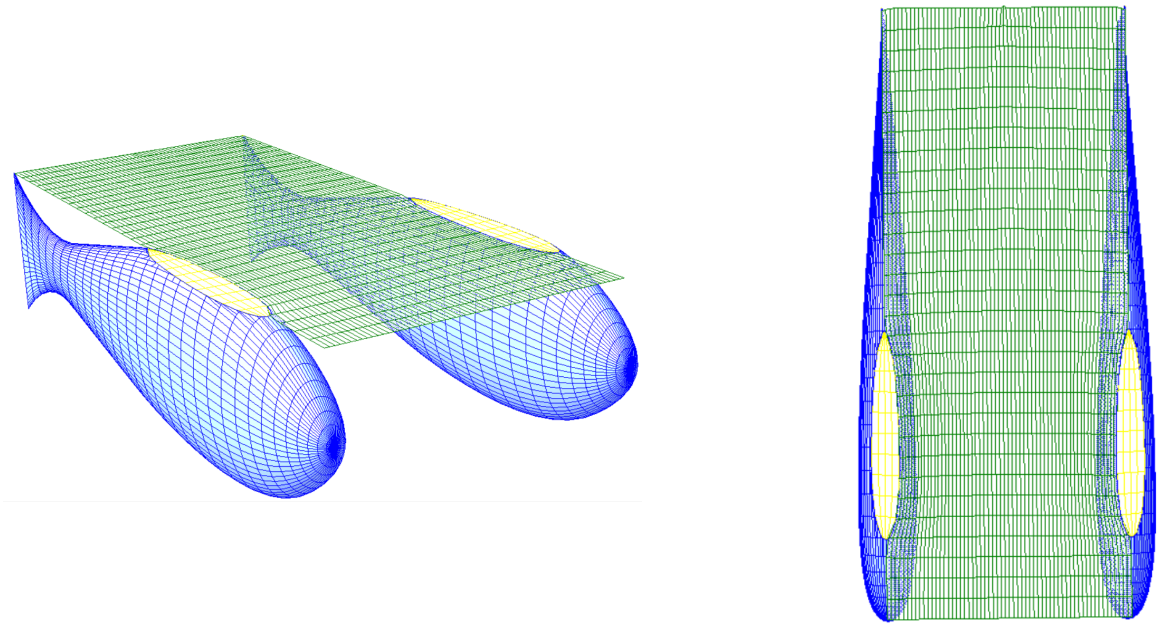

Figure 5.4: Illustrations of the twin fish floater with internal lid and damping lid

5.5 Mooring system data

The mooring system designed in this master thesis is a single point catenary mooring line, as an opposite to most semi-submersible wind turbine systems which use a spread mooring system.

A spread mooring system allows for little movement in any directions, while the single point mooring system will allow for the structure to adjust itself to the loads in which the structure is exposed to. This will result in fewer loads on the mooring line compared to in a spread mooring system. A single point mooring system will also result in reduced cost due to significantly less material.

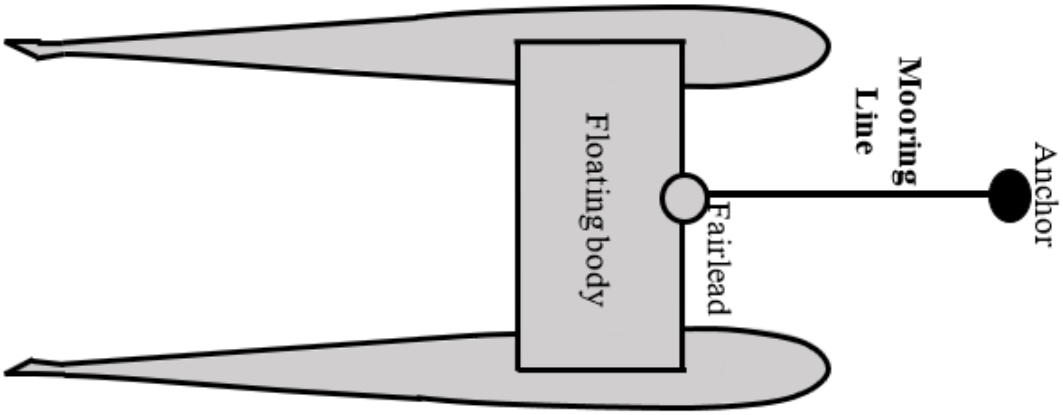

Figure 5.5: Illustration of the twin fish floater with a single point mooring system.

The black points represent the anchor for the mooring lines, while the grey points symbolize the fairlead of the mooring line. The fairlead is not located at the structure for the twin fish in this thesis since no structural analysis have been made on the support structure designed for the twin fish.

5.5.1 Fairlead and anchor position

A challenge was determining where the fairlead should be located for the entire system. Main idea was that the location of the fairlead should be at center of the support system (the connecting plate) between the two twin fish hulls. But, since there has not been any structural calculations on the plate connecting the two hulls, then a fictious point was used for the fairlead located at a site off the model. The anchors final position will be at the seabed, but this could be modelled in two different ways in SIMA (Simo-Riflex).

The position of the fairlead was changed during the analysis. the fairlead was finally designed as a turret in Sima to allow for rotations. Stiff beams connect the supernodes.

5.5.2 Mooring line data

The data for the mooring line is a result from several meetings and iterations done. The data could easily have been put in the result chapter since it answers a part of the reseach question. But, after discussion with my supervisors it was decided to place it here.

The mooring system presented consists of two materials, polyester rope and chain. The data is presented below:

Table 5.6: Characteristics of the mooring line types used for the single point mooring system.

Material	**Diameter [mm]**	**MBL [kN]**	**Stiffness [kN]**
Polyester rope	130	4620	87780
Chain R3	80	4421	526018

The following overall data is provided for the mooring system.The data selected was chosen in cooperation with the supervisors to ensure reliable and standard mooring system. The data below shows the values for the different cross sections used in the mooring system.

Table 5.7: Characteristics of the three segments for the mooring line.

	Segment number		
Characteristics	**1**	**2**	**3**
Cross section properties			
Mass coefficient [kg/m]	11.34	8000	128
External area [m^2]	0.00822	15	0.01631
Internal area[m^2]	0	0	0
Gyration radius [m]	0	0	0
Temperature [C]	20	20	20
Stiffness properties			
Cross section type	bar	bar	bar
Axial stiffness [N]	8.778e+07	1.0e+13	5.2602e+08
Hydrodynamic coefficients			
CQx [Ns^2/m^3]	20.93	1700	46.4
CQy [Ns^2/m^3]	106.6	1500	98.4
CAx [kg/m]	1.36	11000	3.34
CAy [kg/m]	13.61	9000	16.71
CLx [Ns/m^2]	0	0	0
CLy [Ns/m^2]	0	0	0
Capacity parameters			
Tension capacity [N]	1.5e+06	1.5e+06	1.5e+06
Maximum curvature[1/m]	0.3	0.3	0.3

Table 5.8: The final length of each mooring line segment.

Segment number[-]	Length[m]	Number of elements[-]	Element length[m]
1	80	10	8
2	5	1	5
3	1	1	1

The mooring system consists of a polyester rope and a R3 chain. The segments are solid, and therefore have no internal area. Segment number 1 is the polyester rope while segment 3 is the R3 chain. Segment number 2 is a buoyancy element. The length of each segment is not decided and is designed in the thesis.

5.6 Location and Environmental Loads

The location and environmental data is from a location presented in a Research paper by Lin Li et al. The location selected is Norway 5 which is located in the North Sea. Therefore it is possible to use the JONSWAP spectrum as the wave spectrum.

Figure 5.6: Different principles of catenary mooring lines

The location depth selected is for a depth of 100 m, and the data for the environmental wave and wind loads are extracted from the following document "Joint environmental data at five european offshore sites for design of combined wind and wave energy". For designing combined renewable energy concepts, it is important to choose sites with both wind and wave energy resources are substantial. These facilities need to be designed in ultimate limit state based on load effects corresponding to 50 years wind an wave conditions, requiriring a long term joint probabilistic model for wind and wave parameters at potential sites.

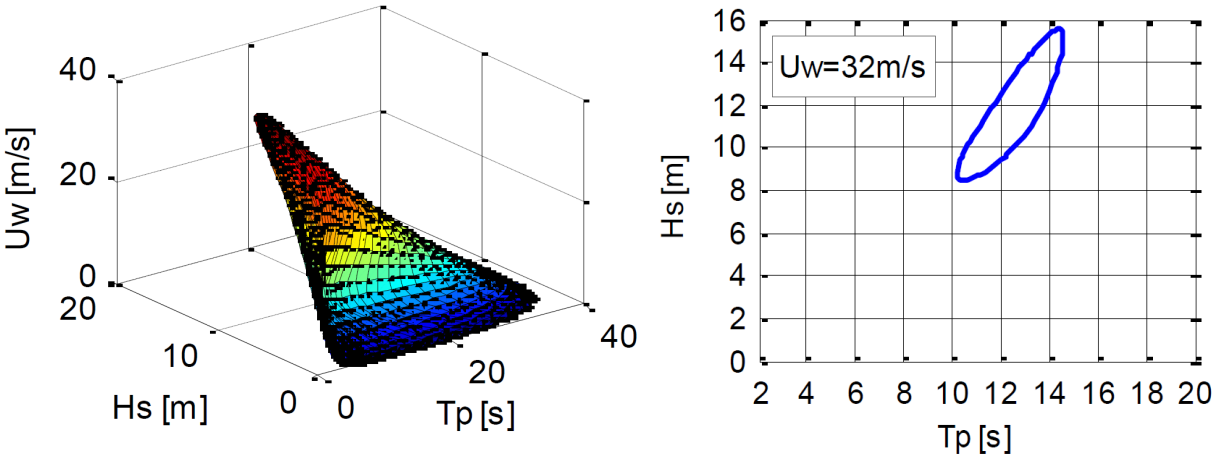

(a) 3D Contour line of Norway 5 location

(b) C2D Contour line of Norway 5 location

Figure 5.7: The environmental contour lines for Norway 5.

The joint distribution are estimated by fitting analytical distributions to the hindcast data following a procedure suggested by (Johannessen et al. 2001). The long term joint distributions can be used to estimate the wind and wave power and assess fatigue issues.

Contour surfaces are established for combined wind and wave parameter. The design points on the 50 year contour surface is established for wind and wave. It is used to estimate long term extreme response by applying short extreme sea states. 1 hour case was used as input and a 2D contour line was created for a U_w of 31.2 m/s . Each point on the 2D contour line has a value for H_s and T_p. The values are presented in the methodology chapter after explanation of extraction.

According to a standard, the loads needs to be considered in several directions, so waves for 180 degrees and 150 degrees were selected.

Table 5.9: The load conditions run in this thesis.

Characteristics	**Direction [deg]**	H_S**[m]**	T_P **[s]**
Contour line	180	var*	var*
Contour line	150	var*	var*
Parked condition	180	15.6	14.5
Parked condition	150	15.6	14.5
Parked condition	180	13.4	13.1
Parked condition	150	13.4	13.1
Low condition	180	1	10
Low condition	150	1	10
Low condition	180	2	10
Low condition	150	2	10

var* stands for the cases where the environmental data is from a 2D contour line.

5.7 SIMA model data for coupled analysis

In the section below all the data input to the SIMA model is presented. Several models were created in SIMA (SIMO-RIFLEX) due to the complexity of the model. The design of the mooring system and the coupled analysis was conducted using SIMA.

5.7.1 Coordinate system

The coordinate system varies throughout the thesis. Originally, the coordinate system is placed as the figure below, at the centre of gravity of the structure, but in z-direction the zero point is the mean water line. The same coordinate system is used in HydroD, GeniE and MOJSLOAD before it is imported into SIMA (SIMO-Riflex). However, in SIMA the center of gravity is defined at a different location, determined by a line constructed for the mooring system.

Since we have an upwind wind turbine, the waves need to be directed against the turbine as shown in the figure.

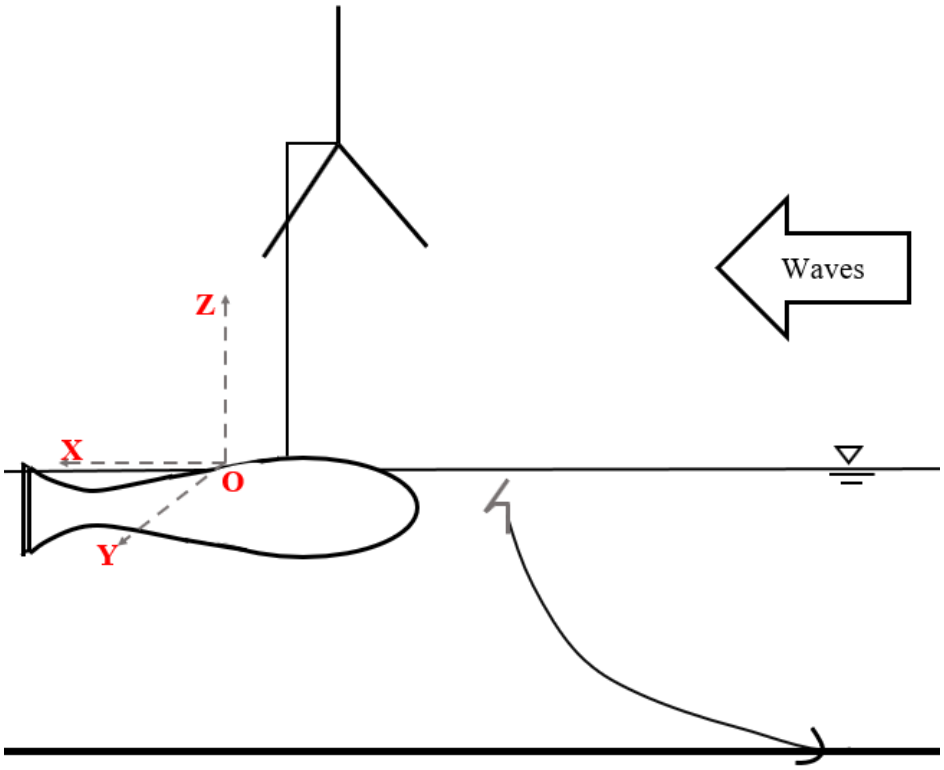

Figure 5.8: Illustration of the twin fish system in Sima with coordinate system and load direction.

5.7.2 Models

The wind turbine is located at the center of the plate connecting the twin fish hull.The fairlead point is always defined as a slave node to the location of the twin fish hull. The fairlead position may either be put on the support structure as decided or the fairlead can be put on the sea surface and can be connected by a rigid imaginary beam. In this thesis, the fairlead position is defined in front of the twin fish wind turbine system.

The anchor position is defined as a fixed supernode, and it can either be modelled at the sea surface or at the sea bed. In SIMA, the mooring line is first set as a rigid straight line, and the fairlead

and anchor are the endpoints of the line. Then the anchor is moved to its fixed position. When the process is done is SIMA, the anchor position is carefully adjusted when doing the dynamic analysis. If we had fixed the anchor at the sea surface will allow that the L_m equals the distance between these points. This has not been done in this thesis.

Several different models were made for the SIMO-RIFLEX coupled analysis. Since there has not been a concept like this before, the modelling was demanding and time consuming, and a stepwise procedure for the models was made to ensure correct modelling. 4 different models were made in SIMA:

1. A dumnmy body with the mooring system.
2. A model which only includes the twin fish body imported from the wamit result files, with a stiffness added in surge.
3. A model with the twin fish body imported from the wamit result files, with a stiffness added in surge, and with the complete wind turbine.
4. A model with the model data imported from the wamit result files, the complete wind turbine, and the mooring line.

Since model 2 does not include the wind turbine or mooring lines, then the data imported from wamit result files does not need to be modified. For model number 3 and 4, the imported data from wamit result files includes the mass and data for the wind turbine as well. A procedure written by Chenyu Luan and Marit Kvittem is explained in the methodology chapter of how one can remove the data for the wind turbine from the imported wamit result files so that the mass of the wind turbine will not be accounted for twice.

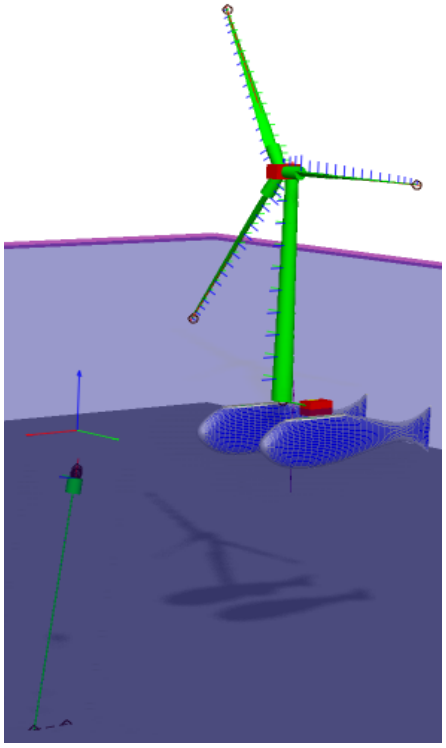

Figure 5.9: The model of the twin fish floater system in Simo-Riflex.

6 | Methodology

This chapter describes the methodology applied in the master thesis, from data gathering, theoretical studies, sensitivity analysis, construction of models and variable selection. Procedures for modelling in sima for coupled analysis is also presented.

6.1 Research

In the introductory phase of the thesis period, a lot of time was devoted to research regarding the necessary theoretical background, as well as good procedures for coupled analysis of a wind turbine. A pre-project was written to acquire a good foundation for basic hydrostatic and hydrodynamic theory. Research within extraction of environmental data and theoretical background behind the calculations in SIMA (SIMO-RIFLEX) was also conducted.

6.2 Software

Several programs were used throughout the thesis period. This chapter describes the various software used to complete the master thesis.

A short overview of software and use is given in the table below.

Program	**Type of program**	**Area of use**
GeniE	Modeling and analysis	Used for detailed modelling
HydroMesh	Subprogram for HydroD	Used for simple mesh in HydroD
HydroD	Hydrostatic and hydrodynamic analysis	Hydrostatic and hydrodynamic analysis
Postresp	Postprocessor for HydroD	Vizualzation and postprocessing
Mojsload	Hydrostatic and hydrodynamic analysis	Hydrostatic, hydrodynamic and verification
Simo-Riflex	Subprograms of SIMA. Modeling, static and dynamic analysis	Modeling, static and dynamic analysis
Excel	Multifunctional program based on spreadsheets	Postprosessing of results
Matlab	Multifunctional program	Sensitivity analysis and postprosessing

6.2.1 GeniE

GeniE, provided by DNV GL, is a program used for concept based finite-element modelling and analysis. GeniE has been used to detail model the structures; creating panel models and mass models of the twin fish. Meshing was conducted in GeniE, generating panel models and mass models for further analysis. In this study T1.FEM and T4.FEM files were exported, the number referencing the superstructure used.

To create the T1.FEM file a mesh smaller than 4 meters was used, meshing the area beneath the water line. The T4.FEM includes the complete mass of the structure, the mass necessary to balance the displacement. A mesh density of 0.5 meters was used for the mass model.

6.2.2 HydroD

HydroD, developed by DNV-GL, is used for advanced hydrostatic and hydrodynamic analysis for fixed and floating offshore structures. The WADAM runs are conducted for every single test case to get hydrostatic qualities, RAOs, added mass and damping, as well as drift forces for the structure.

Either .FEM files or .GDF may be used as panel model and internal surface model. Also, for mass models, either a .FEM file, a mass matrix or an evenly distributed mass may be used to conduct the analysis. The WADAM.LIS file contains most of the results, so the document is thoroughly inspected after each run. The results in the WAMIT files were extracted using Postresp,Matlab or Mojsload. The wizards in HydroD are of good aid for including the necessary data for conducting a hydrostatic or hydrodynamic analysis.

WADAM uses Morisons equation and first and second order 3D potential theory. The incident wave potentials may be defined by Airy/Linear wave theory, analyses are performed in both frequency and time domain approach.

The additional program, Postresp, was used for easily visualizing the results and extracting results for postprocessing. Hydromesh is a subprogram of HydroD and can be used for simplified mesh for creating a surface mesh for free surface damping and other relevant purposes.

HydroD can generate various results, such as hydrostatic data, inertia properties, righting moments, wind heeling moments, GZ-curves and still water sectional loads. The results can also be verified against relevant rules and regulations.

6.2.3 Mojsload

Mojsload is a program developed by my external supervisor, and has been used in both extracting results and for verification of results by comparing calculations in MOjsload with calculations in HydroD. The theory behind Mojsload is based on linear wave theory, and uses Morisons equation and first and second order 3D potential theory.

Mojsload can be used in context with WAMIT , or with HydroD for obtaining results.The control results were run in wamit and mojsload for verification of the results. Mojsload generates several files, among them different .gdf files, information files and all results in excel files for easy read and postprocessing.

6.2.4 SIMO-Riflex

Sima is a program which offers a complete solution for simulation and analysis of marine operations and floating systems.

Sima consists of several subprograms, among them SIMO and Riflex which has been used in this thesis. SIMO is a time domain simulation program developed by MARINTEK for multi body system while Riflex is a non linear FEM program developed by MARINTEK for static and dynamic analysis of slender marine structures. SIMO – Riflex is a state of the art tool for dynamic response analysis of moored offshore structures [43] [44].

6.2.5 MATLAB

Matlab is a multi functional program developed by Mathworks .It is a programming and numeric computation program used by millions to analyze data, develop algorithms and create models.

Matlab is used for extraction of results for environmental contour line (see section...), and for postprosessing results from HydroD and SIMA using simple scripts. It was also used in vizualization of the .gdf files to ensure good quality meshing from HydroD.

6.2.6 Excel

Microsoft Office Excel is a program developed by Microsoft based on spreadsheets. The program has a lot of inbuilt formulae and may also be used for visualization of data in the form of numerous diagrams.

Excel has been used for plotting results, extracting results in mojsload and for comparing results throughout the thesis period.

6.3 Calculation of Displacement

The displacement calculation is based on Archimedes law, where the total mass of the structure necessary to balance out the displacement is calculated.

The calculation was done by hand, but there is a deviation between values in GeniE and values in HydroD. The calculation was therefore used as a preliminary indication of how much the mass of the structure needs to be to balance the displacement. To obtain best possible balance between the displacement mass, and the mass of the structure, some iteration was necessary.

6.4 Mesh size calculation

The mesh size necessary to get proper results is dependent on the wave length. Since the natural period is expected to be about 20 seconds, one can use the following formula to obtain the necessary size of the mesh to get good results:

$$l_{mesh} < \frac{1}{4\sqrt{2}}\lambda \approx \frac{1}{6}\lambda \tag{6.1}$$

A preliminary assumption is that the wave periods considered to be between 3s to 30s.

Therefore the largest mesh size is:

$$l_{mesh,max} < \frac{1}{4\sqrt{2}}\lambda_{min} = \frac{1}{4\sqrt{2}}\frac{gT_{min}^2}{2\pi} = 2.5m \tag{6.2}$$

An iteration process was conducted, and finally two different panel models were used for the thesis: One generated by MOJSLOAD and one from GeniE with a mesh of 1.5 meters. The .gdf file has a larger mesh, but the mesh is more even.

For the mass model a mesh of 0.5 m was used.

Although they all proved to get good results, the .gdf generated by MOJSLOAD was used for the panel model since the meshing was even on both fish.

6.5 Design of the twin fish

The continued design process was based on the final design achieved in the pre-project. The further optimization regarding the hydrodynamic results while achieving good hydrostatic results was a stepwise process. For the optimization regarding the natural period and to study the moonpool resonance effect, the following programs were used: HydroD,GeniE and Mojsload. The subprogram HydroMesh for HydroD was used for creating the necessary mesh.

The procedure for optimization is connected to the idea that lowering the structure further, and reducing the water plane area will lead to better heave natural period. However, this may cause difficulty since lowering the structure further will be detrimental for the stability of the structure. To investigate whether it is possible to achieve better heave natural period, the structure was lowered with an amount and the characteristics were obtained and studied carefully.

The panel model was lowered in HydroD, and mass was defined using the distributed function in HydroD before it was run in HydroD. After investigating several values, an interval was established in which detailed mass models were created which balances the different displacements for each version.

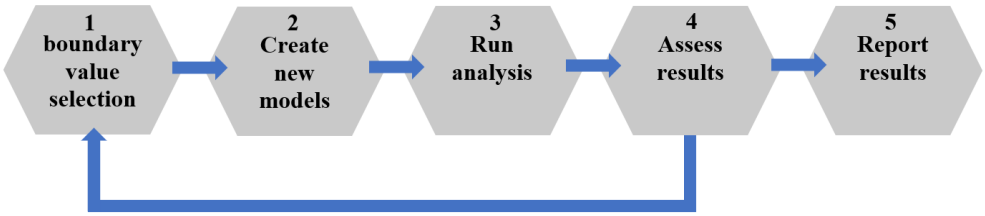

Figure 6.1: Flow chart for optimization for natural period

Another challenge which arose are worse values for RAOs when the structure is lowered further below, since lowering the structure is detrimental to the hydrodynamic responses.

The static results are presented in the result chapter. For the dynamic results a comparison between the raos will be presented, between the "final" twin fish floater and the optimized version.

6.6 Free surface damping

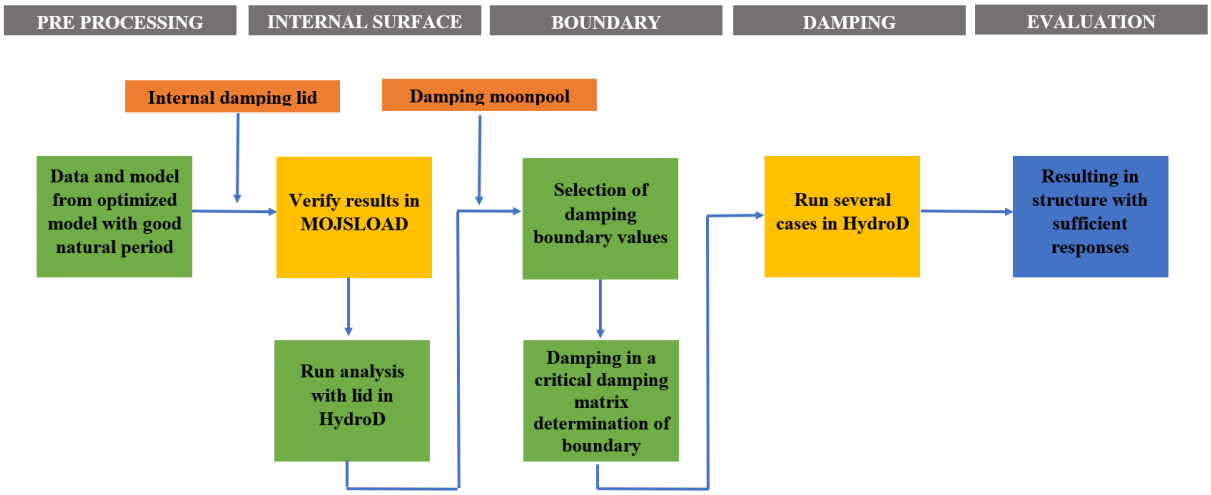

Figure 6.2: Flow chart for irregular frequency and damping

For removal of irregular frequency effects the procedure suggested by DNV GL by using the additional program HydroMesh in HydroD for generating a fixed lid for the internal surface of the structure was conducted.

A symmetrical internal lid was create for the fish hull in HydroMesh. The fixed lid was included as a separate hydromodel. No mass model was included for the panel model. Then, a multibody model was created, including the model for the twin fish, and the fixed lid. Hydrostatic and hydrodynamic analyses were rerun with the new multibody model.

To counteract the effect caused by the moonpool, a damping lid with a mesh was created. The damping lid was created in HydroMesh for the exposed area between the fish with a squared geometry.Then, the mesh was exported as a .FEM file into a Hydro model in HydroD before a multi-body model was created for an analysis run. The damping value was defined in the multi-body model as a percentage. Only the hydromodel with the panel model for the twin fish includes a mass model.

Several damping values were defined and run in HydroD to find the values which generate reasonable hydrodynamic results.

6.7 Extraction of environmental data

The environmental data used in this thesis was extracted using environmental contour lines, a methodology which is reasonable for getting realistic environmental loads on the structure.

The data selected was calculated in matlab scripts and further used in SIMA. Also, the environmental data for parked wind turbine condition was presented in the article for site 14.

Table 6.1: Parameters used for calculating the 2D contour line

Parameters	**Value**
Marginal distribution of U_w	
α_u	2.029
β_u	9.409
Marginal distribution of H_s	
h_0	5.0
μ_{LHM}	0.871
σ_{LHM}	0.506
α_{HM}	1.433
β_{HM}	2.547
Conditional distribution of T_p given H_s	
c_1	1.886
c_2	0.365
c_3	0.312
d_1	0.001
d_2	0.105
d_3	-0.264
Marginal U_w	
α_u	2.029
β_u	9.409
Conditional H_s for given U_w	
a_1	2.136
a_2	0.013
a_3	1.709
b_1	1.816
b_2	0.024
b_3	1.787
Conditional T_p for given U_w and H_s	
θ	-0.255
γ	1.0
e_1	8.0
e_2	1.938
e_3	0.486
f_1	2.5
f_2	3.001
f_3	0.745
k_1	-0.001
k_2	0.316
k_3	-0.145

The environmental contour line generated for this thesis is presented below. It applies for a $U_w = 31.2\ m/s$ to have a reliable value for the ULS. Also, if using a the contour line for a U_w of 33.6 m/s will only generate a point instead of a contour line since it cuts through the 3D contour line at the top.

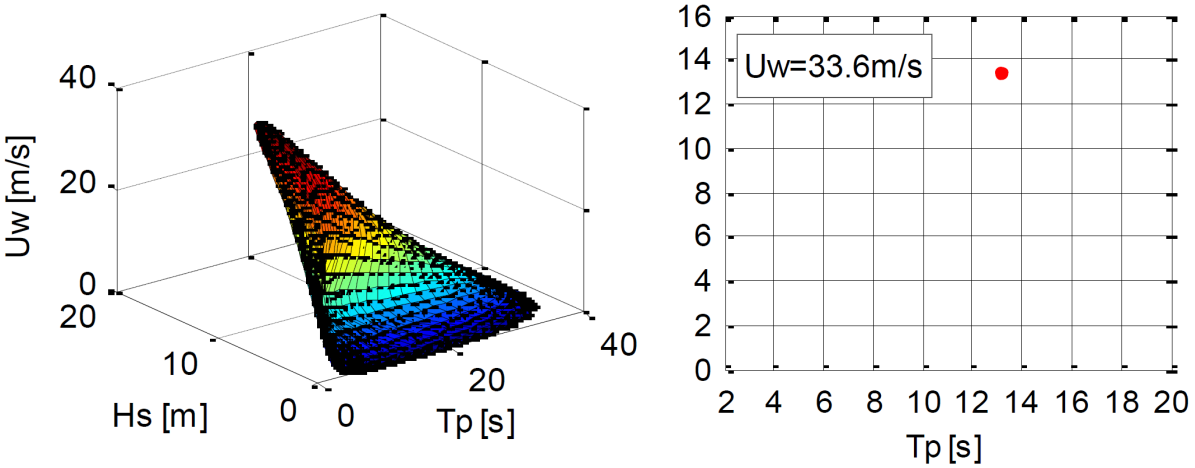

(a) 3D Contour Line for site 14.

(b) 2D Contour line for site 14.

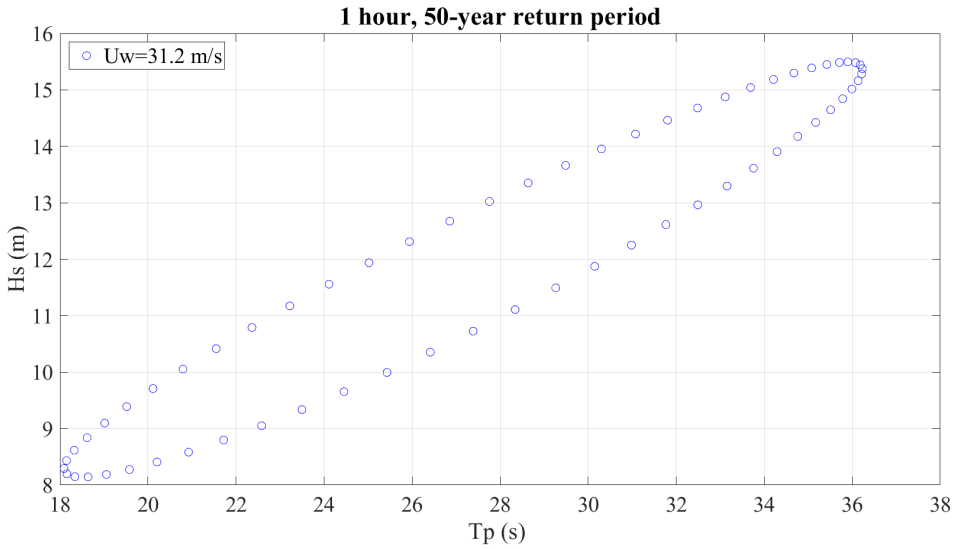

Figure 6.4: 2d Contour Line calculated for the thesis.

6.8 Design of the mooring system

In this thesis the focus was the mooring line tension and the movements in the transverse direction. The mooring line was modelled and based on the results from the analysis, several iterations were made before the results were deemed to be reasonable.

The mooring system design is complex and the standard requirements need to be fulfilled.In the standard it is set that the mooring tension multiplied with safety factors should be significantly less than the mooring line capacity. This applies to collinear direction (180 degrees) and non-collinear (150 degrees) [45].

The static results should reveal little movement in transverse direction due to sufficient stiffness in the mooring, while the global motions displays that the motions in the transverse directions are satisfactory.

6.9 Modelling in SIMA and Coupled analysis

The coupled analysis was conducted in SIMO-RIFLEX, where the twin fish floater, nacelle and hub are modelled as bodies in SIMO , while the mooring system, tower and blades are modelled as RIFLEX elements. The figure demonstrates how the coupled modelling was conducted.

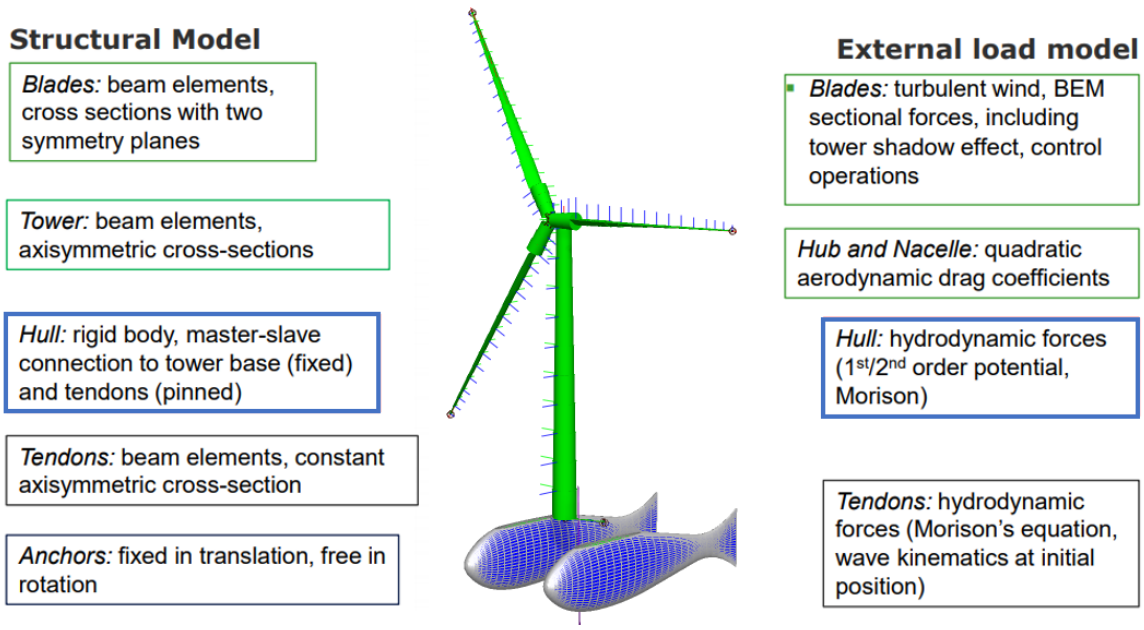

Figure 6.5: Modelling data for a coupled analysis of a floating wind turbine [modified [12]]

The procedure for the analysis is demonstrated in the figure below.

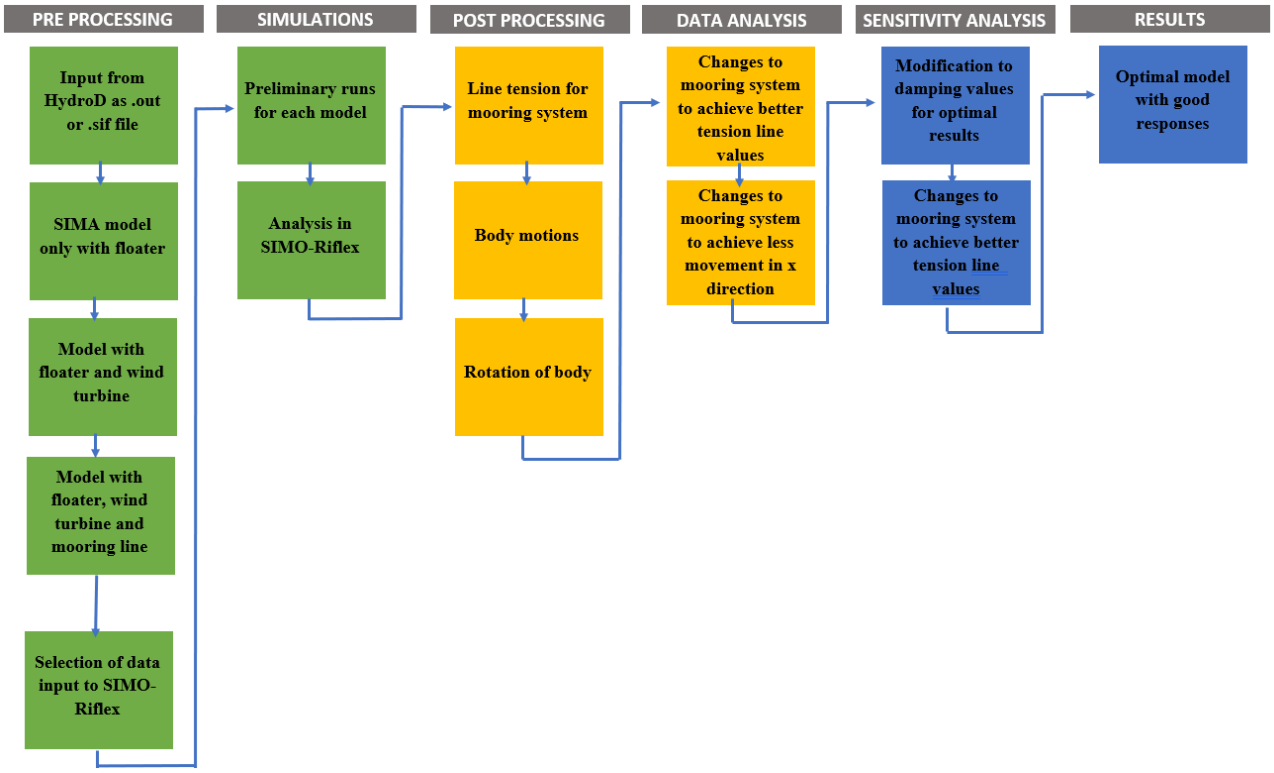

Figure 6.6: Flow chart for the coupled analysis and mooring line design

6.9.1 Buoyancy compensating forces

A short document by Marit Irene Kvitten and Chenyu Luan propose a method introducing buoyancy compensating forces in coupled SIMO-RIFLEX analysis.

Simo-Riflex is used for coupled analysis of platforms where we have a rigid simo body with flexible riflex elements. Restoring matrix and force transfer functions are imported into SIMO through Wadam or wamit result files generated by pressure panel analysis.

A basic assumption in Simo is that the Simo body without the weight of the Riflex-elements, is neutrally buoyant. In reality, it is the Simo body with the weight of the riflex elements which is neutrally bouyant. In Simo the assumption is that the effects of gravity and buoyancy is included in the equation of motion is taken into account in the restoring matrix. This is not the case for Riflex, where gravity and buoyancy is included as nodal forces. This inconsistency between the programs is the reason as to why one needs to define a compensating force in the centre of buoyancy.

This is a good method for modelling when the mooring line weight is applied symmetrically , and is much smaller than the platform weight.

In the case of a floating wind turbine, the platform will not be symmetrically loaded with the weight of the flexible elements (in other words when the centre of gravity and centre of buoyancy of the platform, without the riflex elements - do not have the same coordinates). Using the method for the bouyancy compensating force will create force on the body of the structure.

The proposed method eliminates the issue with an moment on the Simo body, attempting to only have real forces in the model. An upwards specified force at the buoyancy center of the hull to represents the bouyancy and a downwards specified force represents the gravity. However, this is already included in the restoring matrix which is obtained from Wadam or Wamit. In order to not

count the restoring effect twice , this part of the restoring coefficients must be subtracted from the original restoring matrix.

The points presented below will be counted as a general approach to modelling of floating wind turbines in coupled Simo-Riflex:

1. Calculate mass, inertia and mass distribution (mass matrix) for the floating wind turbine platform with and without the wind turbine.
2. Do hydrodynamic panel method analysis in Wadam or Wamit with input describing the whole system of platform and wind turbine.
3. Import output from Wadam/Wamit to Simo.
4. In Simo*sys.dat file, change the following to describe the platform without the wind turbine and mooring lines:
   (a) Mass and inertia
   (b) Centre of gravity
   (c) Add a specified force equal to the weight of the body (W) in the centre of gravity.
   (d) Add a specified force equal to the buoyancy (B) of the body in the centre of buoyancy.
   (e) Subtract the part of the restoring terms (4,4) , (5,5) , (4,6) and (5,6) that are caused by G and B. The restoring forces can also be calculated by Wadam or Wamit by specifying the gravity centre and bouyancy centre at the same point.

$$C(4,4)^{new} = C(4,4)^{wadam} - \rho g \forall z_b + mgz_g \tag{6.3}$$

$$C(5,5)^{new} = C(4,4)^{wadam} - \rho g \forall z_b + mgz_g \tag{6.4}$$

$$C(4,6)^{new} = C(4,6)^{wadam} + \rho g \forall x_b + mgx_g \tag{6.5}$$

$$C(5,6)^{new} = C(5,6)^{wadam} + \rho g \forall y_b + mgy_g \tag{6.6}$$

(a) Forces acting on the neutrally buoyant model.

(b) Simo interpretation where B=G.

Figure 6.7: The buoyancy compensating forces [13].

7 | Results

This chapter presents results obtained in the master thesis period. The section is divided into four main pieces, and are presented in the same way as provided in the figure in the introduction of the report.

7.1 Design of the twin fish floater

The section below shows the results from the design of the twin fish floater system regarding the natural period.

7.1.1 Hydrostatic results

Table 7.1: Hydrostatic results for all 5 cases of the twin fish floater.

		Case number				
Characteristics	**Symbol**	**1**	**2**	**3**	**4**	**5**
Displacement mass [*tonnes*]	Δ	8284.27	8381.2	8451.19	8493.44	8506.45
Displacement volume [m^3]	V	8082.21	8176.78	8245.06	8286.28	8298.97
Waterplane area [m^2]	WPA		106.76	109.91	53.38	1.24
Radius of gyration						
Roll [m]	r_{44}	25.86	25.77	25.77	25.86	26.55
Pitch [m]	r_{55}	29.76	29.69	29.69	29.76	32.01
Yaw [m]	r_{66}	25.2291612	25.24	25.24	25.23	27.19
Centre of buoyancy						
Longitudinal [m]	XOB	10.17	10.17	10.17	10.17	10.17
Vertical [m]	ZOB	-7.5	-8	-8.5	-9.0	-9.5
Metacentric height						
Transverse [m]	GMT	4.12	2.79	0.87	-1.71	-6.33
Longitudinal [m]	GML	5.57	3.76	1.44	-1.47	-6.33
Natural Period						
Heave [s]	T_{n3}	13.29	16.47	20.37	27.50	-
Roll [s]	T_{n4}	28.44	37.55	68.41	-	-
Pitch [s]	T_{n5}	27.92	34.94	56.69	-	-

The table above shows the static results for the cases presented in the *Case and Materials* chapter. The results were not promising, and therefore several other cases needed to be run between the two most promising values. The places marked with a $-$ are unreasonable data and has therefore not been included further.

Table 7.2: New cases run after premliminary analyses.

	Case number			
Characteristics	**1**	**2**	**3**	**4**
Lowered [m]	-1.00	-1.15	-1.25	-1.50
Freeboard [m]	2.30	2.15	2.05	1.80
Displaced mass [kg]	8284.27	8381.20	8451.19	8493.44
ZOB of the floater [m]	-8.00	-8.15	-8.25	-8.50
ZOG of the system [m]	-6.42	-6.57	-6.67	-7.50
Displaced volume[m^3]	8082.21	8176.78	8245.06	8286.28

From further iterations several more cases were investigated which fulfilled the set requirements given in the case and materials chapter. The cases tested were between case 2 and case 3 from table 7.1 The cases were eliminated based on too high or too low values for the natural period and GMT,GML. Lowering the structure -1.25 meters showed the most promising results.

Table 7.3: Best hydrostatic results, case 3.

Characteristics	**Symbol**	**Case 3**
Displacement mass [*tonnes*]	Δ	8418.91
Displacement volume [m^3]	V	8213.57
Waterplane area [m^2]	WPA	136.46
Radius of gyration		
Roll [m]	r_{44}	25.73
Pitch [m]	r_{55}	29.66
Yaw [m]	r_{66}	25.24
Centre of buoyancy		
Longitudinal [m]	XOB	10.33
Vertical [m]	ZOB	-8.34
Metacentric height		
Transverse [m]	GMT	2.10
Longitudinal [m]	GML	2.87
Natural Period		
Heave [s]	T_{n3}	18.15
Roll [s]	T_{n4}	43.6
Pitch [s]	T_{n5}	40.11

This is also the only model with a positive GZ value, which indicates stability, and has therefore been used in further analysis in the thesis.

7.1.2 Hydrodynamic Results

Below the results for the -1.25 m structure is shown. A best balanced mass model is used for the analysis. It is compared to a more even panel model and a more balanced mass model. Selected RAOs are shown below with the two different panel models and mass models shown.

The figure above shows the relevant translational RAOs for the structure. The figure below shows the relevant rotational RAOs for the structure.

The figure above shows a selection for the added mass values. Below the potential damping values are shown for some selected motions.

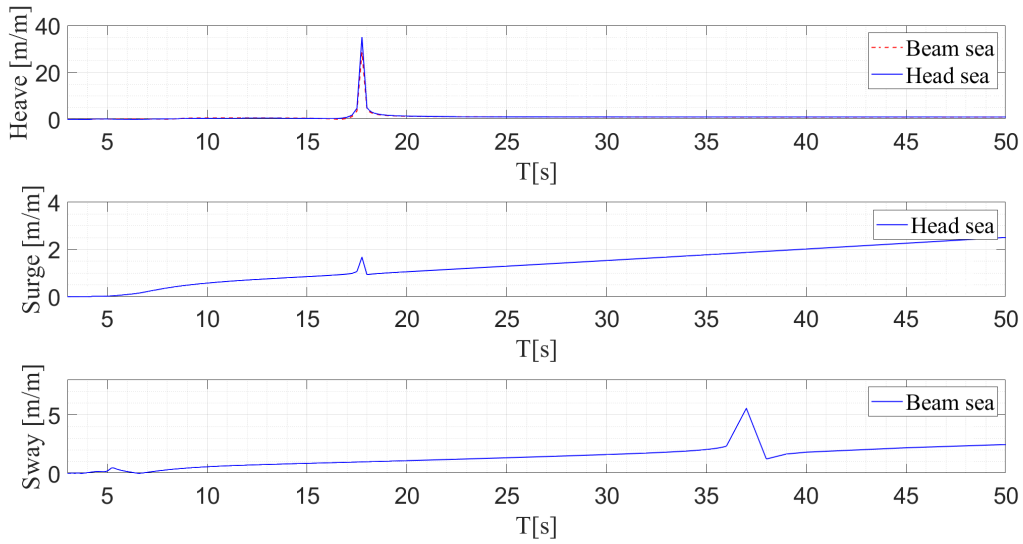

Figure 7.1: Selected translational RAOs for model.Beam sea: 90 deg ; Head sea: 180 deg.

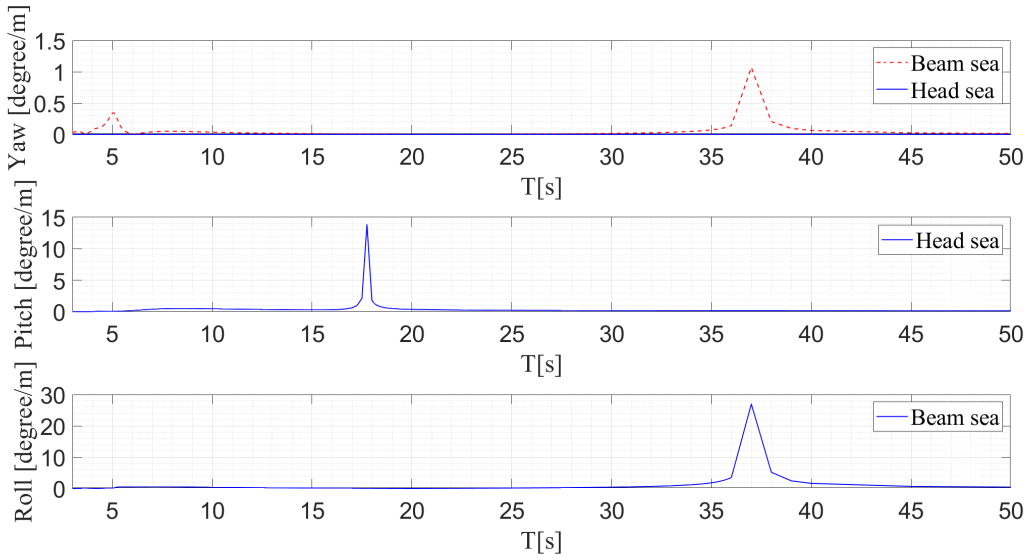

Figure 7.2: Selected rotational RAOs for model. Beam sea: 90 deg ; Head sea:180 deg.

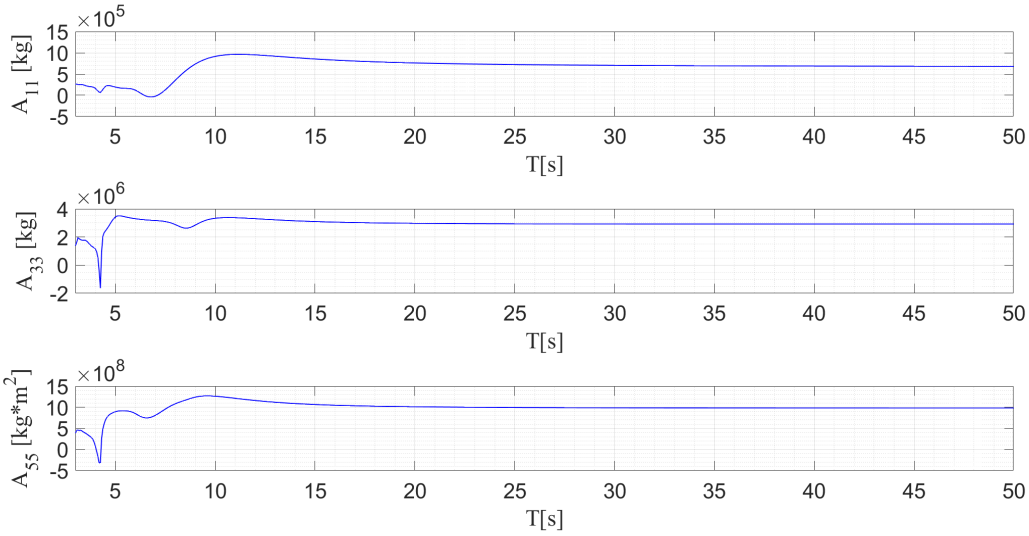

Figure 7.3: Selected added mass values for model. Beam sea: 90 deg ; Head sea:180 deg.

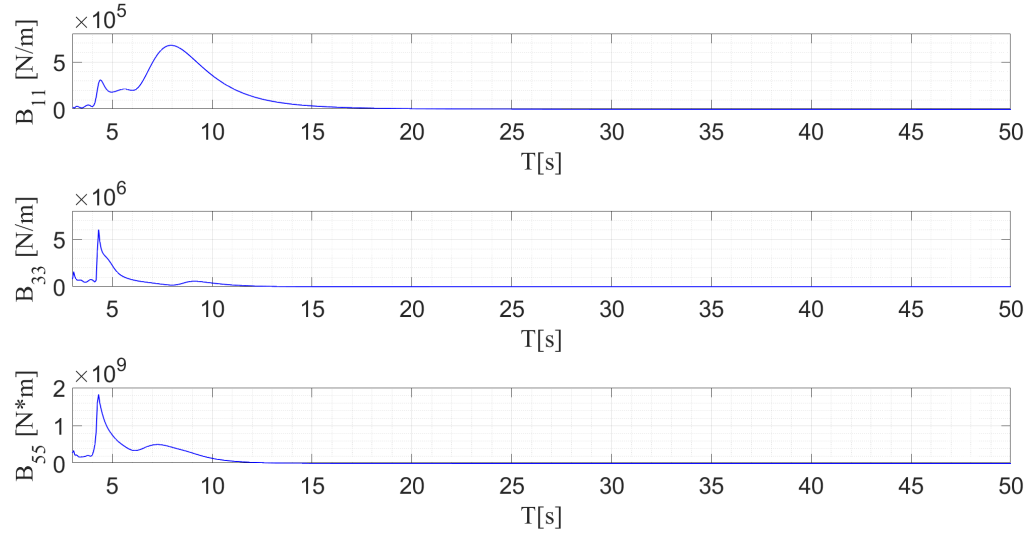

Figure 7.4: Selected potential damping values for model. Beam sea: 90 deg ; Head sea:180 deg.

7.2 Moonpool damping

The results in this section shows the results from the sensitivity analysis for the free surface damping, and for roll and yaw damping. Finally, the results for the damping with the most promising responses are shown. Altough significantly more values were tested for the damping in the moonpool, only a few selected are shown to display clear figures.

7.2.1 Roll damping

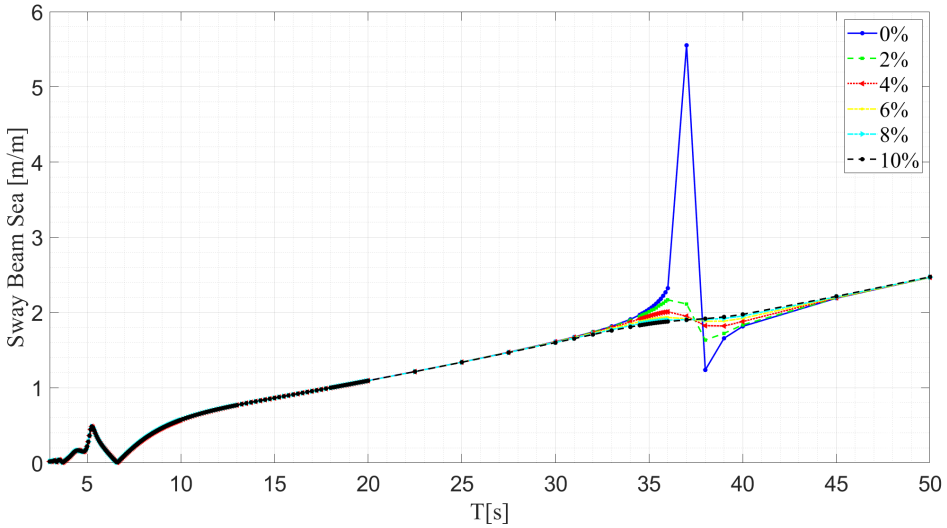

Figure 7.5: Results from the sensitivity study on Sway RAO for twin fish model for 90 degree direction.

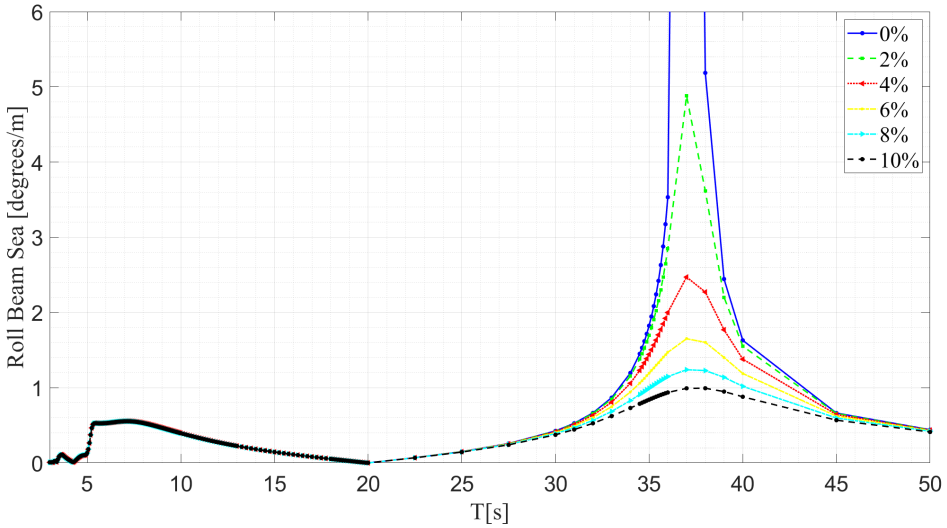

Figure 7.6: Results from the sensitivity study on Roll RAO for the twin fish model for 90 degree direction.

7.2.2 Damping introduced in HydroD

The RAOs below show the RAOs for the structure,when the internal lid was introduced to . Introducing an internal lid in the twin fish hull had no difference on the RAOs, added mass and damping.The values for the different damping are shown in the case chapter, and the results are presented below:

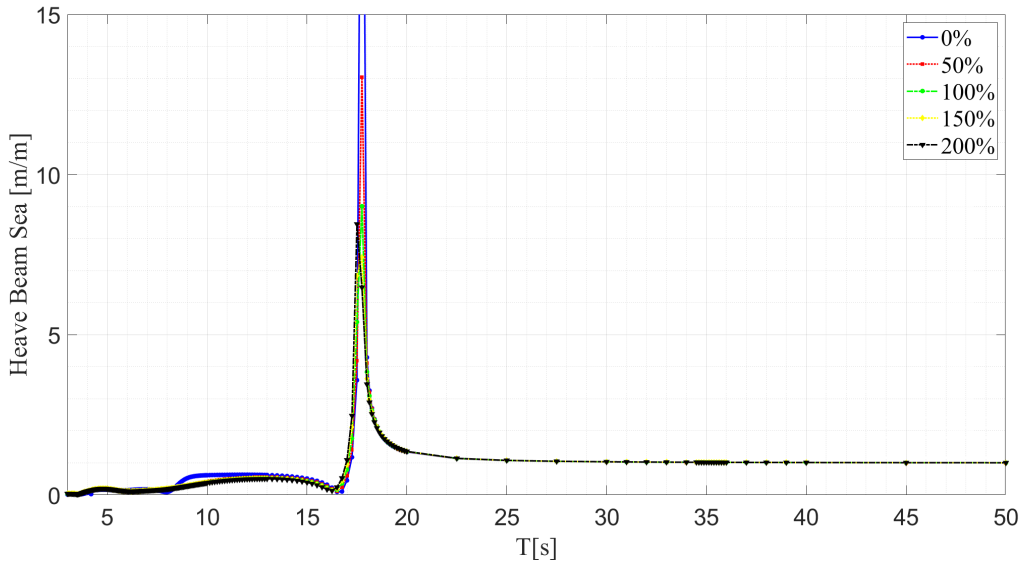

Figure 7.7: Results from the sensitivity study on Heave RAO at 90 degrees when introducing moonpool damping.

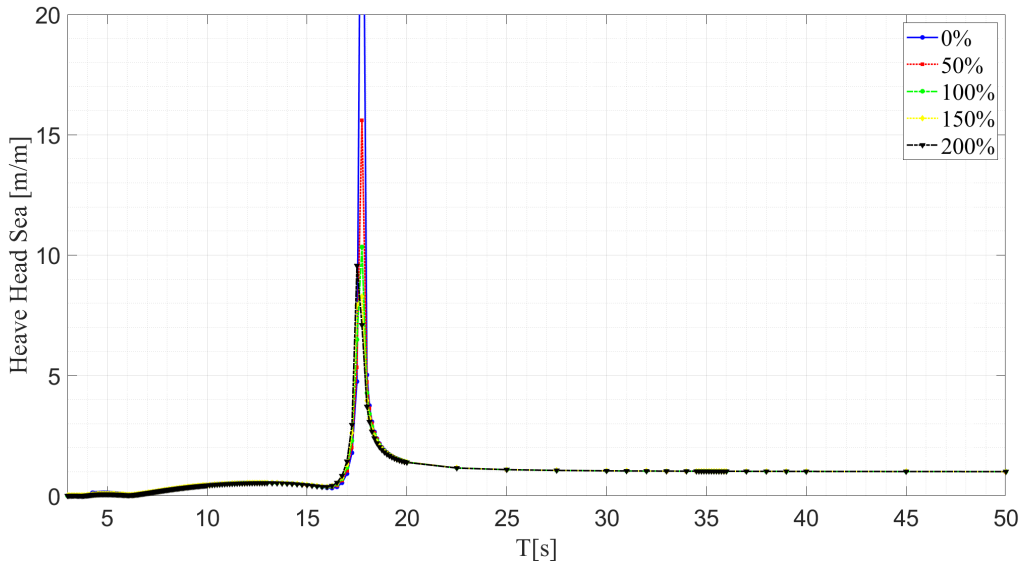

Figure 7.8: Results from the sensitivity study on Heave RAO at 180 degrees when introducing moonpool damping.

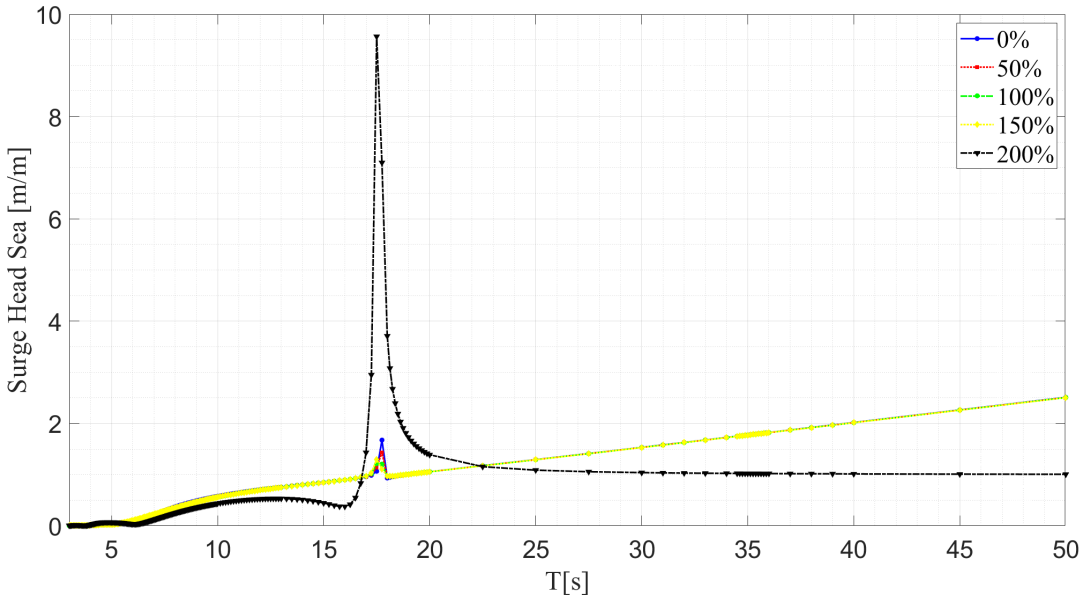

Figure 7.9: Results from the sensitivity study on Surge RAO at 180 degrees when introducing moonpool damping.

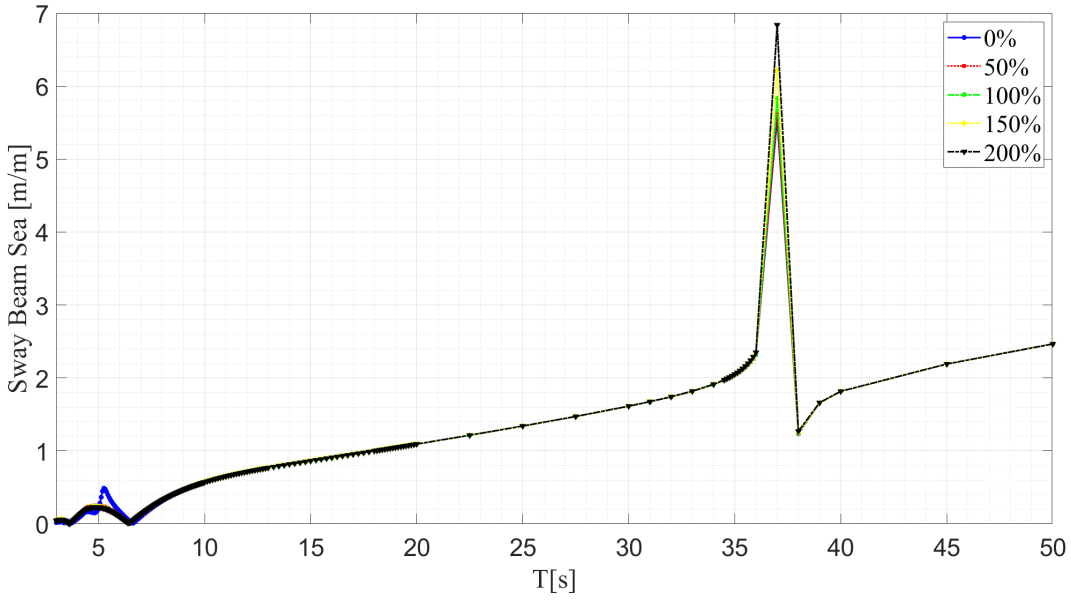

Figure 7.10: Results from the sensitivity study on Sway RAO at 180 degrees when introducing moonpool damping.

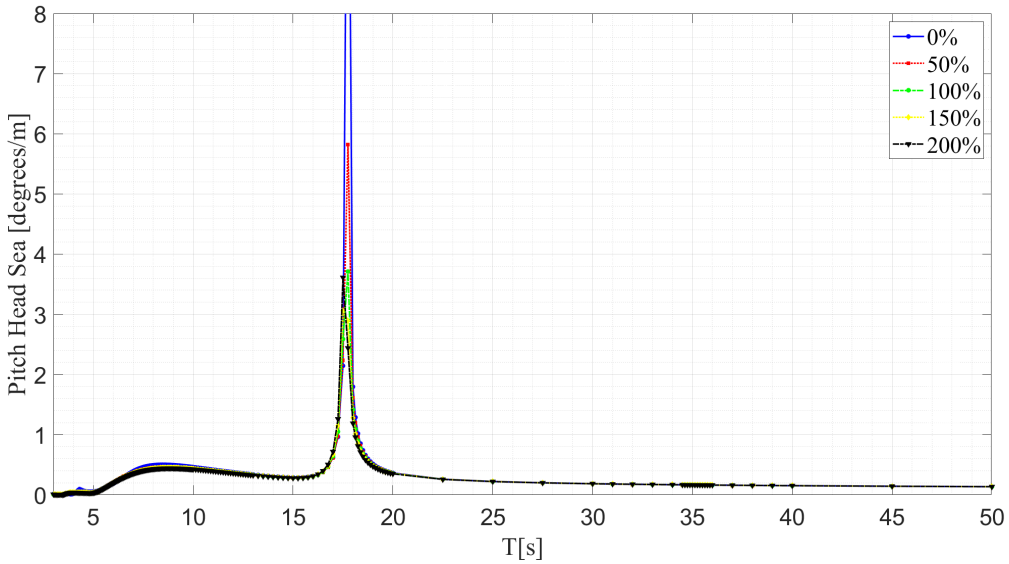

Figure 7.11: Results from the sensitivity study on Pitch RAO at 180 degrees when introducing moonpool damping.

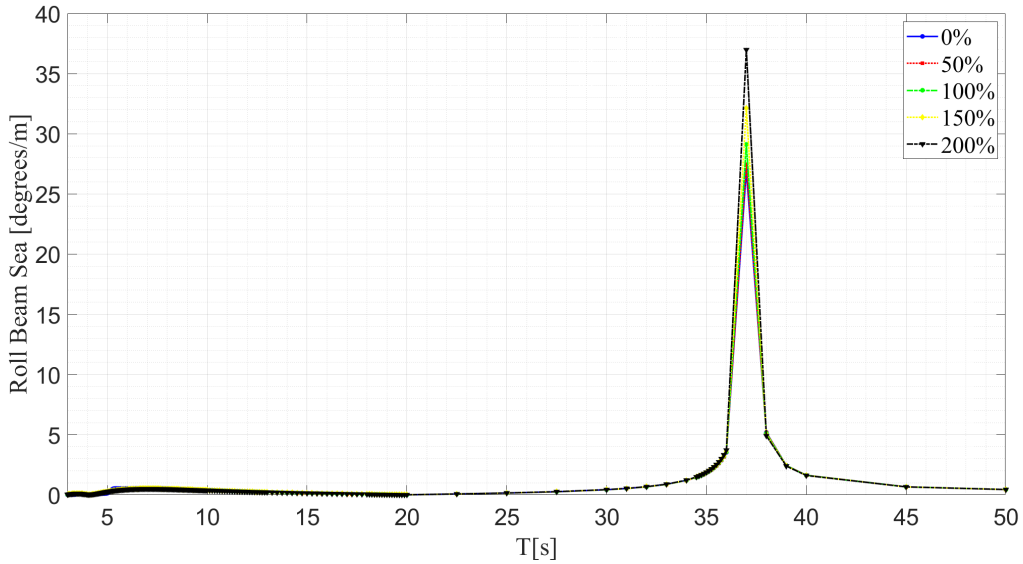

Figure 7.12: Results from the sensitivity study on Roll RAO at 90 degrees when introducing moonpool damping.

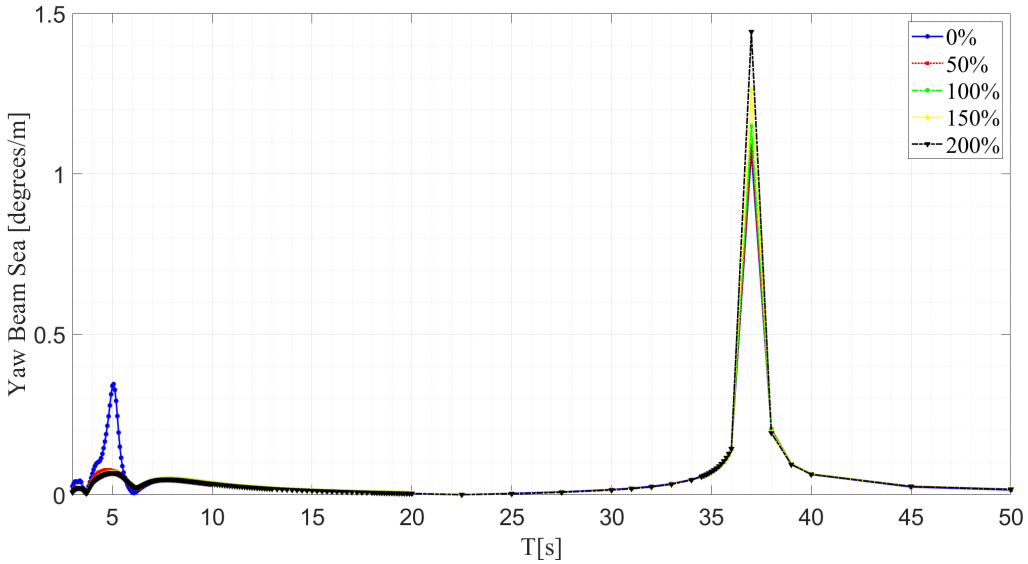

Figure 7.13: Results from the sensitivity study on Yaw RAO at 90 degrees when introducing moonpool damping.

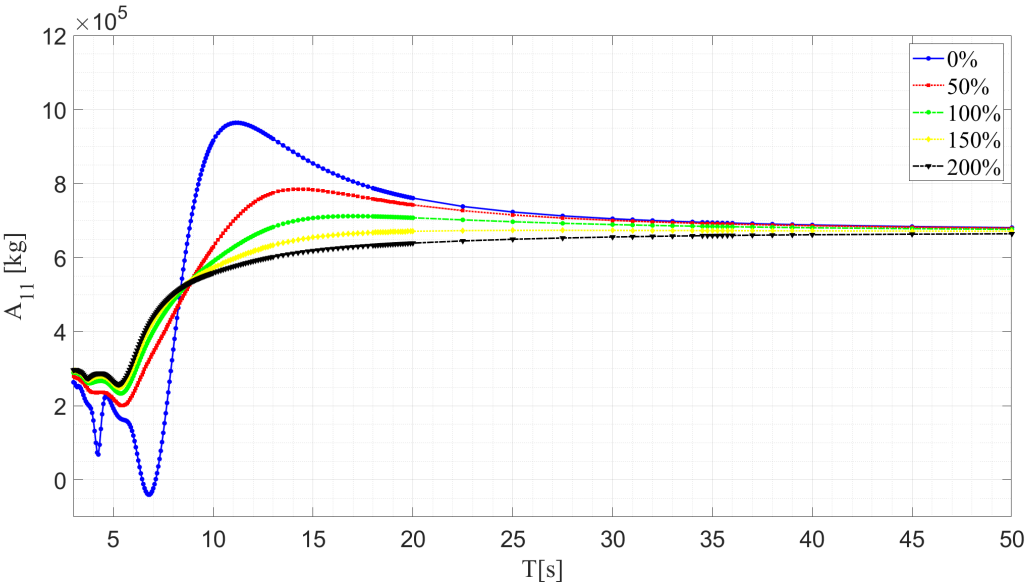

Figure 7.14: Results from the sensitivity study on added mass [A11] when introducing moonpool damping.

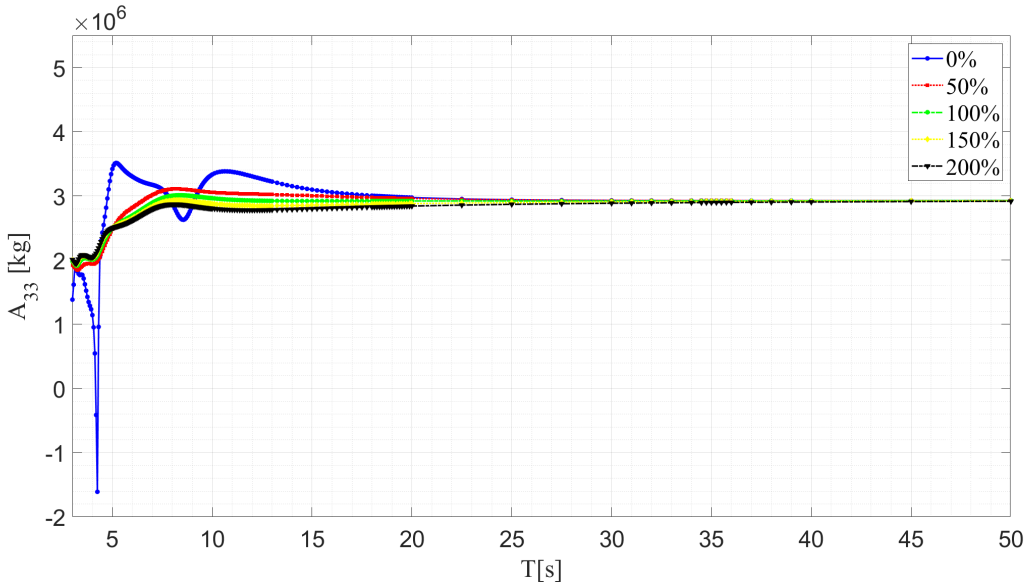

Figure 7.15: Results from the sensitivity study on added mass [A33] when introducing moonpool damping.

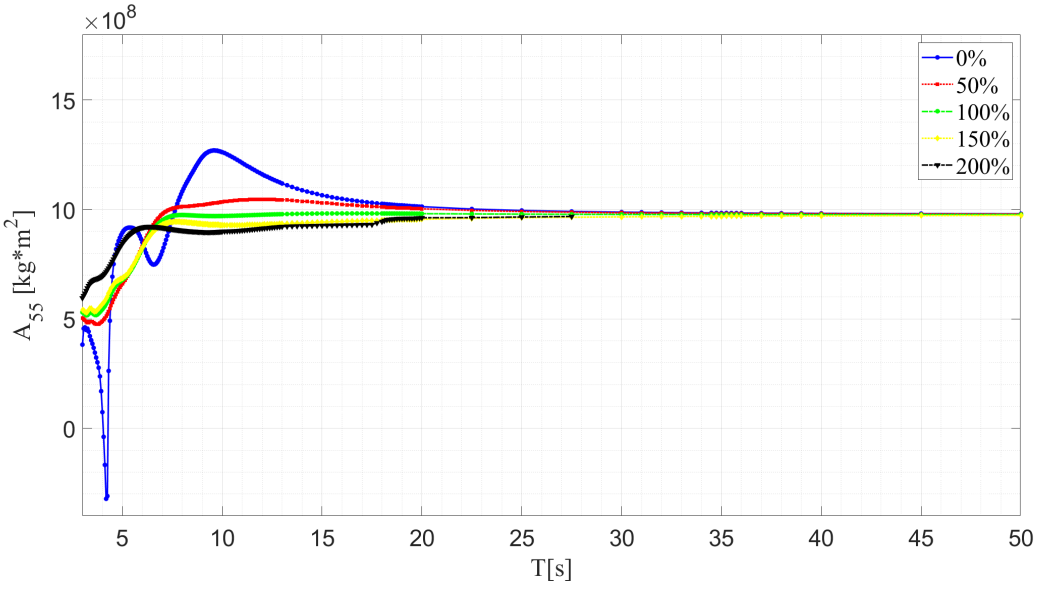

Figure 7.16: Results from the sensitivity study on added mass [A55] when introducing moonpool damping.

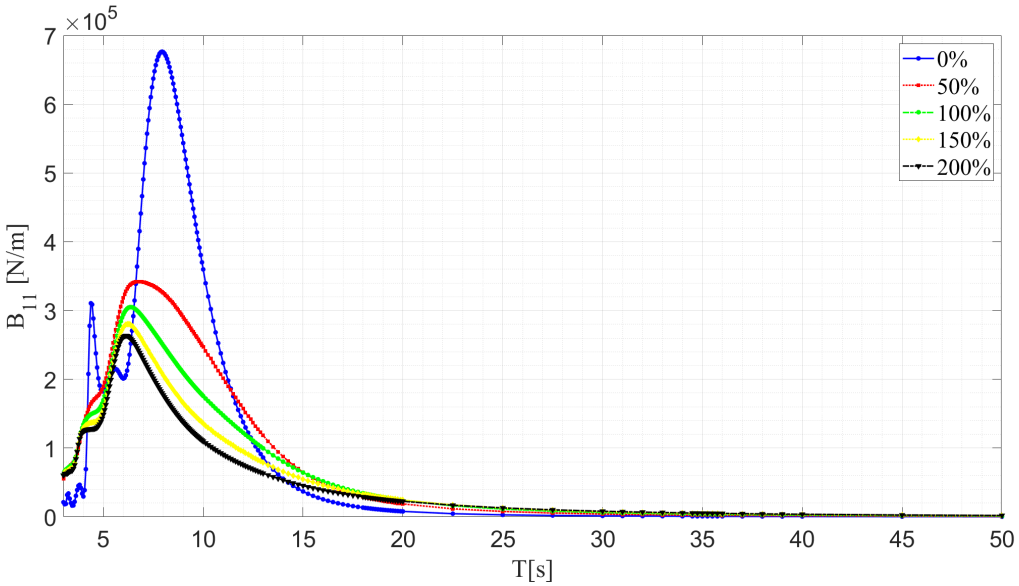

Figure 7.17: Results from the sensitivity study on potential damping [B11] when introducing moonpool damping.

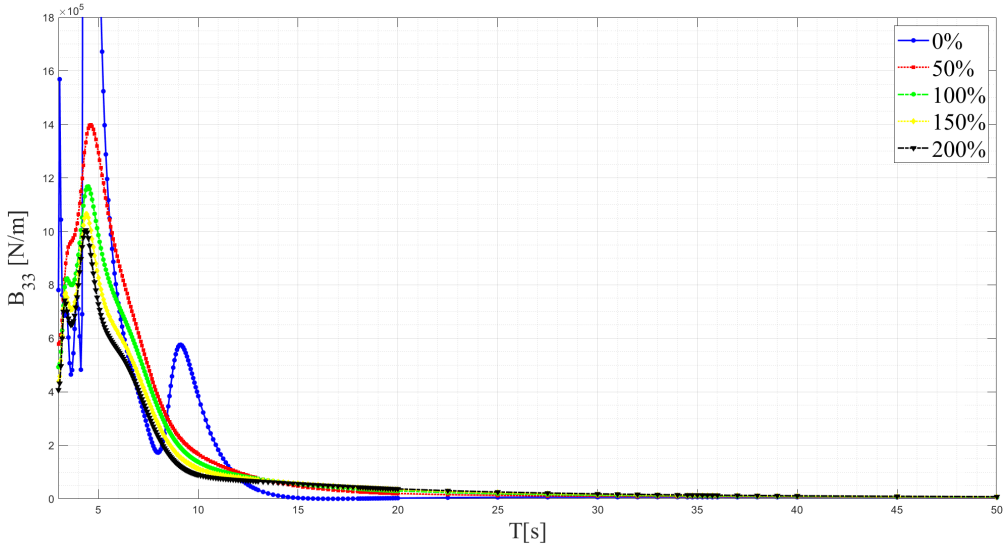

Figure 7.18: Results from the sensitivity study on potential damping [B33] when introducing moonpool damping.

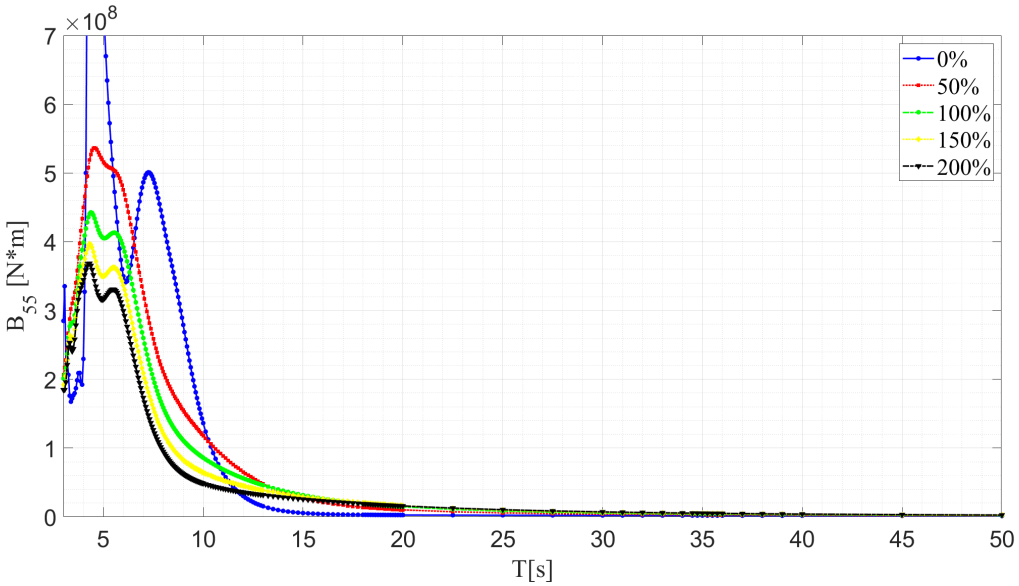

Figure 7.19: Results from the sensitivity study on potential damping [B55] when introducing moonpool damping.

7.2.3 Best results after damping sensitivity study

From the sensitivity analysis for damping, some values were selected which resulted in a significant improvement of the responses of the structure. A damping values of 150 percent and 6 percent roll damping resulted in the best option. The figures below show the final responses of the twin fish floater including damping. These responses were later imported into Sima for the coupled analysis.

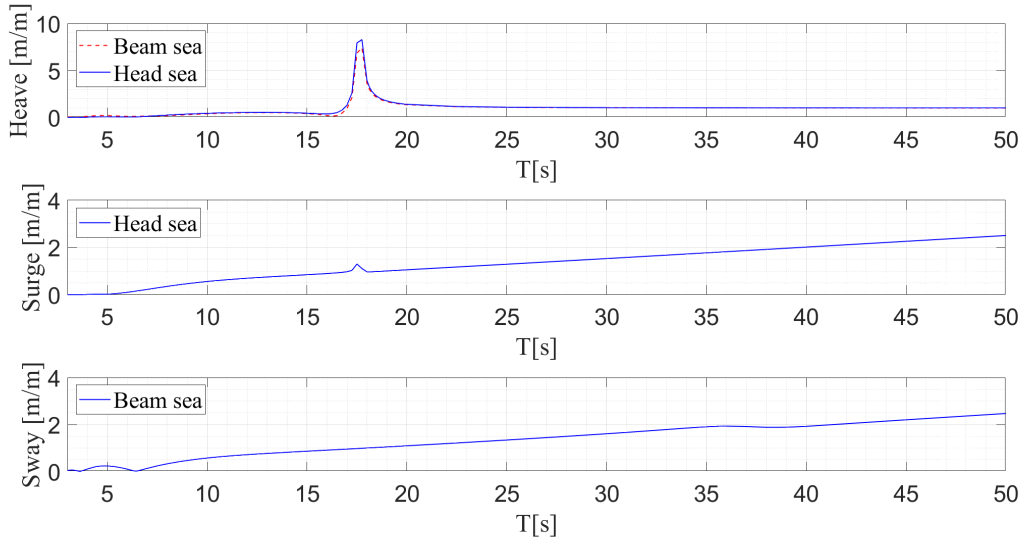

Figure 7.20: Selected translational RAOs for the twin fish floater after introducing moonpool damping and roll critical damping.

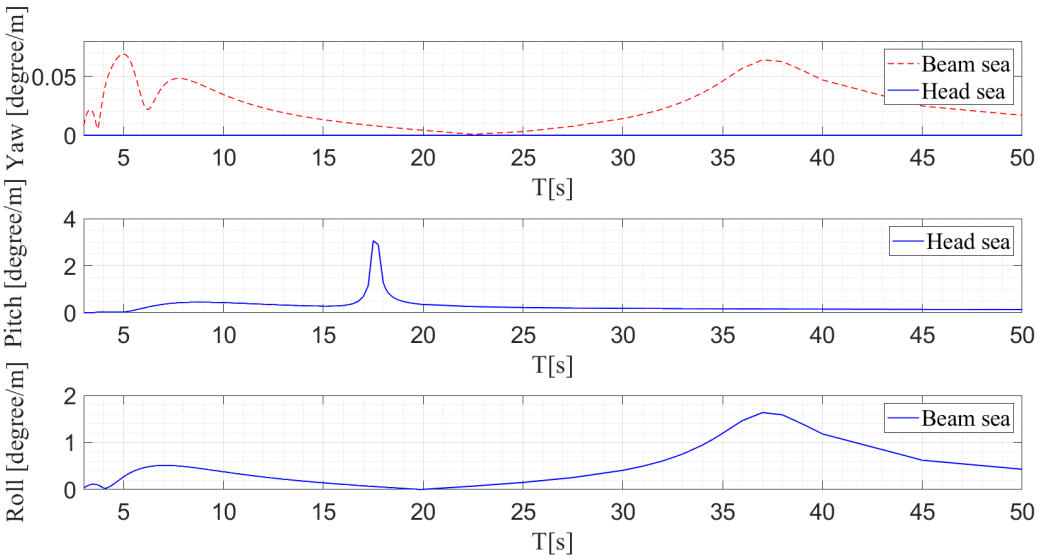

Figure 7.21: Selected rotational RAOs for the twin fish floater after introducing moonpool damping and roll critical damping.

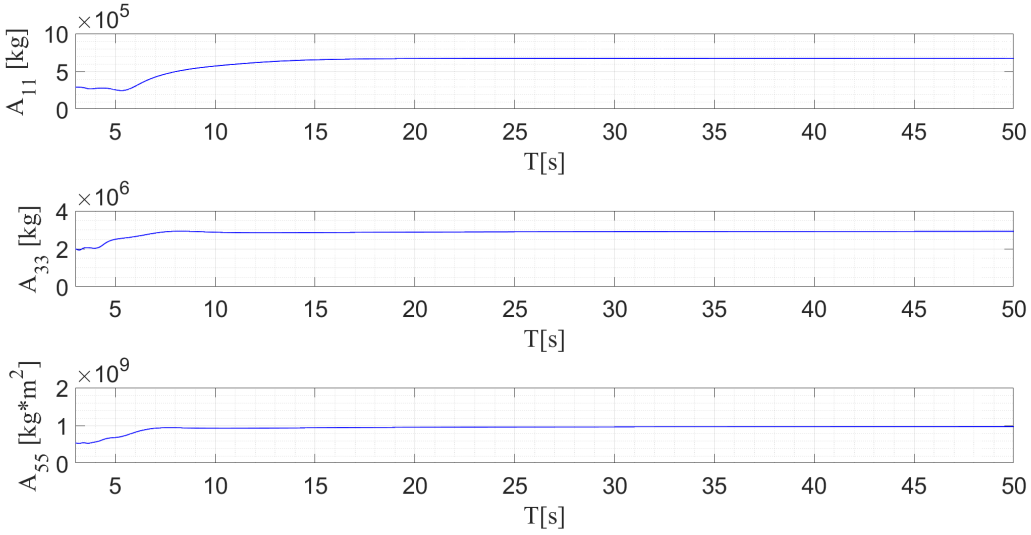

Figure 7.22: Selected added mass values for the twin fish floater after introducing moonpool damping and roll critical damping.

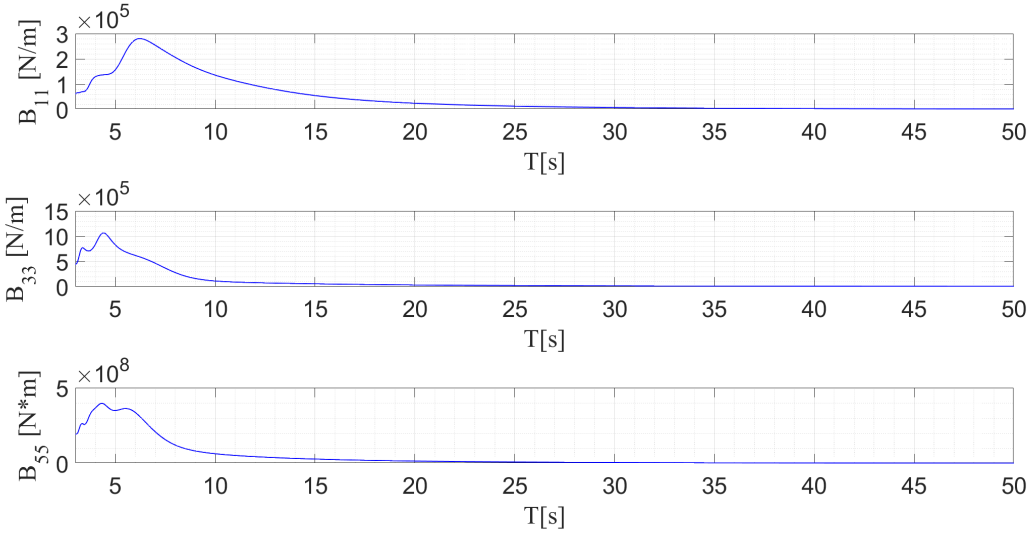

Figure 7.23: Selected potential damping values for the twin fish floater after introducing moonpool damping and roll critical damping.

7.3 Coupled analysis

Below the results for the coupled analysis will be presented. The process of designing a good and correct system with analysis that go through was time consuming and consisted of several models that were constructed. The results below are for the complete model: floater, wind turbine and mooring system. Several conditions were run as presented in *Case and Materials* , but only a few selected values of them are presented.

7.3.1 Global motions of the structure

The figures below are for the condition from the environmental contour line with the highest H_s value which is $15.48m$ while T_p is $36.07s$ for two different wave directions, 180 degrees and 150 degrees. The results are presented for a time period of $600s$

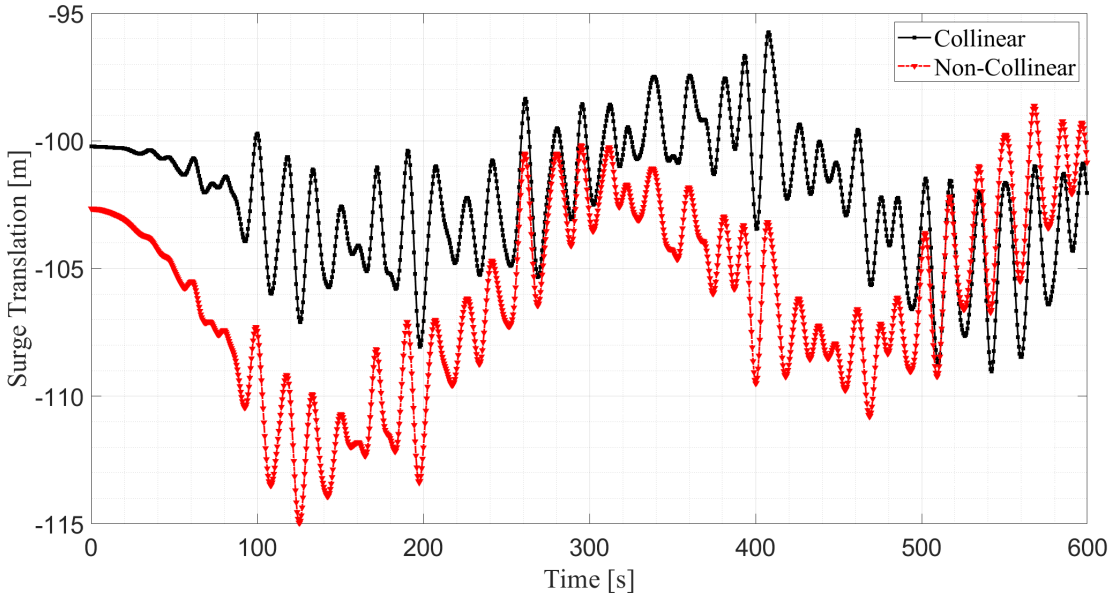

Figure 7.24: Surge translation for the twin fish floater at two wave directions (Collinear - 180 deg, Non-collinear - 150 deg).

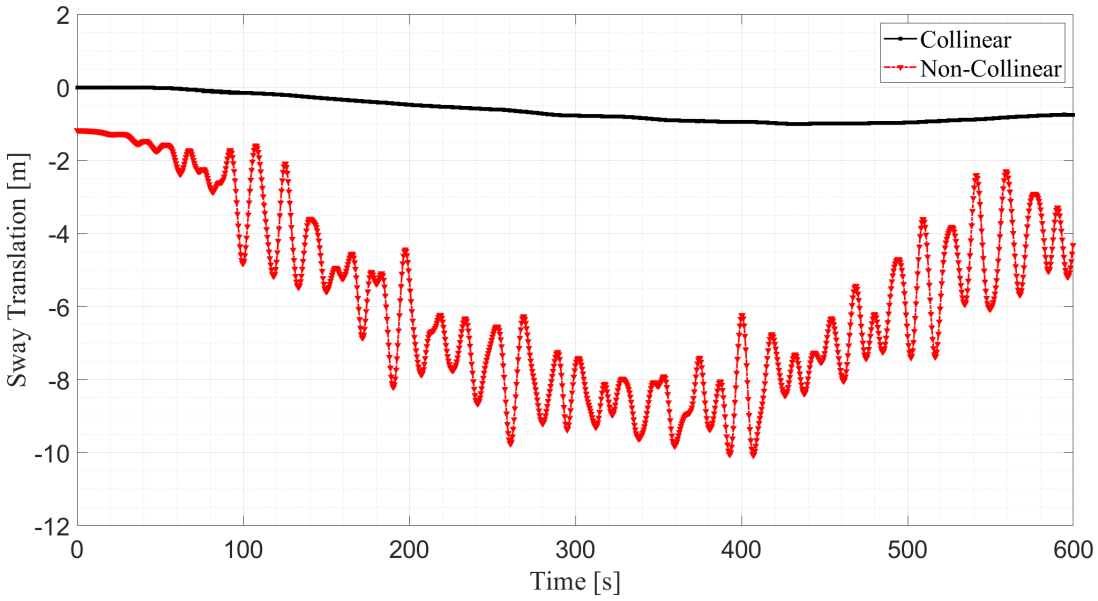

Figure 7.25: Sway translation for the twin fish floater at two wave directions (Collinear - 180 deg, Non-collinear - 150 deg).

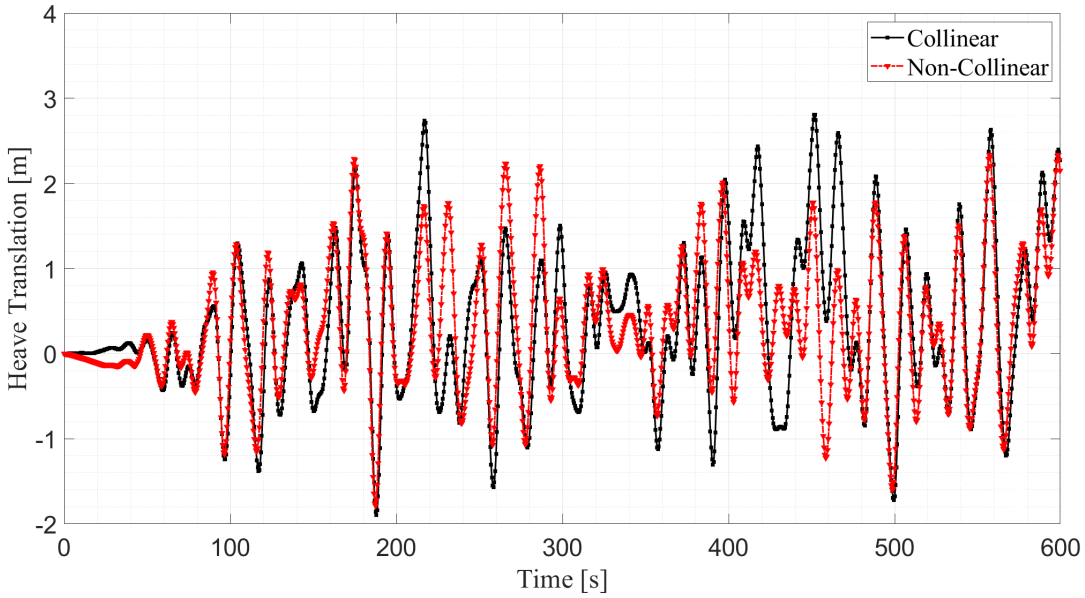

Figure 7.26: Heave translation for the twin fish floater at two wave directions (Collinear - 180 deg, Non-collinear - 150 deg).

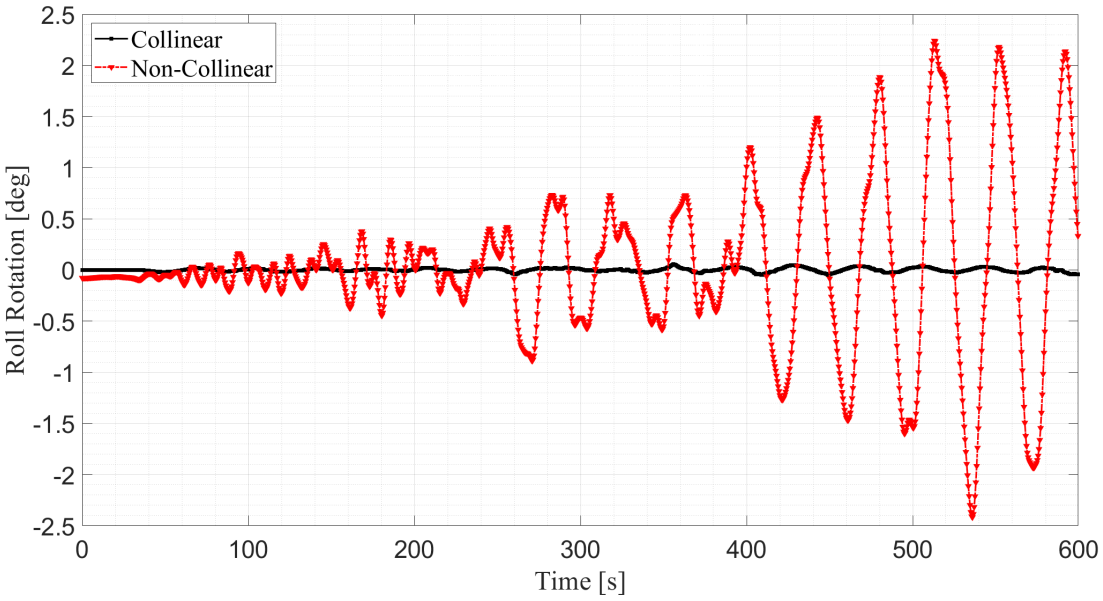

Figure 7.27: Roll rotation for the twin fish floater at two wave directions (Collinear - 180 deg, Non-collinear - 150 deg).

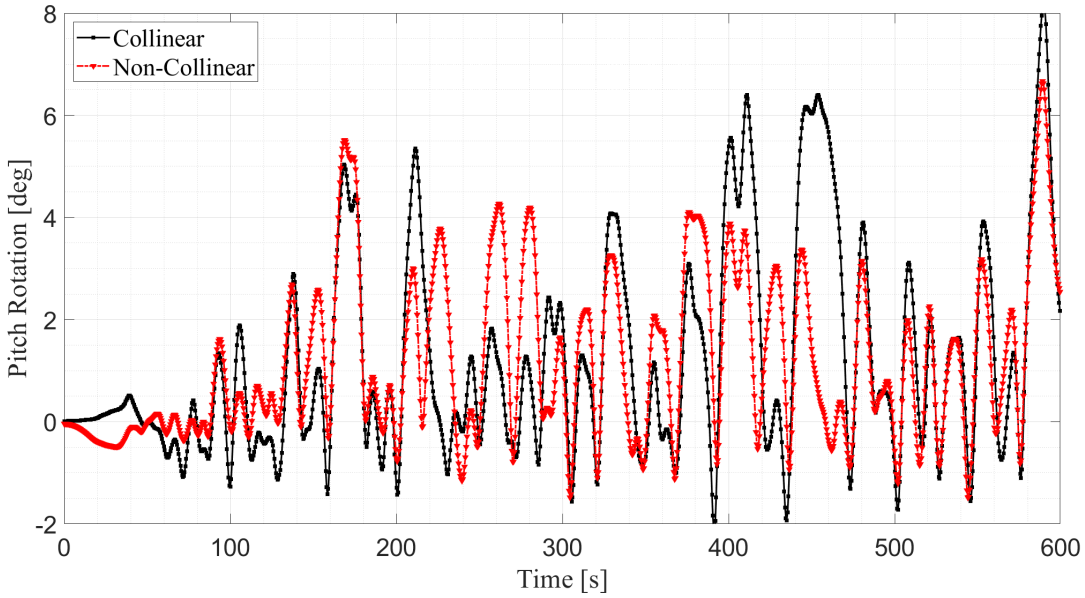

Figure 7.28: Pitch rotation for the twin fish floater at two wave directions (Collinear - 180 deg, Non-collinear - 150 deg).

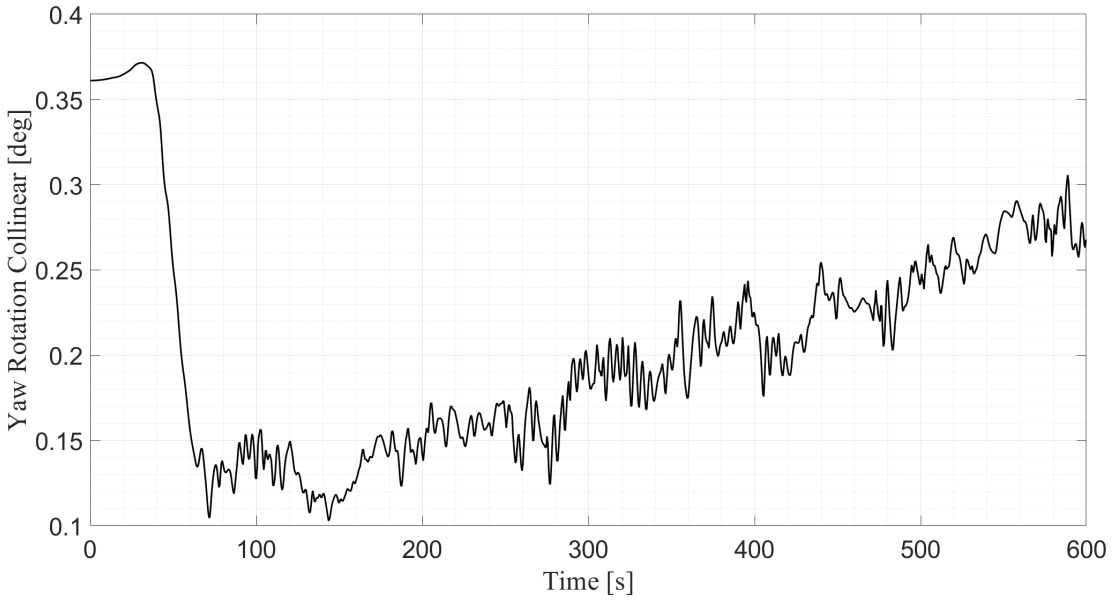

Figure 7.29: Yaw rotations for the twin fish for a collinear wave direction (180 degrees).

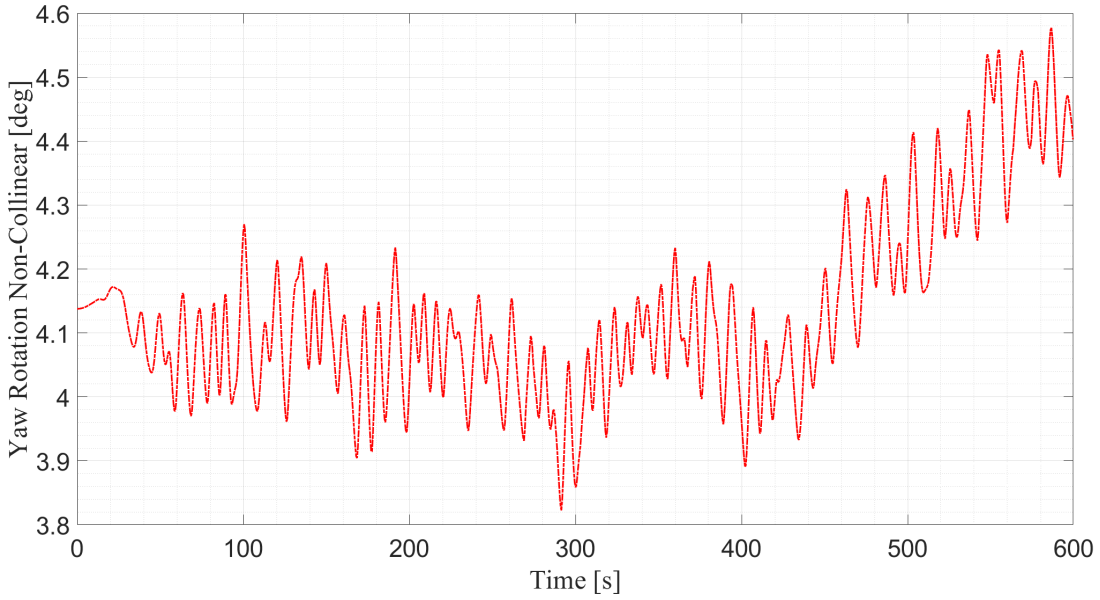

Figure 7.30: Yaw rotations for the twin fish for a non-collinear wave direction (150 degrees).

7.3.2 Global motions for different wave seed numbers

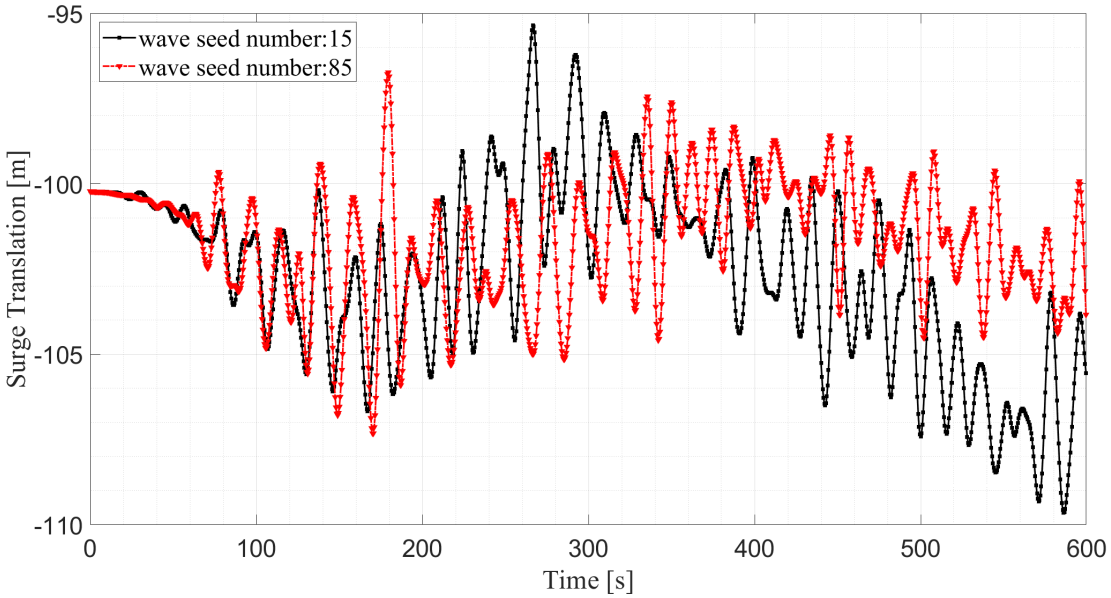

Figure 7.31: Surge translation for twin fish floater at wave seed number 15 and 85.

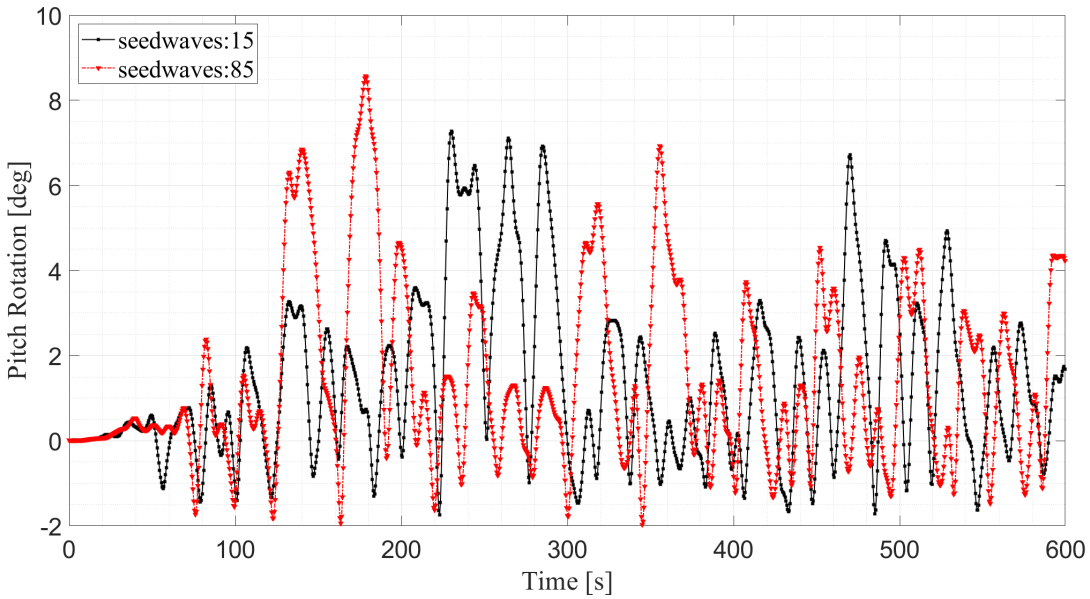

Figure 7.32: Pitch rotation for twin fish floater at wave seed number 15 and 85.

7.4 Design of mooring system

In this section the design of the mooring system will be presented. Several iterations were made to get the preliminary data for the mooring system. Therefore the data presented in the *Case and Materials* chapter can also be considered as results. Only the detailed results for the final mooring line is presented.

7.4.1 Fairlead and turret

The design of the turret structure was conducted to allow for rotation of the structure when influenced by environmental loads. The final turret structure consisted of free supernodes connected by stiff beam elements. The sketch below demonstrates the design of the turret structure.

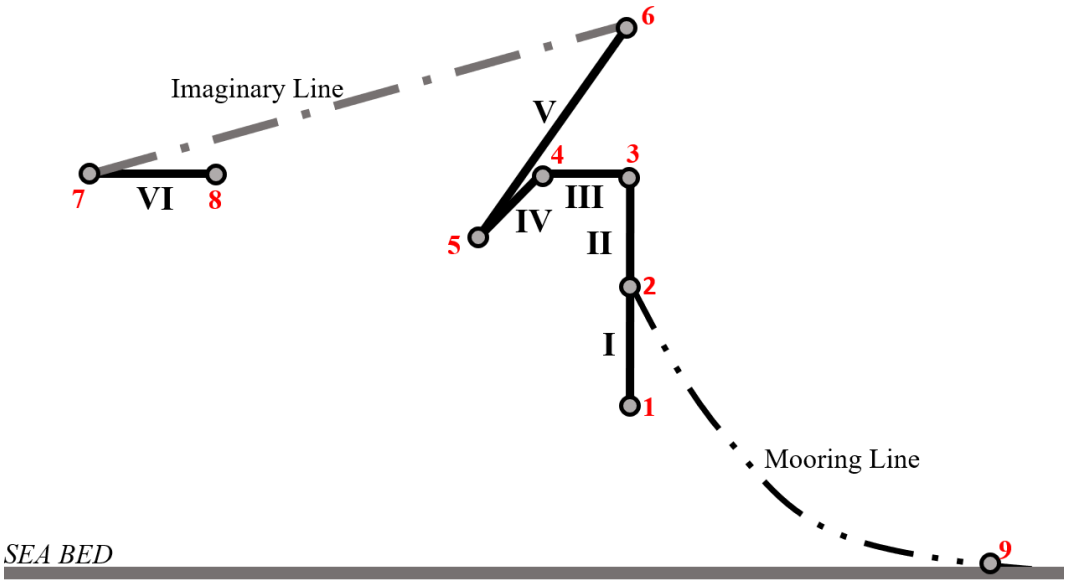

Figure 7.33: Sketch of the turret construction with supernodes and connecting dummy beams.

A line was created connecting supernode 7 and 8, which was later used to define a slender system connection for the twin fish body. The mooring line is attached at supernode 2, while it is anchored at supernode 7.Supernode 7 is fixed, but allows for rotation in all directions.

7.4.2 Static tension of line

We divide between the static line tension, and the dynamic line tension.

The static tension of the line is given in the following table. In the result file from sima (stamod.res), the static tension is given according to each element of the mooring line. The models presented are the two different models, 3 and 4, presented in the *Methodology* chapter.

Table 7.4: Static mooring tension for selected cases.

Node [-]	Case 1 [kN]	Cases Case 1 (150d.) [kN]	Case 2 180[kN]	Case 2(150d.)[kN]
74	359.0	363.0	358.8	357.8
75	359.2	363.2	359.0	358.0
76	359.4	363.4	359.3	358.3
77	359.6	363.6	359.5	358.5
78	359.9	363.9	359.7	358.7
79	360.1	364.1	360.0	359.0
80	360.3	364.3	360.2	359.2
81	360.6	364.6	360.4	359.4
82	360.8	364.8	360.6	359.6
83	361.0	365	360.9	359.9
84	180.3	184.4	180.2	186.1
85	0.08	6.38	0.36	21.5

The numbering of the nodes are from the anchor end (supernode 9) to the fairlead (supernode 2). The static line tension for the different parts of the mooring line is presented above for the highest H_s value in the 2D contour line generated for the thesis. Two different models are displayed, the complete model including the wind turbine (WT) which is the case 1 and the complete model excluding the wind turbine (WOWT) case 2. The results for loads in wave headings 180 deg and 150 deg are shown.

7.4.3 Transverse location

Table 7.5: Final position of body after static analysis.

Condition	$H_s[m]$	$T_p[s]$	X-coordinate [m]
2D Contour Line	15.48	36.08	-100.2
2D Contour Line Non-Collinear	15.48	36.08	-100.2
2D Contour Line	8.274	19.58	-102.6
2D Contour Line Non-Collinear	8.274	19.58	-102.6

The data is from the 2D contour line and includes one parked condition and one condition with low values. The transverse location of the mooring in static analysis is of importance. The body was defined according to the line shown in the figure on the previous page (line 6) between supernode 7 and 8. The location of supernode 7 corresponds to point (0.0.0) for the coordinate system of the model. Since point 7 is defined at -101 m in x-coordinate, then the x-coordinate should not move significantly far from that location.

7.4.4 Dynamic mooring tension

The graph shows the mooring tension for the highest value for H_s is 15.48 m while the T_p is 36.08 s for collinear and non-collinear case.

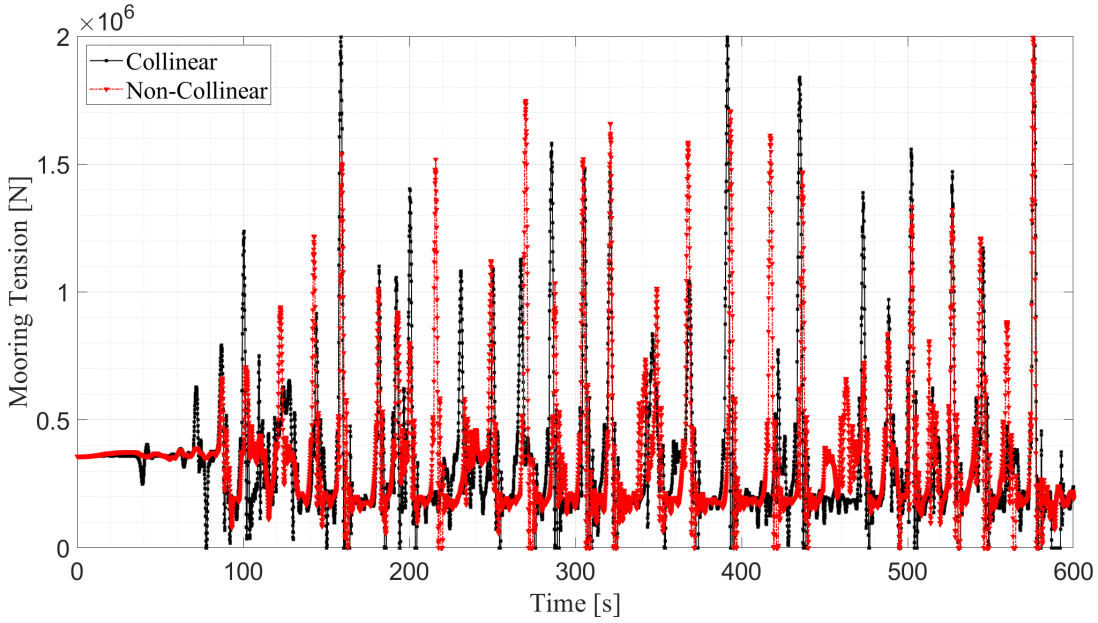

Figure 7.34: Mooring line tension for two wave directions: Collinear - 180 deg, Non-collinear - 150 deg.

7.4.5 Weibull fitting

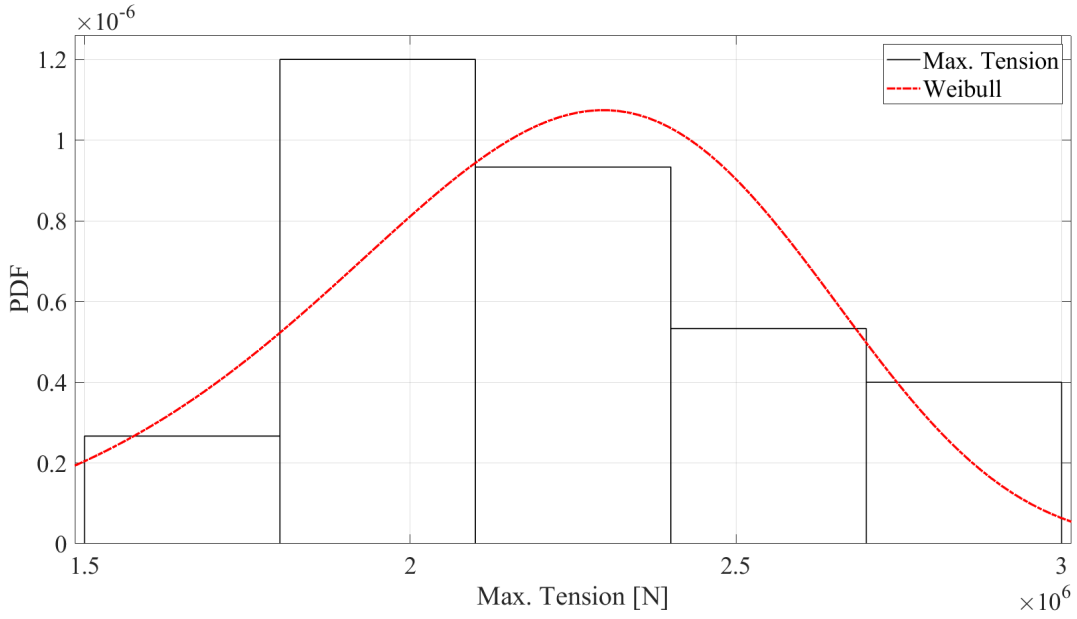

Figure 7.35: The cumulative probability for the maximum tension values for random wave seed numbers.

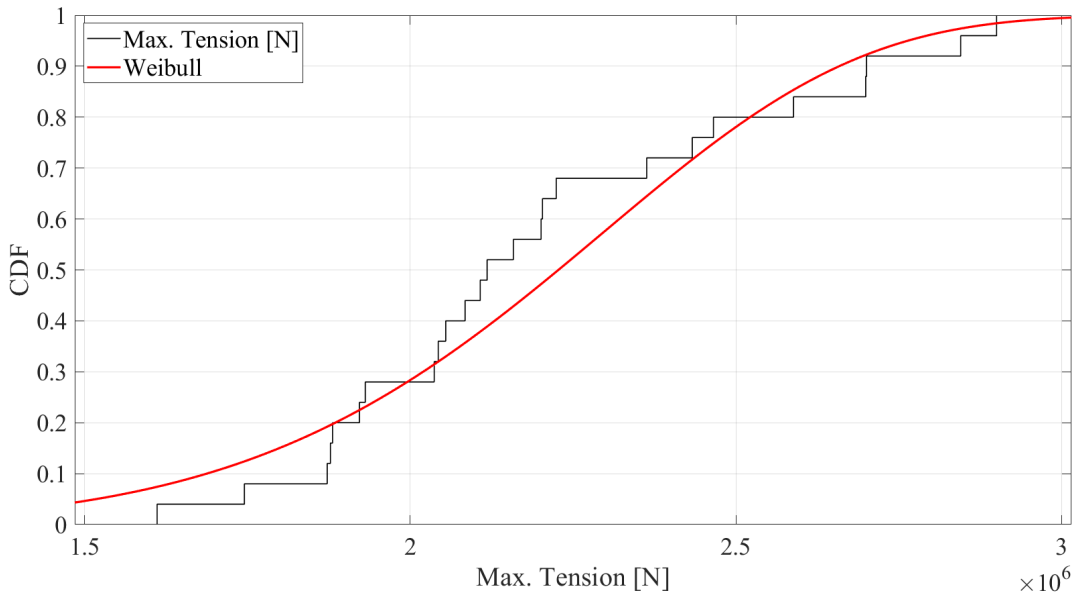

Figure 7.36: The probability for the maximum tension values for random wave seed numbers.

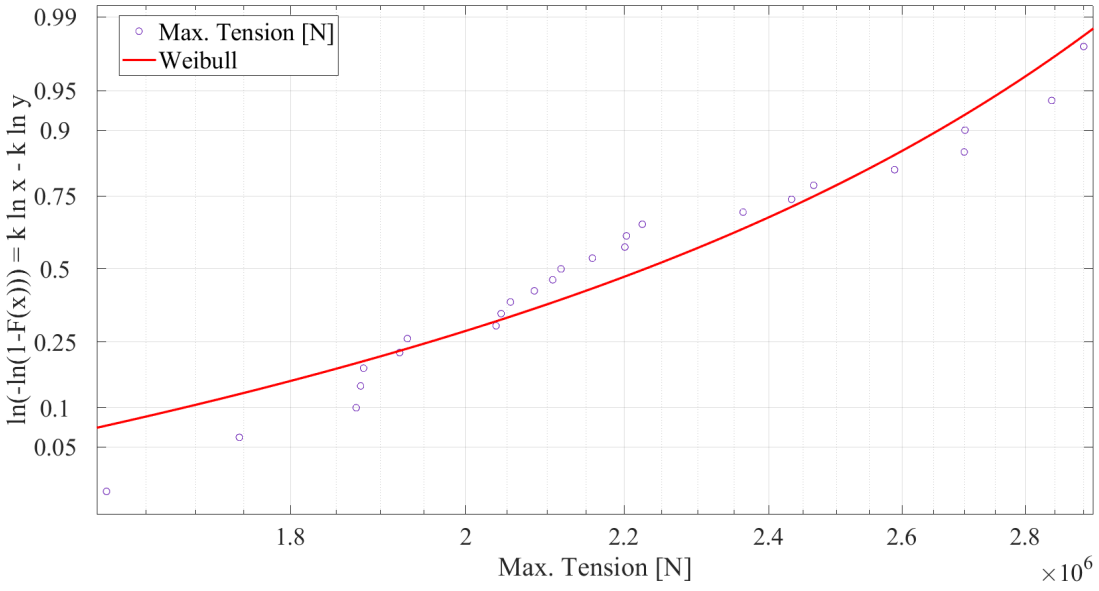

Figure 7.37: The probability plot for the maximum tension values for random wave seed numbers.

8 | Discussion

In this chapter the discussion regarding the steps and procedures conducted to design the novel semi-submersible floater,conducting the coupled analysis and designing the mooring system.

8.1 Design of the twin fish floater

The twin fish floater designed is based on a model designed in a pre-project fall of 2020. The designed showed feasibility, but the natural periods of the structure would result in bad responses.

8.1.1 Hydrostatic responses

From the pre-project, a reasonable model was selected and analyzed. However, the natural period were low and was a indication of a structure with responses that were not ideal. Therefore, as stated in the pre-project, the structure's water plane area needed to be reduced to achieve better natural periods.

Several cases were tested. The preliminary tests were lowering the structure with 0.5 meters between each case, please see the case and materials chapter. However, it was evident that the ideal model was located between lowering the structure 1 - 1.5 meter. A further iteration was conducted in the given area, the cases are presented in the result chapter. From these, the case which resulted in a lowering of 1.25 meter gave the most optimal results from the cases tested. A further lowering beyond 1.25 would result in too high natural periods for a semi-submersible structure , as well as significantly lower GMT and GML values.

Although the ideal would be to achieve a structure with all the natural periods for a value of 20 - 30 seconds, the design shows feasibility with achieving the values presented.

A structure with an elliptical support was also tested as an attempt of achieving better natural periods through a small waterplane area. However, the heave natural period was not improved. Also, the roll natural period became significantly higher. This is an indication that the elliptical support structure is unfit to use. However, a definite answer is not possible to give since only a single design with elliptical support structure is tested. Due to lack of time and other priorities with the thesis this was not investigated further.

8.1.2 Dynamic Results

In the result chapter, only the dynamic results for the final design was shown, which was for the structure which was lowered 1.25 meters more than the original floater from the preproject.

A challenge with the design of a structure with better heave natural periods was that the lowering the structure proved to be detrimental to the dynamic behaviour of the structure. While lowering

the structure resulted in better heave natural period, the amplitudes of the RAOs increased significantly which is detrimental to the structure's responses. It was therefore a challenge ensuring that the requirements for the natural periods were fulfilled while the responses are not neglected.

But, from the preproject period a challenge regarding the potential damping of the structure was discovered, where the potential damping values were significantly higher than for the 5 MW CSC , and the V - shaped semi-submersible. This was an indication of a an amplification effect caused by the moonpool of the structure. This challenge is related to the issue with worse dynamic behaviour, but the solution and further investigation of the issue was conducted. If the results were improved by introducing a damping lid to the structure, then the main cause of the detrimental responses will be removed.

8.1.3 Verification of results

The results from HydroD were compared to the results generated by MOJSLOAD. In the beginning, several issues were discovered in MOJSLOAD, which later proved to be an error in the algorithm, which was later corrected.

The results for the bodies used for damping sensitivity analysis can not be verified in MOJSLOAD since these models are multibody models and MOJSLOAD is not able to recognize these separate bodies. If the results from the damping sensitivity analysis were to be verified then WAMIT needed to be used with a different procedure for creating the internal surface and the mesh of the moonpool, as described in the WAMIT manual in the section on damping.

8.2 Free surface damping

In this section the discussion regarding removal of irregular frequencies through implementing a internal surface in the fish hulls and the sensitivity analysis for damping for the moonpool is discussed below.

8.2.1 Irregular frequency removal

The irregular frequency is removed from the dynamic responses through introducing internal surface lids within the fish hulls. The reason is that the internal lid functions as a war of removing numerical errors caused by the computer program. A comparison of the results for the removal of the irregular frequency compared to the results before were not presented as the procedure had no effect on the results, indicating no numerical errors in the presented responses of the structure.

8.2.2 Damping introduced in HydroD

Several sensitivity studies were carried out for the structure as the pre-project indicated a piston effect caused by the moonpool between the fish, and it showed detrimental values compared to the 5MW-CSC and the V-semi.

The damping introduced in HydroD is related to the moonpool between the two fish hull. A plate without mass was created for the area, and meshed in the subprogram Hydromesh. The procedure proved to be difficult as Hydromesh could not register the exact area between the fish hulls. Therefore another panel model was modelled in GeniE in which the moonpool area would be easier to detect in HydroMesh. The new model included plates which cut through the necessary area.

The mesh of the moonpool area was studied carefully, and the conclusion is that it suits the area well and follows the contour of the twin fish, and therefore will give reliable results.

A wide range of values were tested for damping - ranging from 0 to 400 percent. The hydrodynamic values were significantly improved when damping was introduced, which is displayed in the result chapter for the RAOs, added mass and potential damping values. The main features were that with increasing damping percentages introduced into the damping lid, the hydrodynamic characteristics have smaller amplitudes.It was evident that introducing more than 150 percent damping would result in that the values for RAOs would become worse again, while the added mass and potential damping amplitude values continued to decrease.

From the theory presented, values more than 1 (= 100 percent) will result in numerical incorrectness and therefore are unvalid in the given area presented. However, the values for damping were still significantly larger than what was reasonable for a feasible structure,and this needed to be investigated further byt introducing damping values of more than 100 percent. For the continued modelling in Sima (SIMO-Riflex) the responses of the structure with 150 percent damping was imported in.

Including the sensitivity analysis conducted for the damping lid in the moonpool area, a critical damping matrix was introduced for the twin fish floater due to the high roll and yaw RAOs. The values investigated for yaw and roll damping are within reasonable selection of damping for other floaters.

From the sensitivity analysis for yaw, it proved that it did not have any effect on any of the six motions of the structure. However, the sensitivity analysis for roll damping indicated a coupling effect between roll, yaw and sway. When higher values of roll was introduced, the values for roll,swat and yaw decreased in all of these DOFs. Introducing some damping for roll resulted in decreased

values for all of these motions, butt not any decrease for the added mass values or the potential damping values.

8.2.3 Final results from HydroD

Introducing some damping to the structure had a significant effect on the responses of the structure, improving them greatly. The most reasonable results from the sensitivity analysis is achieved after introducing 150 percent damping, and 6 percent roll damping. For roll damping the value could be less and still achieve good responses.

From the results presented in the result chapter, the values for the RAOs were still significantly large, and this needed to be studied further. But, this is also an indication that the model is not feasible since these large amplitudes around the natural periods could be detrimental to the structure.

8.3 Design of mooring system

Below the discussion for the design of the mooring system will be presented. The design of the mooring system and the coupled analysis for the structure are intertwined as the design of the mooring system could not be conducted without using the model created for the coupling analysis.

8.3.1 Different models

The goal with the design of the mooring line was designing a single point mooring system, instead of a spread mooring system which is currently most used for semi-submersible structures. A spread mooring system will keep the structure at a fixed heading since it will withhold the structure from several directions, and will therefore take up significantly large forces. A single-point mooring system consists of one mooring line, attached at the sea bed by an anchor, and attached at the floater using a fairlead. The single-point mooring system will allow the structure to rotate depending on the direction of the environmental loads.

Different mooring line designs were created based on the fundamental data presented in the case and materials chapter. The span of the lengths of the mooring system span between 95 - 125 meters, while the movement of the structure and the tension of the mooring line determined if changes had to be made on the mooring system. The static tension of the line had to not exceed a certain value for the mooring line to be considered as a good design.

There are several design objectives connected to the design of the mooring system. The mooring line capacity is one of them, where the analysis conducted in Sima (SIMO-Riflex) verify that the tension of the mooring does not exceed the capacity of the mooring line. Another factor which is of great importance is the global or local motions of the system, ensuring that the motion responses are sufficient. Codes and standards related to design of mooring system need to be fulfilled.

Some of the design objectives which have been irrelevant to investigate in this thesis are concrete mooring equipment and installation requirements, necessary clearances and offset. If all considerations would have been taken into account, then it would be difficult answering the set research question within the given time.

The final model shows good tension data, while the structure is kept at place at reasonable values.

8.3.2 Tension of line

The tension of the line is presented both as static tension and as dynamic tension, in the time domain. For the static line tension, the table presented demonstrates the forces on the two most distinct models from the Simo-Riflex analysis; the complete model without the wind turbine (WOWT) and complete model with the wind turbine (WT) at two different wave directions, 180 and 150 degrees.

The nodes listed are the nodes in which the mooring line has been divided into. From the result chapter, the complete data for the mooring system is given, and it displays that the mooring system is divided into three segments - which are again divided into smaller elements. In total the mooring system consists of 12 nodes for which the static tension is given. The maximum tension for a collinear case is 360.8 kN while the lowest value given is 0.08 kN. The static tension of the non-collinear case presents similar values, although a little larger than for a collinear load direction.

It is worth mentioning that that the wind turbine characteristics have been accounted for in both models, since it's characteristics is included in the imported files from HydroD, the model with the wind turbine is more correct since the wind turbine elements are modelled as slender elements

(Riflex) in SIMA. The tension values do not differ greatly from the two models, but the difference is more evident for the non-collinear cases.

8.3.3 Dynamic mooring line tension

The figure presented in the results displays the mooring tension in time domain for the highest value of H_s which is 15.48m with a T_p of 36.08s. It shows that the mooring tension varies significantly throughout the studied time period with a maximum value of about 2000 kN. The direction of the loads also influence the tension of the mooring line.

Also, the maximum tension for a parked condition where H_s equals 15.4 m and T_p ... is plotted for randomized selection of seed waves, from the value of 1 to 103.

The mean value was subtracted from the maximum tension value before it was plotted to a weibull distribution. There is a good correspondence between the values and the distribution. This is shown in the CDF and the probability plot.

8.3.4 Transverse motion

In the thesis, the transverse motion relevant for the mooring system, is the motion in x - direction, the surge motion of the structure. Both the transverse location of the entire system in the static analysis, and the dynamic movement in surge is presented in the paper, the dynamic movement will be discussed in the *Coupled Analysis* section of the *Discussion* chapter.

As stated in the theory chapter, the main function of a mooring system is keeping the structure at place in transverse movement. The challenge with a single point mooring system is that it is only attached at a single point compared to a spread system. A spread system keeps the structure at place at multiple directions - taking up larger forces than a single point mooring system. A spread mooring system restrains the structure from moving in multiple directions.

The original position of the structure is at -101m. From the table presented in the result chapter, the static analysis demonstrate that the location of the body does not change significantly more than the original position. The cases presented is for the lowest and higest H_s value provided from the 2D contour line created for a U_w value of 31.2 m/s.

8.4 Coupled analysis

8.4.1 Global motions of the structure

The global motions presented in the results chapter were for the 2D contour lines generated for the thesis. The highest H_s case was selected, 15.48 m with a T_p of 36.07 s. The linear and collinear motions are shown for the case. The surge translation shows that there are significant movements, but the motions of the structure share the same characteristics for both collinear and non-collinear direction. The same applies for heave translational motion.

However, the sway translation shows significantly larger motions for non-collinear than collinear. The same applies for the roll motion, where the collinear loads have significantly less than for the non-collinear case. From the graph it appear as if the rotation of roll is increasing as time passes. The pitch rotation has smaller amplitudes for the non-collinear loads compared to collinear loads.

Finally , for yaw rotation it is a clear drop the first seconds, before the values increase. For the non-collinear load condition, the maximum value throughout the time period studied is about 4.6 degrees, even though the inflicted load has an angle of 30 degrees compared to the structure. This may indicate that the structure does not have the desired characteristic, that it aligns itself with the direction of the loads. There is some resistance in the structure towards aligning itself according to the loads, which may result in larger loads on the mooring line than expected.

8.4.2 Effect of wave seed on global motions

In the results, an example with two different wave seeds for the same case is displayed. It is evident that the seed wave number has an effect on the motions, but the motions share many of the same characteristics. It is still important to include the results for a more reliable consideration of the load effects.

9 | Conclusion

In this master thesis, the twin fish floater has been designed with better hydrodynamic characteristics. Then, a coupled analysis was conducted for the structure including a design of a single point mooring system to keep the structure at place.

The research questions defined in this thesis were the following:

How can the twin fish floater wind turbine system be designed?

With the subquestions:

1. What are the dynamic characteristics of the system under influence of environmental loads?
2. How can the mooring system of the twin fish wind turbine system be designed to keep the structure at place?

The dynamic characteristics of the twin fish floater under influence of environmental loads was assessed by conducting a coupled analysis. The final model displayed significant displacements. The direction of the environmental loads also greatly influences the motion responses, both the translational and the rotational. The significant differences was displayed in roll motion where the non-collinear loads resulted in clear displacements which appears to increase when time passes. The Yaw rotation displayed that even though the direction of the structure is changed, the floater has some difficulties aligning itself to the load directions. The translational movement in sway shows large differences between the collinear and non-collinear loading, resulting in significant displacements.

The twin fish floater was designed with a single point mooring system using a catenary mooring line. A turret was designed and used as the fairlead to allow the structure to rotate in accordance with the existing load directions. The supernodes making up the turret was connected by beam elements.The anchor is fixed, but allows for rotations. The mooring line is divided into three distinct segments, a R3 chain, a Polyester rope and a buoy.

The tension in the mooring line are well below the capacity, and the movement in translational direction is sufficient. Weibull fitting was conducted and it showed good fitting.

10 | Suggestions for further work

In this thesis a design of a novel semi-submersible concept has been conducted.A single point mooring system was designed for the twin fish floater.Although the results show some feasibility, there are several challenges that have appeared which should be considered if any progress should be made with the design:

- A detailed structural design of the connecting structure with the wind turbine support.
- Several more fish shapes should be studied since the current fish shape experiences great displacements, such as in roll.
- Investigate the structure's responses during operational conditions.

Bibliography

[1] E. G. Energy, "The world of wind turbines." Available at `https://ege-windturbines.com/en/news/` (2021/05/01).

[2] IEA, "Global energy review 2020: Global energy and co_2 emissions in 2020," tech. rep., Paris, 2020.

[3] Pelastar, "Pelastar." Available at `https://pelastar.com/` (2021/05/06).

[4] P. P. Inc., "Windfloat." Available at `https://www.principlepowerinc.com/en/windfloat` (2021/05/06).

[5] GWEC, "Global offshore wind report 2020," tech. rep., Brussel, 2020.

[6] Y. Ma, "Fishtailing behaviour of single point mooring floating wind turbines," tech. rep., 2020.

[7] S. A. A. Najim, "My own illustrations." Own drawings, master thesis, 2021.

[8] I.-I. E. Commission, "Iec: 61400-3:wind turbines - part 3: Design requirements for offshore wind turbines," tech. rep.

[9] O. M. Faltinsen, *Sea Loads on Ships and Offshore Structures*. Cambridge: Cambridge University Press, 1 ed., 1990.

[10] M. Schabrich, "Coupled dynamic analysis of a floating dock system for installation of a spar wind turbine," tech. rep., 2019.

[11] D. I. J. Wichers, *Guide to single point moorings*. WMooring Inc., 1 ed., 2013.

[12] DNV GL, *Sesam User Course-Sima Coupled Motion Analysis,Wind Turbines*.

[13] C. Luan and M. I. Kvittem, "Use of buoyancy compensating force in coupled simo-riflex models." Procedure from authors,NOWITECH/Centre for Ships and Ocean Structures, 2013.

[14] Masson-Delmotte, V., P. Zhai, H.-O. Pörtner, D. Roberts, J. Skea, P. Shukla, A. Pirani, R. P. W. Moufouma-Okia, C. Péan, S. Connors, J. Matthews, Y. Chen, X. Zhou, M. Gomis, E. Lonnoy, T. Maycock, M. Tignor, and T. W. (eds.), "Global warming of 1.5°c. an ipcc special report on the impacts of global warming of 1.5°c above pre-industrial levels and related global greenhouse gas emission pathways, in the context of strengthening the global response to the threat of climate change, sustainable development, and efforts to eradicate poverty," tech. rep., World Meteorological Organization, Geneva, Switzerland, 2018.

[15] IEA, "Global energy review 2020: Global energy and co_2 emissions in 2020," tech. rep., Paris, 2020.

[16] IEA, "Global energy review 2020." Available at `https://www.iea.org/reports/global-energy-review-2020/global-energy-and-co2-emissions-in-2020` (2020/11/12), 2020.

[17] International Renewable Energy Agency (IRENA), "Renewable energy capacity statistics 2021," tech. rep., Abu Dhabi, 2021.

[18] E. Kjetil Malkenes Hovland, "Ferd-selskap satser på flytende havvind-konsept." Available at https://e24.no/olje-og-energi/i/vAavK5/ferd-selskap-satser-paa-flytende-havvind-konsept (2021/06/07).

[19] S. Nagothu, A. Østby, L. M. Pauchon, and M. S. Dale, "Kartlegging av den norskbaserte fornybarnæringen i 2019," tech. rep., Skøyen, Oslo, 2020.

[20] Jinjin Guan and Harald Zepp , "Factors affecting the community acceptance og onshore wind farms: A case study of the zhongying wind farm in eastern china," *Sustainability*, 2020.

[21] "Offshore wind power," 2009.

[22] P. A. Lynn, "Onshore and offshore wind energy : an introduction," 2012.

[23] Chenyu Luan and Torgeir Moan and Zhen Gao, "Design and analysis of a braceless steel 5-MW semi-submersible wind turbine," no. 35, pp. 46–129, 2016.

[24] GustoMSC, "Tri-floater." Available at https://www.gustomsc.com/our-markets/offshore-wind/floating-wind/tri-floater-and-spinfloat%20 (2021/01/27).

[25] GustoMSC, "A floating barge for offshore wind turbines." Available at https://www.bw-ideol.com/en/technology(2021/01/27).

[26] M. Karimirad and C. Michailides, "V-shaped semisubmersible offshore wind turbine: An alternative concept for offshore wind technology," *Renewable Energy*, vol. 83, pp. 126–143, 2015.

[27] IEA, "Offshore wind outlook 2019:world energy outlook special report," tech. rep., 2019.

[28] IEA, "Renewable and non-renewable electricity generation in oecd countries, 2008-2018," tech. rep., 2020.

[29] N. Government, "Renewable energy production in norway." Available at https://www.regjeringen.no/en/topics/energy/renewable-energy/renewable-energy-production-in-norway/id2343462/ (2021/04/01).

[30] FVN, "Samler krefter for flytende havvind." Available at https://www.fvn.no/nyheter/okonomi/i/869Wkx/samler-krefter-for-flytende-havvind (2021/01/27).

[31] Equinor, "Hywind tampen:the world's first renewable power for offshore oil and gas." Available at https://www.equinor.com/en/what-we-do/hywind-tampen.html (2021/05/01).

[32] J. Journée and W. Massie, *Offshore Hydromechanics*. Delft University of Technology, 1 ed., January 2001.

[33] P. Moriarty and A. H. N. R. E. Laboratory, "Aerodyn theory manual," tech. rep., 2005.

[34] J. Newman, "Marine hydrodynamics," 2017.

[35] R. Hibbeler, "Mechanics for engineers : statics," 2012.

[36] D. GL, "Recommended practise: Coupled analysis of floating wind turbines," tech. rep., 2019.

[37] M. Karimirad and T. Moan, "A simplified method for coupled analysis of floating offshore wind turbines," *Marine Structures*, vol. 27, no. 1, pp. 45–63, 2012.

[38] SINTEF Ocean, *SIMO 4.18.1 Theory Manual*.

[39] L. Li, Z. Gao, and T. Moan, "Joint environmental data at five european offshore sites for design of combined wind and wave energy devices," vol. 137, 06 2013.

[40] S. A. A. Najim, "Hydrostatic and hydrodynamic analyses of the twin fish supported floating wind turbine." Preproject, Hydrostatic, Hydrodynamic, novel concept, 2020.

[41] J. Jonkmann, S. Butterfield, W. Musial, and G. Scott, "Definition of a 5 mw reference wind turbine for offshore system development," tech. rep., New York NY, 2009.

[42] J. Jonkmann, "Definition of the floating system for phase iv of oc3," tech. rep., Golden,CO,USA, 2010.

[43] SINTEF Ocean, *Riflex 4.18.1 User Guide*.

[44] SINTEF Ocean, *SIMO 4.18.1 User Manual*.

[45] D. GL, "Dnvgl-os-e301:mooring position," tech. rep., 2018.

Appendices

A Appendix 1

- .stask files from SIMA/SIMO-Riflex
- Preproject thesis
- Models from HydroD
- Project plan
- Meeting Documentation
- A3 Poster